# Pathway-centric computational approach identifies molecular changes associated with antibiotic resistance in *Staphylococcus aureus*

By

Laura K. Harris

A Dissertation Submitted

In partial fulfillment of the Requirements for the Degree of

Doctor of Philosophy in Biomedical Informatics

Department of Health Informatics

Rutgers, The State University of New Jersey

School of Health Professions

May 2020

APPROVAL PAGE

X_____

Antonina Mitrofanova (Co-advisor)

X_____

Masayuki Shibata (Co-advisor)

X_____

Fredrick Coffman

X_____

Susan Gunn

X_____

External Reviewer

ACKNOWLEDGEMENTS

I thank my mentors, Drs. Antonina Mitrofanova and Masayuki Shibata, for the countless hours of mentoring they have provided over these past few years. Thank you to Dr. Susan Gunn for her expertise with the experimental portion of the work. Thank you also to Dr. Fredrick Coffman for being a committee member and advising on the work.

# DEDICATION

I dedicate this work to my husband, Robert W. Harris, and two daughters, Serena P. Harris and Lilly A. Harris, all who have sacrificed so much to support me in completing this degree.

TABLE OF CONTENTS

ABSTRACT

**Background**: Antibiotic resistant *Staphylococcus aureus* (*S. aureus*) infections are a major medical concern due to loss of antibiotic sensitivity. Genome-wide analyses, including sequencing and gene expression, identified genes associated with antibiotic resistances, such as *vraSR* whose mutations are associated with vancomycin, daptomycin, and oxacillin resistances. Pathway enrichment analysis using Fisher's Exact Test (FET) provides insight into pathway activity, though pathway roles in resistance are not fully elucidated. These studies applied a pathway-centric computational approach to examine antibiotic resistance (*i.e., vraS*-driven) and response (*i.e.,* treatment inducible) changes in *S. aureus.*

**Method**: This is the first application of Gene Set Enrichment Analysis, which improves upon FET by removing gene selection requirements, to obtain pathway signatures (*i.e.,* pathways ranked by activity change) from normalized enrichment scores reflecting 164 individual pathway activities in *S. aureus*. The pathway panels were obtained (most up- or down-regulated pathways separately), for *vraS*- and *graSR*-driven resistance signatures. A similar process was repeated to examine vancomycin susceptibility (*i.e.,* difference in response between resistant and sensitive strains). Pathway activity in *vraS*-driven resistance panels was then examined in various antibiotic (vancomycin, oxacillin, or linezolid) susceptibilities to identify commonalities and differences in individual pathway activities. One novel pathway was selected and its association to antibiotic sensitivity was experimentally verified.

**Results**: This approach correlated pathway activity changes, like up-regulated histidine biosynthesis, with established genetic associations to antibiotic resistance. Further,

pathway activity changes with known associations to vancomycin susceptibility such as down-regulated TCA cycle activity was also identified. Both examinations identified pathways with no prior association to antibiotic resistance. Inverse correlations between pathway activity changes and susceptibility to vancomycin and oxacillin/linezolid were seen (pathway activities up-regulated in vancomycin susceptibility were down-regulated in linezolid susceptibility) regardless of strain resistance level. Lysine biosynthesis was identified as a top candidate pathway for targeting to overcome resistance and verified by lysine or aspartate supplementation. Thus, lysine biosynthesis as a co-therapeutic target could restore antibiotic efficacy.

**Conclusion**: This pathway-centric approach identified pathway activity changes associated with antibiotic sensitivity which can be targeted to help reverse antibiotic resistance.

# LIST OF TABLES

LIST OF FIGURES

# CHAPTER 1

## INTRODUCTION

Many cells contain thousands of genes that drive complex molecular interactions supporting life. Breakthroughs in high-throughput experimental technology, such as microarray and RNA-seq, allow researchers to quickly examine expression of thousands of genes for a biological sample to get a broad perspective of cellular activity which allows for a comprehensive examination of specific biological processes. This is a massive improvement over laboratory techniques like reverse transcriptase-polymerase chain reaction (RT-PCR) and Northern blot that only test for a few select genes per experiment[1]. Since inception, microarray technologies have been used extensively to examine gene expression, polymorphisms, chromosomal aberrations, and copy number variations to answer a wide-variety of scientific inquiries including cancer and antibiotic resistance (*i.e.*, loss of sensitivity to an antibiotic therapy) research[1,2]. Its extensive use has generated large volumes of data which need further analysis to elucidate connections between observed gene changes and the molecular interactions they impact in order to fully understand cellular processes that produce phenotypic variations (*i.e.*, observable characteristics or traits). To accomplish this, researchers use statistical methods, such as enrichment analysis, to identify pathways (*i.e.*, ordered succession of cell molecular interactions leading to change in a cellular process or state) from genes selected for their statistical significance (*e.g.*, T-test p-value<0.05) that neglect genes with insignificant changes in expression from microarray data. While these methods identify individual pathways of scientific interest, they are limited because they consider pathways whose enrichment is based on statistically significant genes, missing broader pathway changes

(*i.e.*, accumulated via small gene expression changes) which contribute to phenotypic variations that result from activity of multiple pathways simultaneously, a perspective that is needed to fully understand cellular processes. To overcome this limitation, I used Gene Set Enrichment Analysis (GSEA), a well-established computational tool that does not neglect genes with insignificant changes when calculating enrichment, to examine antibiotic resistance, and was the first to use GSEA on *Staphylococcus aureus* (*S. aureus*). Further, I was the first to apply a new computational approach using GSEA that defines and compares pathway signatures (*i.e.*, pathway lists ranked by activity as defined by differential mRNA (*i.e.*, gene) expression) to detect activity changes associated with antibiotic resistance. I applied my pathway signature approach to multiple resistance studies across different antibiotic classes to identify pathways affecting development of antibiotic resistance, which was the first analysis of its kind to the best of my knowledge. Finally, I experimentally established biological relevance for one of the top pathway candidates identified from my computational approach.

## 1.1 Background on Antibiotic Resistance

Bacteriology, the study of bacteria, is one area of biological exploration where mRNA expression data is used extensively, but with limited benefit to humanity's overall understanding of cellular processes, such as antibiotic resistance which was the focus of this work. Bacteria are an entire taxonomy domain of single-celled microorganisms that are found in most habitats on Earth including soil, water, and within and on humans[3]. Researchers estimate there is at least one bacterium for every human cell in the body[4]. Bacterial species associated with humans have either a mutualist (beneficial) or commensal (neutral) relationship with us, while some bacteria are pathogens (harmful to

human health)[3]. Bacterial pathogens cause an average of nearly 14 million infections annually[5]. While much scientific attention is given to true pathogens that can cause disease in healthy individuals, such as *Yersinia pestis* (causative agent of bubonic plague), opportunistic pathogens that cause disease in immunocompromised people, such as *Pseudomonas aeruginosa* (common cause of burn infections), are bigger public health concerns because they already inhabit most humans in commensal relationships, waiting for the human immune system to decline before establishing infection[3,6]. For this reason, opportunistic pathogen infections are an ongoing clinical challenge[7].

To treat infections of true (*i.e.*, able to cause infection in healthy humans) and opportunistic pathogens clinically, antibiotics are useful therapeutic agents[3]. Antibiotics have been used for decades as the primary treatment and prevention method for a wide variety of communicable diseases and endogenous infections[8-11]. Over 70 billion antibiotic doses are consumed worldwide every year[1,12] which save millions of lives[11]. Table 1 lists antibiotics commonly prescribed for bacterial infections, grouping them by their mechanisms of action. Cell wall synthesis inhibitors are preferred for treating gram positive infections, like those caused by *S. aureus*, because they target exposed peptidoglycan, a polymer consisting of amino acids and sugars that form a mesh-like layer unique to the bacterial cell wall[3]. On the other hand, gram negative bacteria have an outer membrane protecting their peptidoglycan layer from the outside environment. Thus, for gram negative bacteria, protein synthesis inhibitors are preferred since the ribosomal subunit size is different between bacteria and humans. Both bacteria and humans have similar cell membrane structure, nucleic acid and folate synthesis processes, thus antibiotics that target these cellular components are less desirable[3].

Table 1. Antibiotics Commonly Used to Treat Bacterial Infections

| Mechanism of Action[a,b] | Group | Example Antibiotics[b,c,d] |
|---|---|---|
| Cell wall synthesis inhibitors | β-lactams | Penicillin (*e.g.*, methicillin, oxacillin, and flucloxacillin) |
| | | Cephalosporin (*e.g.*, ceftobiprole) |
| | Glycopeptides | Vancomycin |
| Protein synthesis inhibitors | 30S ribosomal subunit | Aminoglycosides (*e.g.*, kanamycin) |
| | | Tetracycline |
| | 50S ribosomal subunit | Macrolides (*e.g.*, erythromycin) |
| | | Glycylcyclines (*e.g.*, tigecycline) |
| | | Oxazolidinones (*e.g.*, linezolid) |
| | | Lincosamides (*e.g.*, clindamycin) |
| Cell membrane depolarizers | Lipopeptides | Daptomycin |
| | | Polymyxin (*e.g.*, colistin) |
| Nucleic acid synthesis inhibitors | Quinolones | Ciprofloxacin |
| Folate synthesis inhibitors | Sulfonamides Trimethoprims | Trimethoprim-sulfamethoxazole |

[a] Madigan, M.T. Et al.[3]
[b] Kapoor, G. Et al.[13]
[c] Pantosti, A. Et al.[14]
[d] Velkov, T. Et al.[15]

Unfortunately, antibiotics are losing their efficacy (*i.e.*, clinical treatment failure) due to the rapid emergence of antibiotic resistant infections[11,16], a problem regarded as one of the 21st century's major public health concerns by the World Health Organization[8,9,11,17-19]. In the United States alone, almost two million Americans contract hospital acquired infections, resulting in 99,000 deaths annually and most of these infections involved antibiotic resistant pathogens[11,20]. Resistant pathogens are not limited to clinical-based infections. They are prevalent in the community with over 53 million people worldwide possibly who are colonized unknowingly with resistant pathogens, posing as a potential risk to self and others[21,22]. As resistance spreads, predictions of up to 10 million deaths per year worldwide from antibiotic resistant infections by 2050 have been reported[23]. Besides prolonged hospital stays[11,20], increases in mortality rates[11,20],

long-term disability rates[11], and hospitalization for patients[24,25], resistant infections substantially increase medical costs per patient[11,26] resulting in significant economic and societal costs[21,24,27-29]. The estimated annual total economic burden to the United States economy is $20 billion in health care costs and $35 billion in lost wages[11,20]. Finding ways to more effectively treat antibiotic resistant infections is critical to improving patient outcomes and relieving an already overburdened healthcare system[11].

Of particular concern is antibiotic resistant *S. aureus*, an opportunistic Gram-positive bacterial pathogen that causes a varied assortment of infections including superficial skin and surgical wound infections, bone and joint infections, food poisoning, toxic shock syndrome, pneumonia, endocarditis, and bacteremia[14,21,30,31]. During the pre-antibiotic era, prior to the discovery of penicillin, *S. aureus* patients with bacteremia had a mortality rate of more than 80%[21,32]. The introduction of penicillin and subsequent antibiotics dramatically improved patient prognosis[21,33]. All *S. aureus* isolates were sensitive to penicillin when first introduced in the early 1940s. However, now more than 90% of human *S. aureus* isolates are penicillin resistant[14,21,31]. Methicillin, a semisynthetic penicillin derivative, was originally designed in 1959 to overcome the spread of penicillin resistance[21,31]. However, methicillin resistant *Staphylococcus aureus* (MRSA) isolates were found the following year[21,34] and today MRSA is a serious threat to public health[11]. MRSA is the second most common cause of bloodstream infections worldwide and the most common cause of infective endocarditis in the developed world[35-37]. The Center for Disease Control and Prevention in 2011 estimated 80,000 invasive MRSA infections and 11,285 related deaths in the United States (around 15% mortality rate)[21,38]. As seen in other bacteria, MRSA infections among the general

population (*i.e.*, community-acquired) have steadily increased during the past decade[11], resulting in *S. aureus* strains that now exist with resistance to one, two, or more (*i.e.*, multi-drug resistant, MDR) antibiotics[11,21,39,40]. It will not be long before there is an untreatable strain of *S. aureus*[41] as is already seen in other infectious bacterial species such as *Acinetobacter spp.* and *Klebsiella pneumoniae*[42,43].

Several antibiotic resistance mechanisms have been elucidated.

Table 2 summarizes resistance mechanisms employed by *S. aureus* and other bacterial species. High-level, sudden onset antibiotic resistance typically involves the procurement of a detectable genetic marker such as a chromosomal mutation or externally-acquired genes that deactivate the antibiotic, often by physical alteration of the antibiotic or its target[3,14,21,44,45]. Further, efflux pumps that remove antibiotics from the cell, preventing them from reaching their targets, have been found across bacterial species and commonly contribute to multi-drug resistances of antibiotics across all mechanisms of action[44,46-50]. Multi-drug resistance can also arise from accumulation of several externally-derived genes and/or chromosomal mutations, each encoding resistance to a particular antibiotic[51]. However, genetic markers are not consistently found in multi-drug and low-level (*i.e.*, intermediate) resistances, presenting a challenge for treatment management[14,44,45].

Table 2. Overview of Antibiotic Resistance Mechanisms

| Group[a] | Mechanisms of Resistance |
|---|---|
| β-lactams | • Acquire penicillinase to cleave β-lactam ring to inactive it[b,c]<br>• Mutate penicillin binding proteins so β-lactam ring cannot bind[b,c] |
| Glycopeptides | • Mutate cell wall so glycopeptides cannot bind[b,c,d] |
| 30S ribosomal subunit | • Mutate 30S subunit so drug cannot bind[e] |
| 50S ribosomal subunit | • Modify methylation of ribosome to inhibit drug binding[f]<br>• Mutate 50S subunit so drug cannot bind[b] |
| Lipopeptides | • Increase voltage difference across the membrane[b,g]<br>• Mutate membrane proteins that bind drug[g] |
| Quinolones | • Mutate DNA gyrase and/or topoisomerase IV[b,h] |
| Sulfonamides | • Mutate dihydropteroate synthase[b]<br>• Use alternative pathways of folate synthesis[b] |
| Trimethoprim | • Mutate dihydrofolate reductase[b]<br>• Use alternative pathways of folate synthesis[b] |

[a] Madigan, M.T. Et al.[3]
[b] Pantosti, A. Et al.[14]
[c] Peacock, S.J. Et al.[21]
[d] Gardete, S. Et al.[45]
[e] Chopra, I. Et al.[47]
[f] Quiles-Melero, I. Et al.[52]
[g] Tran, T.T. Et al.[53]
[h] Hooper, D.C. Et al.[48]

Low-level resistances frequently arise from "persister" cells that survive antibiotic exposure and are common in reoccurring infections. Unlike high-level resistant species which can flourish in the presence of antibiotic, "persister" cells grow after antibiotic treatment has stopped[44]. Persistence has been observed in most bacterial species, particularly for slow growing pathogens such as *Mycobacterium tuberculosis* (causative agent of Tuberculosis) that require months of antibiotic therapy with a high risk of patient non-compliance[44]. Mechanisms used by "persister" cells are not well understood, particularly since a small percentage of any bacterial population exists in a transient state of resistance meaning "persister" cells may have temporary resistance[54]. Despite producing similar antibiotic resistant phenotypes, there is considerable diversity in which

gene mutations are accumulated across resistant bacterial species and resistant strains of the same species[55,56]. While gene mutation studies provide useful information such as the effects of mutation on gene expression, a pathway-centric perspective using GSEA can identify pathway contributions to antibiotic resistant phenotypes, which complements scientific understanding of how variations in accumulated gene mutations contribute to the development of antibiotic resistant bacteria[44].

## 1.2 Statement of the Problem

Despite science's understanding of antibiotic resistance mechanisms, humanity struggles to control *S. aureus* and other bacterial infections. Due to increases in the global spread of resistant infections like MRSA[18] and their development into MDR strains in recent decades[11], there is a need for new antibiotic therapy options, either with different mechanisms of action than those currently in use[57] or that suppress existing resistance mechanisms to make current therapies useful again[58]. Not having these options will cause significant economic and medical hardships.

Targeting changes in pathway activities to overcome antibiotic resistance has shown promising preliminary outcomes[44,59-62]. Researchers have been able to restore vancomycin efficacy in resistant *S. aureus* by inhibiting amino sugar and purine biosynthesis[59], combine cysteine or other small thiols with rifampicin or isoniazid to kill "persister" and fully resistant *Mycobacterium tuberculosis*[62], and use exogenous alanine, glucose, or glutamate to restore kanamycin function in *Edwardsiella tarda* and *Escherichia coli* (causative agents of gastrointestinal distress)[60,61]. Continued exploration into pathway activity can provide new co-therapy options for antibiotic resistant infections.

Pathway activity can be inferred from observing differential changes in mRNA expression. Statistical methods, such as pathway enrichment analysis, a common technique used for interpreting differentially expressed gene lists by comparing gene list membership to memberships of known pathways individually[63], have been used to identify pathways involved in antibiotic resistance. However, most pathway enrichment analysis methods are complicated by selection methods for gene list membership and do not consider all pathway activities simultaniously[64-69]. GSEA improves upon these methods by removing the gene selection requirement. Further, by using pathway signatures to detect activity changes across all well-established pathways, scientists can get a higher-level vantage of cellular processes that contribute to resistance. Pathway-centric computational approaches, like the one proposed here, can improve how mRNA expression is used to interpret pathway activity changes associated with antibiotic resistance. When applied to mRNA expression datasets examining resistant and sensitive strains, my computational approach could identify pathway targets useful for the development of novel co-therapeutic options to clinically combat the worldwide antibiotic resistance problem. Without these advancements, antibiotic therapy will continue regressing into a post-antibiotic era where common infections, minor injuries, and surgeries, once again threaten the lives of billions of people worldwide[11,70].

## 1.3 Goal and Aims of the Study

The overall goal of this study was to elucidate molecular changes associated with antibiotic resistance in *S. aureus* through computational mRNA expression and biological pathway activity analyses to identify targetable pathways for co-therapeutic development to overcome antibiotic resistance. To do this, I applied a computational approach that

uses GSEA to define and compare pathway signatures from *S. aureus* mRNA expression datasets that examine 1) mutation-driven resistance (*i.e.*, comparison of resistant and sensitive *S. aureus* under the same treatment condition to identify the contributions of known or established mutations to loss of antibiotic sensitivity)[56,71-76], 2) antibiotic response (*i.e.*, comparison of *S. aureus* with and without antibiotic treatment, regardless of strain resistance level)[77], and 3) antibiotic susceptibility (*i.e.*, difference in treatment response between resistant and sensitive strains) to accomplish the following aims:

- Aim 1: Identify pathway activity changes associated with mutation-driven resistance
- Aim 2: Identify pathway activity changes associated with vancomycin susceptibility
- Aim 3: Compare pathway activity changes associated with mutation-driven resistance to pathway activity changes associated with vancomycin, oxacillin, and linezolid susceptibilities and responses

I used my approach to identify and confirm inferred pathway activity changes associated with mutation-driven resistance, and antibiotic susceptibility and response in *S. aureus*, focusing around vancomycin because of its alarming treatment failure rate clinically[11,56]. Pathway activity changes identified for mutation-driven resistance were then compared to changes associated with susceptibility and response to one of three antibiotics individually (vancomycin, oxacillin, or linezolid) in both sensitive strains and strains with varying resistance levels. The purpose of this analysis was to identify pathway activity changes occurring via selective pressures from antibiotic exposure[56,78-81] that potentially contribute to developing resistance in sensitive strains. These changes

have the potential to restore antibiotic sensitivity if used as a co-therapeutic target. The outcome of this work could demonstrate a path to improve clinical outcomes by predicting valuable pathway targets for co-therapeutic options to preclude or overcome antibiotic resistance in *S. aureus*. Further, my approach is directly applicable to other antibiotic resistant bacterial species and could be instrumental in predicting antibiotic co-therapies targeting pathway activity changes that can be used to restore the efficacy of current antibiotic therapies.

# CHAPTER 2

# REVIEW OF LITERATURE

This work applied a new computational approach based on pathway signatures using Gene Set Enrichment Analysis (GSEA) to analyze mRNA expression data to determine changes in pathway activities associated with antibiotic resistance in *S. aureus*. This chapter begins with the specifics of known antibiotic resistance mechanisms for vancomycin, oxacillin, daptomycin, and linezolid. I then detail the GSEA algorithm/software[67] used in this work and include a discussion of its benefits and challenges. This chapter concludes with an overview of popular pathway databases commonly used in pathway enrichment analysis with a discussion on which databases were best to use in my study.

## 2.1 Review of Experimentally Recognized Antibiotic Resistance Mechanisms

This section is a review of antibiotic resistance mechanisms in *S. aureus* as they pertain to my study. Since vancomycin and oxacillin are cell wall synthesis inhibitors, I begin with a brief review of cell wall construction for gram positive bacterial species like *S. aureus*. The cell wall is an important cellular structure located outside of the cytoplasmic membrane that maintains cell shape and internal osmotic pressure[82]. Bacterial cell walls contain peptidoglycan (PTG), which is unique to bacterial species, making them excellent targets for antibiotic therapies[3,56,82,83]. PTG is comprised of strands of alternating glycan sugars, N-acetyl glucosamine (NAG) and N-acetyl muramic acid (NAM), crosslinked by amino acid bridges, forming a complex, thick, rigid, three-dimensional layer that surrounds the entire cell[3,82]. The enzyme, transpeptidase, creates these crosslinks by binding to the D-Alanine:D-Alanine (D-Ala: D-Ala) ends of NAM

molecules (Figure 1). Cell wall synthesis inhibitors, such as penicillin, oxacillin, methicillin, and vancomycin, prevent transpeptidation resulting in a weak peptidoglycan layer[3,82]. Penicillin and its derivatives, oxacillin and methicillin, use their β-lactam ring structures to bind transpeptidase, thus preventing transpeptidase binding to D-Ala:D-Ala ends for cross-linkage (Figure 1)[3,83]. Vancomycin binds to D-Ala:D-Ala ends causing steric hindrance, preventing the transpeptidase from binding and inhibiting cross-linkage (Figure 1)[14,19,83]. Disrupting cell wall formation stalls bacterial growth or invokes cell lysis, thus killing *S. aureus* cells[3,19,83].

Daptomycin is a cell membrane disrupter that upsets the electrical potential all cells produce across their cell membrane that is driven by a charged ion concentration gradient. Daptomycin does this by using calcium to insert itself by anionic phospholipid phosphatidylglycerols, a common component in cell membranes, then oligomerizing before translocating throughout the cell membrane to form an oligomeric pore resulting in ion leakage and dissipation of cell membrane potential (Figure 1)[84-86]. Losing the tight control of ion flux that generates cell membrane potential radically alters cellular osmotic pressure, often producing lethal consequences for the cell.

Linezolid is a protein synthesis inhibitor. Protein synthesis inhibition hinders protein production for essential cellular metabolic machinery and structural components, leading to issues with all cellular processes leading to cell death[3]. Protein synthesis requires the formation of a ribosomal complex consisting of a large and small ribosomal subunit sandwiched around mRNA[3]. Linezolid specifically binds to the peptidyl transferase site of the large ribosomal subunit (50S), physically inhibiting formation of the initiation complex (Figure 1)[87-89]. Established resistance mechanisms for all

antibiotics discussed here including linezolid circumvent these processes and are discussed in the remainder of this section.

Figure 1. Bacterial cell wall synthesis and mechanism of action of antibiotics commonly used to treat *S. aureus* infections: oxacillin, vancomycin, daptomycin, and linezolid

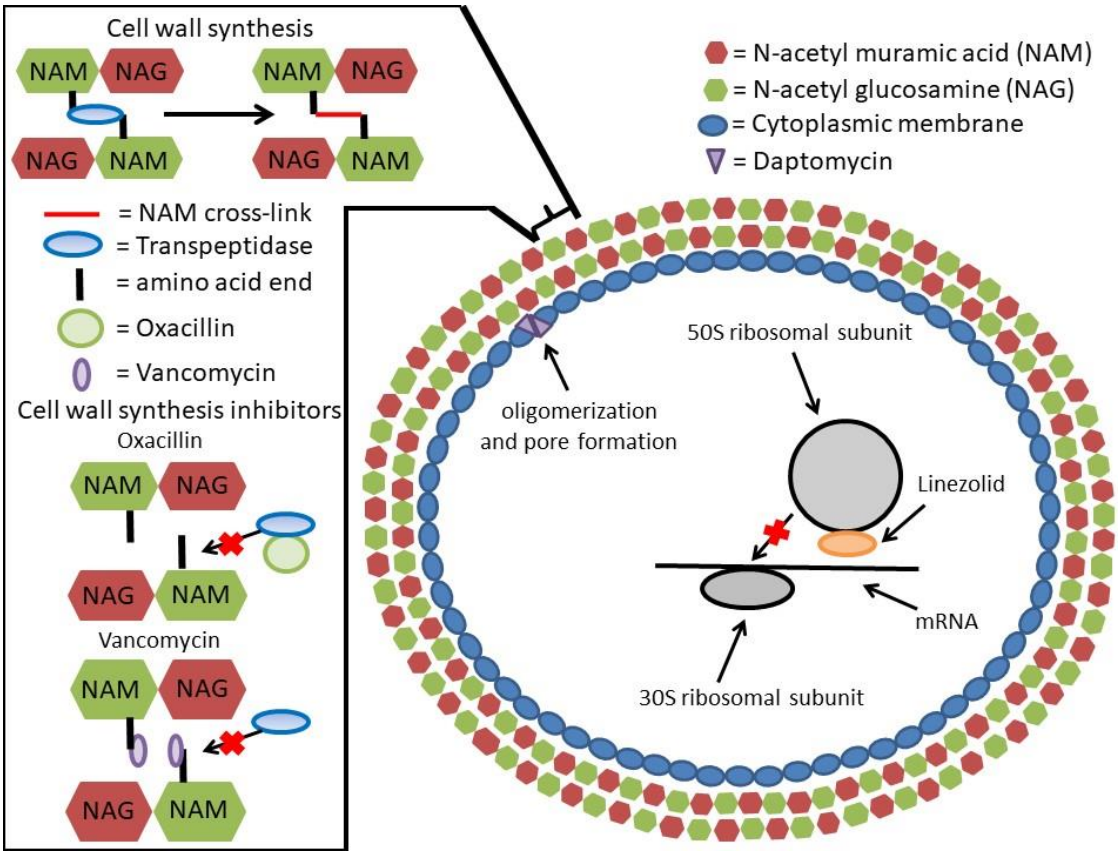


Cell walls are composed of alternating N-acetylmuramic acid (NAM, red hexagon) and N-acetyl glucosamine (NAG, green hexagon) sugar layers to form peptidoglycan. Transpeptidase (blue oval) cross-links (red line) NAG-NAM sugar layers by the amino acid ends (black line) of NAM sugars to give peptidoglycan in bacterial cell walls rigidity from osmotic pressure. Cell wall synthesis inhibitor antibiotics inhibit peptidoglycan formation. Oxacillin (green circle) acts by binding to transpeptidase so it cannot bind NAM ends (red X) to form cross-links. Vancomycin (purple oval) attach to amino acid ends, preventing transpeptidase binding and cross-link formation. Daptomycin (purple triangle) inserts its itself into the cytoplasmic membrane (dark blue oval) leading to oligomerization and eventually pore formation that disrupts membrane integrity. Linezolid binds to 50S ribosomal subunits (gray circle), inhibiting it from binding 30S

ribosomal subunits (gray oval) and preventing translation complex formation around messenger ribonucleic acid (mRNA, black line). Without the ability to produce proteins, cellular processes slow to a halt leading to death.

### 2.1.1 Vancomycin Resistance

Vancomycin resistance in *S. aureus* uses one of two different mechanisms[90]. Vancomycin resistant *Staphylococcus aureus* (VRSA) infections are characterized by high-level minimum inhibitory concentration (MIC) of ≥16mg/L, sudden-onset resistance that arise from acquisition of the Tn*1546* transposon from a vancomycin-resistant enterococci plasmid during a mixed infection with MRSA[14,56,81,83]. VRSA is marked by *van* operon, a group of 7 genes that produce modified peptidoglycan precursors containing a terminal D-Ala:D-Lac instead of D-Ala:D-Ala while also eradicating susceptible wild-type D-Ala:D-Ala ends[14,56,81]. Vancomycin has a much lower affinity for the D-Ala:D-Lac ends than the wild-type D-Ala:D-Ala ends[14,56,81], thus conveying the observed resistance phenotype. Fortunately, VRSA infections are rare with only 14 isolates reported in the United States by 2016[56,91].

Vancomycin intermediate *Staphylococcus aureus* (VISA) infections are of greater clinical concern with incidences of VISA infections steadily increasing and death tolls in the tens of thousands annually[56,59]. VISA infections lack the *van* operon and are usually associated with low-level resistance (MIC 2-8mg/L)[56,92], persistent infection, long hospitalizations, and prolonged or failed vancomycin treatment[56]. They commonly develop in MRSA patients treated with vancomycin for an extended period of time[82], resulting in altered physiology and metabolism to sustain growth during vancomycin exposure[59,93]. Thickened cell walls that are high in uncross-linked peptidoglycan chains with the D-Ala:D-Ala ends are associated with intermediate resistance[14,94,95]. Evidence

suggests overproduction of the D-Ala:D-Ala ends in thickened cell walls act as decoys blocking vancomycin in external layers and diverting it from reaching its intended targets[14,96]. With continued exposure, the cell wall clogs with trapped vancomycin, further hindering vancomycin effectiveness and leading to the development of full vancomycin resistance[14,97]. VISA is usually preceded by an intermediate phenotype, heterogenous VISA (hVISA), where the infection is a mixed population of sensitive (MIC $\leq$2mg/L) and resistant (MIC $\geq$4mg/L) cells[56]. This makes VISA and hVISA infections difficult to detect due to the low vancomycin doses needed for testing despite variations in testing methods (*i.e.*, E-strip, broth dilution)[56]. Further, VISA and hVISA infections can enter a transient resistance state like other bacterial "persister" infections, which is thought to be controlled by ATP depletion triggering entrance into the stationary growth phase where cells become metabolically dormant and do not divide[54,56,98], making them difficult to treat and resulting in frequent reoccurring infections. Taken together, it is easy to see why VISA infections are worrisome clinically.

Further, the mechanisms behind the development of VISA resistance are not completely understood[14]. VISA isolates share phenotypic characteristics, such as thickened cell wall, but there is substantial variation across strains in how these traits are produced (*i.e.*, types and number of genes mutated and specific mutations used)[59,99]. Table 3 summarizes genes associated with VISA. Most genes associated with VISA are part of the "cell wall stimulon"[100]. Researchers theorize that resistance develops from a series of step-wise gene mutations[14,56], and the majority of mutations has become associated with certain *S. aureus* lineages[101,56]. For example, several nonsynonymous single-nucleotide polymorphisms associated with VISA phenotype are part of two- and

three- component regulatory systems, such as *graRS*, *vraTSR* and *walKR*, which alter expression of over 100 cell wall biosynthesis, including genes required to produce D-Ala:D-Ala ends[56,59,72,100,102-104]. Over 40 of those genes, termed the "cell wall stimulon", are controlled by *vraSR*, resulting in cell wall synthesis when induced by cell wall damage. Alternatively, active *walKR* controls expression of autolysins, which are proteins needed for cell wall turn-over during division. In vancomycin sensitive strains, *vraSR* remains inactive since it does not detect cell wall damage during vancomycin exposure while *walKR* continues to be active to support cell division, the combination resulting in cell lysis. Further, when the cationic antimicrobial peptide (CAMP) switch, *graSR*, is activated it suppresses *walKR* expression and induces activity of over a dozen cell wall synthesis genes, such as *vraFG*, *vraDE*, *mprF* and *dltABCD*, that overlap and complement "cell wall stimulon" activity. Mutations that cause the over-expression of *vraSR*, *graSR*, and/or several of the cell wall synthesis genes they control (*e.g.*, *mprF*), and/or under-expression of *walKR* result in increased cell wall thickness and decreased cell division (*i.e.*, slow growth), the classic VISA phenotype[45,56,73,74,105-107]. Further, seemingly unrelated mutations that down-regulate activity of global regulators, such as *rpoB* which encodes the RNA polymerase β-subunit, are linked to VISA phenotype (*i.e.*, increased cell wall thickness)[45,56,108-112]. This demonstrates the complexity of identifying consistent genetic markers behind VISA development and highlights the need for an additional perspective.

Table 3. Genes Associated with VISA Phenotypes

| Phenotype | Genes | Role in VISA Phenotype |
|---|---|---|
| Cell wall thickening and reduced autolytic activity | *graRS* | Up-regulates over 13 genes including *vraFG*, *vraDE*, capsule operon, *mprF*, *dltABCD*, *fmtC*, *mgrA* and *rot*, down-regulates *walKR* and *agr*, and is associated with nucleotide metabolism |
| | *pbp4* | Reduced rates of peptidoglycan cross-linking and transpeptidation |
| | *sarA* | Reduced production of autolysins responsible for cell wall recycling |
| | *mgrA* | |
| | *clpP* | Cell wall thickening, slow growth, and reduced autolysis |
| | *stp1* | |
| | *walKR* (*yycFG*) | Limited *walKR* activity lowers rates of autolysis and increases cell wall thickness |
| | *yycH* | Lowered expression of autolysis genes |
| Up-regulated cell wall stimulon | *vraSR* | Associated with reduced vancomycin susceptibility, up-regulates 40 cell wall stimulon genes including *vraFG* and *mprF* |
| | *vraFG* | Associated with reduced vancomycin susceptibility |
| | *prsA* | |
| | *isdE* | |
| | *fmtC* (*mprF*) | Increased net negative charge of cell wall and reduced peptidoglycan cross-linking |
| | *spoVG* | Increased capsule production |
| | *capA-capP* | |
| Down-regulated global regulators | *arg* | Attenuation of virulence and reduced vancomycin susceptibility |
| | *rot* | |
| | *rpoB* | Associated with reduced vancomycin susceptibility |
| | *rsbU* | |
| | *yjbH* | |
| | *vraT* (*yvqF*) | Up-regulates *vraSR*, reduced vancomycin susceptibility |
| Decreased Production of Virulence Factors | *sbi* | Altered IgM binding |
| | *spa* | Observed alterations in opsonization and phagocytosis |

**Source**: Adopted From McGuinness WA, Malachowa N, DeLeo FR (2017). Vancomycin Resistance in *Staphylococcus aureus*. Yale Journal of Biology and Medicine, 102(43), pp.269-281[56,99,102,113,114].

Researchers are looking at pathway activity in VISA isolates experimentally to better comprehend resistance mechanisms and find links between reversable alterations in the core metabolism of *S. aureus* and VISA phenotype[107]. Changes in acetate catabolism

due in part to reduction of tricarboxylic acid (*i.e.*, Kreb's, citrate, TCA) cycle are associated with VISA phenotypes[59], suggesting *S. aureus* may use a variety of metabolic changes to develop vancomycin resistance. Increases in wall teichoic acid and peptidoglycan precursor biosynthesis, urea cycle, arginine metabolism, nucleotide metabolism[56] such as purine biosynthesis, and carbon flow through the pentose phosphate pathway are associated with VISA phenotypes[59,107]. This highlights the importance of examining pathway changes to fully understand developing vancomycin resistance mechanisms.

### 2.1.2 Oxacillin Resistance

Researchers have characterized two mechanisms *S. aureus* uses to resist β-lactam antibiotics (*i.e.*, penicillin and its derivatives). Initial penicillin resistance occurred through acquisition of the plasmid-borne *bla* operon, which contains an extracellular enzyme, β-lactamase, that inactivates β-lactams by hydrolyzing their β-lactam rings so they can no longer bind transpeptidase[14]. Methicillin and other next generation β-lactams (*e.g.*, oxacillin and flucloxacillin) have a semi-synthetic penicillinase-resistant β-lactam ring[14]. MRSA is characterized by high-level resistance (MIC >2mg/L) that is associated with acquisition of the plasmid-borne *mec* operon that encodes a mutated transpeptidase that lacks β-lactam affinity[14,19,31]. Most cases of β-lactam resistance clinically are MRSA, though occasionally β-lactam resistant strains lacking the *mec* operon arise from chromosomal mutations that alter transpeptidase affinity for β-lactam antibiotics[21]. Regardless, oxacillin resistance is relatively well characterized at the genetic level compared to resistance to other antibiotics.

### 2.1.3 Daptomycin Resistance

Despite being a cell membrane disrupter rather than a cell wall synthesis inhibitor antibiotic, daptomycin resistance (MIC >1mg/L) often presents in MDR *S. aureus* strains alongside VISA phenotypes with several genes implicated across antibiotic resistance[84-86]. The most frequently described mutation associated with daptomycin resistance is in *mprF*. For daptomycin resistance, *mprF* that encodes an enzyme that attaches lysine to phosphatidylglycerol, thus conferring resistance by reducing binding of daptomycin to bacterial membranes. However, mutations in *mprF* are also associated with VISA phenotypes[56] due to its role in cell wall synthesis under the direction of VISA regulator genes like *graSR*, *vraSR* and *yycFG* (also known as *walKR*)[53,115]. Evidence in MRSA strains suggest that *mprF* mutations conferring daptomycin resistance are also associated with over-expression of *vraSR*, and inactivation of *vraSR* alone can increase daptomycin sensitivity[71,72]. Recent work has shown a single missense mutation in *mprF* can confer resistance to daptomycin and vancomycin while improving oxacillin susceptibility[104]. Further, mutations associated with VISA in genes that are not directly related to cell wall synthesis, such as *rpoB*, have been implicated in daptomycin resistance. The diverse and often interconnected MDR mechanisms used by *S. aureus* to overcome daptomycin therapy impedes clinical treatment and further supports the need to examine antibiotic resistance from a broader pathway activity perspective.

Interestingly, daptomycin has structural similarities to cationic antimicrobial peptides (CAMPs) made by the mammalian innate immune system from which polymyxin antibiotics like colistin (*i.e.*, polymyxin E) are derived[86,116,117]. Colistin is commonly used as a last option, due to human toxicity issues, to treat gram negative

MDR infections[118,119]. Unfortunately, *S. aureus* has an intrinsic resistance to polymyxins in part because of their affinity for lipopolysaccharide (LPS) which is not found in gram positive bacteria[15,117,120]. However, genes associated with daptomycin resistance, such as *mprF* and *graSR*, are also associated with intrinsic resistance to CAMPs in *S. aureus*, leading researchers to question the overlap of resistance mechanisms[76,116].

### 2.1.4 Linezolid Resistance

Rarely (<1% of clinical isolates), *S. aureus* infections develop resistance to linezolid (MIC >4mg/L). One mechanism reported involves changing the large ribosomal subunit through a single nucleotide chromosomal mutation in the peptidyl transferase site[14]. *S. aureus* has around five ribosomal RNA encoding genes and three ribosomal proteins L3, L4 and L22, encoded by *rplC*, *rplD* and *rplV* genes, respectively, have been linked to linezolid resistance[52,87,121-123]. Researchers theorize that linezolid resistance arises from multiple ribosomal subunit mutations, which accumulates based on selective pressure from linezolid exposure, likely in a gene-dosage effect (*i.e.*, as mutations accrue higher linezolid doses are required for successful treatment)[14,52,87,124,125]. Another way to acquire linezolid resistance is through a plasmid containing genes that confer cross-resistance to other protein synthesis inhibitors[87] . For example, the *cfr* gene that encodes a methyltransferase that modifies an adenosine in the large ribosomal subunit has been linked to resistance of phenicol, lincosamide, oxazolidinone, pleuromutilin and streptogramin A, commonly referred to as the PhLOPSA phenotype[87,126,127]. Also, linezolid resistance has been linked to acquiring the *lmrS* gene that encodes a major facilitator superfamily protein, an MDR efflux pump[49,128]. *S. aureus* uses a variety of mechanisms to develop linezolid resistance.

## 2.2 Review of Computationally Identified Antibiotic Resistance Mechanisms

While experimental examination has successfully identified several resistance mechanisms, substantial expertise and resources are needed to accomplish this, which slows clinical progress in treating resistant infections. Use of computational methods, such as gene expression and pathway enrichment analyses, can provide insight into biological processes, thus focusing experimental efforts and speeding clinical progress. Here, I added to the genome sequencing and mutational analysis just reviewed to discuss resistance mechanisms identified through gene expression and pathway enrichment analyses as they pertain to this work.

### 2.2.1 Documented Gene Expression Analysis Findings

Most gene expression studies, including those used in this work and described earlier, use gene expression analysis to report changes in individual differentially expressed genes identified through statistical comparison (*e.g.*, fold change threshold and/or T-test p-value). Several experimentally established resistance genes have been identified via gene expression analysis, including most of them finding confirmed experimentally that I discussed in the prior section[76,101,129]. For example, gene expression analysis in studies examining how *graSR* mutations affect antibiotic resistance in *S. aureus* have confirmed the association of *mprF* and the *dltABCD* operon with daptomycin and colistin resistance as determined by fold change ratio difference[76,129]. Another study using gene expression analysis found increased expression of VISA associated cell wall stress genes, *vraSR*, *vraFG*, *vraDE*, *fmtA*, *murZ*, and *tcaA*, were found in a high level vancomycin and low level daptomycin resistant strain as determined by fold change ratio difference[101], showing that computational gene expression analysis

can identify resistance mechanisms. Gene expression analysis can detect changes in operon expression if several genes in the same operon have similar changes, such as the *vra* operon in VISA (*vraSR*, *vraFG*, and *vraDE*). However, operon expression changes do not directly correlate with pathway activity changes as an operon can belong to multiple pathways[130,131]. For this, pathway enrichment analysis is needed.

### 2.2.2 Documented Pathway Enrichment Analysis Findings

For microbiological studies, Fisher's Exact Test or one of its variants is used to calculate the significance of enrichment between the generated gene list and individual pathways from a pathway knowledgebase. This analysis can be done at the time of gene expression analysis or can be performed post hoc on publicly accessible mRNA expression datasets. Few gene expression studies examining antibiotic resistance collect differentially expressed genes identified through statistical comparison to generate a gene list for pathway enrichment analysis. One such study performed pathway enrichment analysis on differentially expressed genes from gene expression data examining vancomycin resistant phenotypes (*i.e.*, sensitive and VISA strains, both untreated) using Kyoto Encyclopedia of Genes and Genomes (KEGG) pathways identified decreased expression of quorum sensing genes, supporting experimental findings that *agr*, an accessory gene regulator for a quorum sensing system plays a role in vancomycin resistance, and implicating the entire *arg* pathway in the VISA phenotype. This pathway enrichment analysis with KEGG also implicated some new pathways associated with vancomycin or linezolid susceptibility (*i.e.*, antibiotic treated versus untreated VISA strains), like increased glycine, serine, and threonine metabolism, and decreased quorum sensing[56,132]. KEGG has been further used in pathway enrichment analysis to identify

TCA cycle's role in vancomycin resistance, a finding which is leading to the development of new therapeutic co-targets[59]. In other antibiotics, pathway enrichment analysis of oxacillin resistance gene expression datasets using KEGG have found up-regulation of glycolysis, arginine biosynthesis, and TCA cycle and downregulation of pentose phosphate, amino acid and nitrogen metabolism pathways[133]. Pathway enrichment using FET also reported increases in β-lactam resistance pathway activity including over-expressed antimicrobial resistance proteins, VraF and VraG, in methicillin treated *S. aureus* biofilms and altered glucose metabolism regulation when MRSA was treated with water extract from *Galla chinensis*, a nontoxic Chinese herbal medicine thought to have antibacterial properties[134,135]. Unfortunately, there are no pathway enrichment analysis studies examining linezolid resistance in *S. aureus*, but pathway enrichment analysis using FET in other bacterial species, like *Enterococcus faecalis*, with both KEGG and Gene Ontology, another pathway knowledgebase, have identified changes in peptidoglycan biosynthesis, valine, leucine, and isoleucine degradation, and metabolic processes[136]. However, these pathway enrichment analyses using Fisher's Exact Test are limited because they compare gene list membership based on differential expression with a statistical cut-off to individual pathways, therefore not considering the entire genome from a pathway perspective.

The number of studies that use GSEA for pathway enrichment analysis in microbiology is minute, with only one study that examined macrolide resistance in *Streptococcus pneumoniae* that used GSEA to identify genes of interest between gene expression datasets then used FET to detect pathway enrichment in identified genes[137]. This *Streptococcus pneumoniae* study stated that a substantial percentage of GSEA-

identified genes using this approach had genome annotation issues (*i.e.*, hypothetical proteins), which limited the ability of their approach to detect pathway activity changes associated with resistance[137]. My work here used GSEA to generate pathway signatures, an improvement in pathway enrichment analysis compared to prior studies that have been performed 1) on *S. aureus* using FET, and 2) examining antibiotic resistance using GSEA in any pathogen.

## 2.3 Review of Gene Set Enrichment Analysis

My study utilized Gene Set Enrichment Analysis (GSEA)[67,138] , a method originally developed by Subramanian, et al., and a software provided by the Broad Institute. GSEA has been used extensively to examine alterations in human pathways, single nucleotide polymorphisms, and methylation patterns in cancer[67,139] and diabetes[138]. However, only a few microbial projects have used GSEA, primarily being applied to examine connections between viruses and cancer growth[66,140,141]. In this section I discussed in detail how GSEA works and its benefits and challenges compared to other methods used to select differentially expressed genes and compare them to known pathways.

### 2.3.1 Method and Software Implementation

The reader familiar with the GSEA software[67,138] may skip directly to section 2.3.2.

The overall objective of GSEA is to assess whether members of a gene set appear enriched at one end of the reference signature. GSEA software begins by creating a *reference signature*, which I defined as a list of items (probes, gene symbols, locus tags, or pathways) ranked in order of differential expression or activity from high to low. Using a phenotype label file, GSEA identifies which samples in expression dataset

correspond to which experimental group. It uses that information to calculate a user defined statistic, such as Welch T-test, for between two conditions (*i.e.*, untreated and treated) for each item. This statistical score represents how strong of a connection an item has to a phenotype. Items are then ranked in order of those statistical values from high to low, forming the *reference signature*.

GSEA then goes item by item through the reference signature, comparing each item to the *query gene set*, which is an unranked list of items (genes or pathways corresponding to the type of item in the reference signature) with knowledge-based biological relevance (*i.e.*, pathway or tail of a reference signature from another study). GSEA calculates a running-sum statistic, called the *enrichment score*, which represents the extent the query gene set is overrepresented at the top or bottom (*i.e.*, most extreme T-scores) of the reference signature. If an item in the reference signature matches an item in the query gene set (*i.e.*, hit), the enrichment score changes based on its ranking statistic value. The $P_{hit}$ equation is: $P_{hit} = \Sigma_{gj \epsilon S\ j \leq i} |r_j|^p / N_R$, where $N_R = \Sigma_{gj \epsilon S\ j \leq i} |r_j|^p$, $g_j$ is the item in the reference signature under consideration, S represents the query gene set, j is the position of the item being evaluated, i symbolizes the most recent position evaluated in the reference signature, $r_j$ is the item's ($g_j$) ranking score (*i.e.*, T-score), and p is 1. To consider the weight of each item based on its ranking score, p is set to 1. If p is set to 0, as is done in the Kolmogorov-Smirnov statistic, no consideration is given to the ranking score of each item. $N_R$ becomes a constant for each query gene set, calculated as the sum of the absolute value of ranking scores for all hits. If an item in the reference signature does not match any item in the query gene set (*i.e.*, miss), the enrichment score changes by a constant based on reference signature and query gene set defined as $P_{miss} = \Sigma_{gj \notin S\ j \leq i} 1 /$

($N-N_H$), where N is the number of items in the reference signature and $N_H$ is the number of items in the query gene set.

The *maximum enrichment score*, abbreviated ES(S), is the maximum deviation from $P_{hit}-P_{miss}$ to zero with the fewest number of reference signature items. Any hits located in that range are defined as *leading edge* items. Leading edge items are the core of the query gene set that contributes most to the enrichment signal. This is illustrated by the *enrichment plot* that GSEA produces (Figure 2).

Figure 2. Example Enrichment Plot

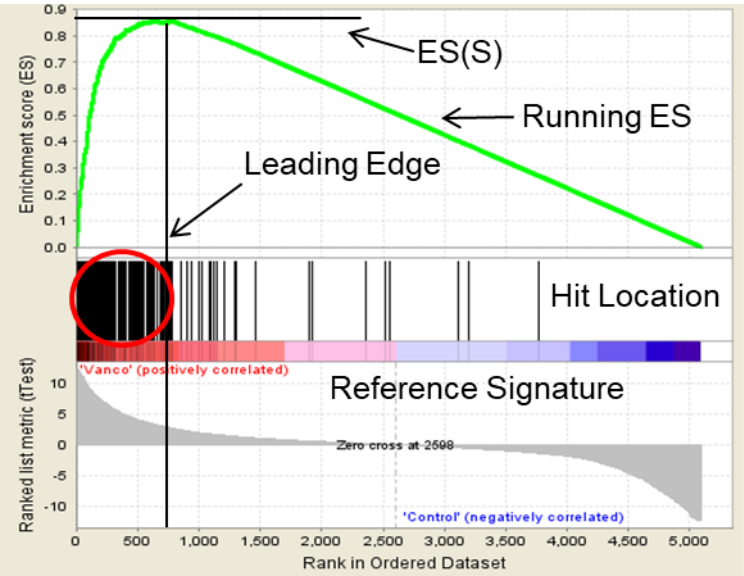


**Source:** Adopted From Subramanian A, Tamayo P, Mootha VK, Mukherjee S, Ebert BL, Gillette MA, Paulovich A, Pomeroy SL, Golub TR, Lander ES, Mesirov JP (2005). Gene set enrichment analysis: a knowledge-based approach for interpreting genome-wide expression profiles. Proceedings of the National Academy of Sciences, 102(43), pp.15545-15550[67].

Significance of the ES(S) is estimated through 1,000 iterations with permutations of items from the reference signature. A new ES(S) is calculated per iteration, designated ES(S,π) where π represents a number 1 to 1,000. The ES(S,π) from all iterations are

plotted to create a histogram (Figure 3), which represents a random distribution of scores. As a result, the *nominal p-value* is the true ES(S) compared to a random distribution of scores as calculated using nominal p-value = number of ES(S,π) ≥ ES(S) / number of ES(S,π) with the same sign as ES(S), where ES(S) is the true enrichment score and ES(S,π) is maximum enrichment score for any one of the 1000 iterations. The positive or negative portion of ES(S,π) that matches ES(S)'s sign (+/-) is used.

Figure 3. Example Histogram

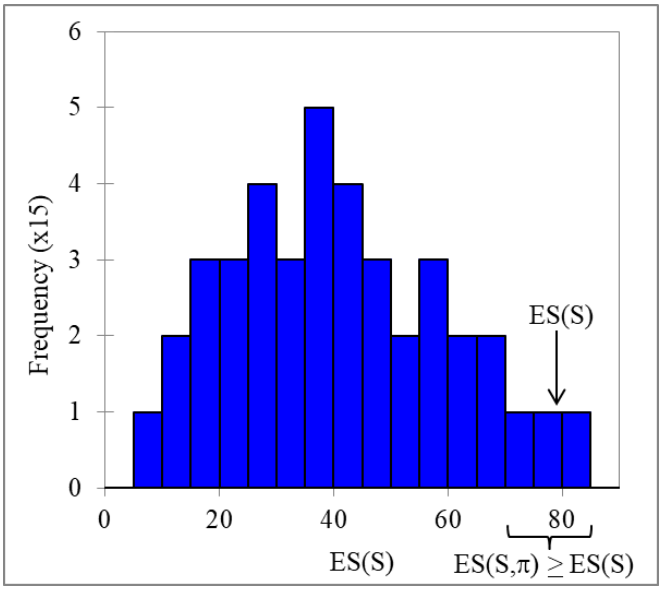


**Source:** Adopted From Subramanian A, Tamayo P, Mootha VK, Mukherjee S, Ebert BL, Gillette MA, Paulovich A, Pomeroy SL, Golub TR, Lander ES, Mesirov JP (2005). Gene set enrichment analysis: a knowledge-based approach for interpreting genome-wide expression profiles. Proceedings of the National Academy of Sciences, 102(43), pp.15545-15550[67].

To compare across multiple reference signatures and/or query gene sets, maximum enrichment scores are normalized. Particularly, using normalized enrichment scores (NES) helps remove the effect of different gene set sizes. The NES(S) formula is NES(S) = ES(S) / mean[ES(S,π) with the same sign as ES(S)], where ES(S) is the true enrichment score and ES(S,π) is maximum enrichment score for any one of the 1000

iterations. Similar to nominal p-value, the portion of ES(S,π) that is appropriate (+/-) to that particular ES(S) is used.

### 2.3.2 Advantages and Disadvantages of GSEA Compared to Other Methods

Compared to GSEA, Fisher's Exact Test (FET)[142,143] is predominantly used in microbiology for analyzing mRNA expression data because it is easy to perform and interpret with no special software or statistical understanding required[69]. FET determines if there are non-random associations between groups. Groups are often created by quantifying the interest of each gene, usually with a T-test or ANOVA p-value, then counting candidate genes that meet or fall short of an appropriate cut-off (*i.e.*, $p<0.05$)[69,144,145]. FET uses a 2x2 contingency table to compare the proportion of differentially expressed genes from a dataset found in and excluded from a pathway and proportion of pathway genes compared to the total number of genes in the database via and calculates a p-value using hypergeometric (*i.e.*, sampling without replacement) distribution. Results from FET can have substantial variation based on how differentially expressed genes are selected and its use on mRNA expression datasets has been criticized for 1) ignoring biological knowledge regarding how genes work together[144], and 2) being unable to detect significance in gene sets containing several members undergoing subtle expression changes[67].

Subramanian designed GSEA to overcome some of FET's shortcomings. By using query sets with an established biological relevance, GSEA results keep within a biological context[67]. GSEA is versatile in that query sets can be identified from various sources including biological pathways, chromosomal locations, computational analysis of genomic information, or signatures from other gene expression studies[67,146]. Further,

Subramanian and colleagues used human cancer datasets to show that GSEA is sensitive in identifying gene sets with several members undergoing subtle expression changes that are statistically insignificant individually via single gene methods (*i.e.*, T-test) yet may be significant collectively[67], since GSEA considers all genes in a dataset rather than those above a particular cut-off point. However, GSEA has its limitations[69,147]. It has been criticized for detecting gene sets without biological relevance (*i.e.*, false positive)[147,148] and its inability to distinguish gene sets with biological significance (*i.e.*, false negative)[149]. While other algorithms are available to improve GSEA's error rates, such as SAM-GS[147], Sub-GSE[149], and more recently AbsFilterGSEA[148], these programs are less readily available and user-friendly, so GSEA remains a popular software for analyzing mRNA expression data[67,138-141].

Comparison of GSEA and FET has produced varied results. Irizarry, et al., used the same human cancer datasets Subramanian and colleagues used to introduce GSEA[67,138] to compare GSEA to the $\chi^2$-test[144]. The FET and $\chi^2$-test both compare independent, not correlated groups to determine independence between two variables, though the $\chi^2$-test loses accuracy compared to FET because it assumes large sample sizes so it uses approximations[150]. Irizarry and colleagues showed that both GSEA and $\chi^2$-test identified the same gene sets as interesting, but GSEA had several false positives that favor small gene sets[144]. They recommended the use of the $\chi^2$-test over GSEA for this reason, in addition to the $\chi^2$-test being more user-friendly[144]. However, Abatangelo and associates used cancer expression datasets from human cell cultures and patient samples to find that GSEA is better than FET at detecting gene sets with subtle differences in the distributions of gene expression levels in a gene set between two phenotypic

conditions[151]. They praised GSEA for its ability to detect true distribution changes despite phenotypic differences being caused by a wide range of altered pathways, and did not observe GSEA's limitations[151]. Meanwhile, Tintle and his colleagues took an interest in GSEA for bacterial use, comparing it to FET on both simulation and real expression data from *Salmonella typhimurium* and *Escherichia coli*. They found FET lacked robustness and power compared to GSEA[69]. Tintle, et al., also saw that GSEA was overly sensitive to gene sets with few differentially expressed genes (*i.e.*, false positives), but they were unable to predict if this was an inherent flaw with GSEA software[147] or if adjusting the weight of GSEA's weighted K-S-like statistic for bacterial datasets would overcome this sensitivity issue[69]. Consideration for potential detection errors will be given when interpreting results from my *S. aureus* work here.

## 2.4 Overview of Pathway Databases

There are several publicly accessible databases that contain pathway information that can be applied to genes of interest. Subramanian and colleagues introduced the Molecular Signature Database (MSigDB)[152-154] when they introduced the GSEA software[67]. MSigDB now houses eight gene set collections with over 10,000 gene sets for various human genome characteristics and cellular processes, particularly cancer, metabolic, and immunological gene sets[154]. Reactome is a free, manually curated, peer reviewed pathway database, which contains 10,719 human genes which accounts for 53% of the 20,338 predicted human protein-coding genes[155,156]. Unfortunately, MSigDB and Reactome do not have gene sets for *S. aureus*.

Gene Ontology (GO) is a popular source of cellular information for bacteria[68,157,158] GO is a comprehensive knowledge base of gene functions and products

that was designed to unify the representation of genes and proteins across all species[159]. GO currently includes experimental findings from almost 140,000 published papers and it is often used as a part of the genome annotation process[157-159]. GO classifies gene functions along three aspects: molecular function (*i.e.*, molecular activities of gene products), cellular component (*i.e.*, where gene products are active), and biological process (*i.e.*, pathways and larger processes made up of the activities of multiple gene products). GO biological processes consist of multiple molecular activities and must have more than one distinct step[157,158]. GO provides easy, user-friendly enrichment analysis for gene lists of interest through collaboration with the Protein Analysis Through Evolutionary Relationships (PANTHER) Enrichment Analysis Tool[160].

For bacterial pathways, the Kyoto Encyclopedia of Genes and Genomes (KEGG) database is arguably regarded as one of the leading pathway databases in the field[68,159,161,162]. KEGG is an integrated database resource containing manually curated fifteen databases broadly categorized into three information categories: systems, chemical, and genomic[163]. The systems information category contains KEGG pathway and KEGG module databases. The KEGG pathway database consists of manually drawn pathway maps that represent current knowledge of molecular interaction, reaction, and relation networks for metabolism, genetic and environmental information processing, cellular processes, organismal systems, human diseases, and drug development. KEGG modules are an assortment of manually defined functional units used for biological interpretation and annotation of sequenced genomes. There are four types of KEGG modules: pathway modules, signature modules, structural complexes, and functional sets[163]. Pathway modules embody tighter functional units than KEGG pathways and are

therefore closer to actual biological pathways[163,164]. Signature modules include markers of phenotypes, which in the case of *S. aureus* are exclusively drug resistance gene sets. Structural complex modules contain genes that form molecular machineries. Any other type of essential gene set not previously categorized falls into the functional sets module category. KEGG does not have an easy, user-friendly way to perform enrichment analysis on a group of genes. External programs, such as Database for Annotation, Visualization and Integrated Discovery (DAVID), have been developed to provide an interface for KEGG pathway-based enrichment analysis[165,166].

A lesser known source for bacterial pathway information includes the SEED and its associate database, the Pathosystems Resource Integration Center (PATRIC)[167-169]. In 2005, the Fellowship for Interpretation of Genomes began the Project to Annotate 1000 Genomes, resulting in the SEED. Their initial data version in 2005 included 180,177 proteins with 2,133 different functional roles across 383 different organisms and the project has only expanded[167]. The SEED differs from other resources as it is based on expert curated groups of functionally related protein families (*i.e.*, subsystems) that span several diverse genomes whose annotations are computationally extended to new subsystem members rather than gene-by-gene annotation approaches employed by other resources[167]. This produces more accurate and faster annotations since experts in each subsystem oversee initial annotations that are applied across diverse genomes[167]. The SEED constantly assimilates different types of genomic data from a variety of sources, including KEGG[167,169]. In 2011, the SEED developers were commissioned by the National Institute of Allergy and Infectious Diseases to apply the subsystem approach to annotation to priority disease-causing microbial pathogens, such as *S. aureus*[168,170].

PATRIC, an organism-focused resource to provide scientists with genomic information for priority pathogens, was the result[168,170]. Like KEGG, PATRIC does not yet have a user-friendly interface for enrichment analysis nor do DAVID or many other external programs connect to it.

To explore these pathway database variations in bacteria, Tintle and his colleagues evaluated gene set consistency across pathway databases, including GO, KEGG, and the SEED, in 17 diverse bacteria including *S. aureus* Mu50 (MRSA/VISA) strain[68,171]. While KEGG had the least number of gene sets, it had the largest average gene set size[68]. Using their consistency metrics, differential expression, absolute expression, and correlation between expression values, they found GO was more consistent than KEGG gene sets, regardless of gene set size or organism differences, but the SEED was able to outperform both GO and KEGG in all consistency metrics[68]. I considered pathway database variations in my project, particularly since all knowledgebases have been extensively updated since Tintle's study several years ago (2012) including addition of antibiotic resistant pathways in KEGG's last update[162].

## 2.5 Conclusion

Gene mutation studies have revealed several mechanisms associated with individual and multiple antibiotic resistances, such as involvement of *vraSR* and *graSR* in daptomycin, vancomycin and oxacillin resistances. Examination of differential gene expression for individual genes can also find changes associated with resistances, such as increased expression of *vra* operon genes (*vraSR*, *vraFG*, and *vraDE*) associated with VISA. Pathway enrichment analysis using FET complements differential gene expression for individual genes by detecting pathway activity changes associated with antibiotic

resistances such as decreased TCA cycle associated with vancomycin intermediate resistance. FET is limited by its requirement to select a subset of genes for enrichment analysis. GSEA overcomes the limitations of this gene selection requirement by considering all genes rather than a subset. My innovative project was the first to apply GSEA to examine *S. aureus*. However, use of GSEA to examine antibiotic resistance in *Streptococcus pneumoniae* by comparing gene expression changes directly was limited by incomplete and inaccurate genome annotation[66]. To overcome this limitation, I used GSEA to define pathway signatures derived from comparing mRNA expression datasets containing *S. aureus* samples of antibiotic resistant and sensitive strains with or without antibiotic treatment to KEGG pathways. The overall goal of this analysis was to elucidate and verify experimentally pathway activity changes associated with antibiotic sensitivity.

# CHAPTER 3

# ANTIBIOTIC RESISTANCE IN *STAPHYLOCOCCUS AUREUS*

## 3.1 Background

*Staphylococcus aureus* (*S. aureus*) causes a wide variety of life-threatening infections[21,59]. Despite the discovery of a wide array of antibiotics[3,13,14], *S. aureus* infections are a public health threat due to increasing antibiotic resistance (*i.e.*, clinical treatment failure)[11]. The most serious is methicillin resistant *Staphylococcus aureus* (MRSA), which is resistant to the β-lactam class of antibiotics, like oxacillin and flucloxacillin[11,172], that inhibit cell wall synthesis by directly inactivating transpeptidase activity[21,172]. MRSA infections are commonly treated with vancomycin[82,90,173], a different kind of cell wall synthesis inhibitor that indirectly disables transpeptidase activity by binding to its target, D-alanyl-D-alanine carboxyl terminus of cell wall precursor molecules[45,59,174]. Yet, vancomycin treatment is losing favor due to increasing morbidity and mortality rates from resistant infections[175] and worldwide resistance prevalence[176]. In cases of vancomycin-resistant infections, the protein synthesis inhibitor linezolid is a preferred therapy[14,177,178]. However, clinicians have reported multifocal outbreaks of linezolid resistant *S. aureus*[52,87,179] with lethal consequences[174,180,181]. For linezolid resistant *S. aureus* infections, the cell-membrane-targeting lipopeptide daptomycin is a preferred therapy and while rare, daptomycin resistant infections are reported[86,116]. To complicate treatment options further, some *S. aureus* infections are caused by multi-drug resistant (MDR) strains[182]. Limited treatment options coupled with increasing mortality and continued spread of antibiotic resistant *S. aureus* infections have been major clinical challenges for infectious disease management[11,183].

Antibiotic resistant *S. aureus* infections are particularly troublesome clinically, in part because of an incomplete understanding of individual and shared resistance mechanisms. A good example of this is vancomycin resistance. Vancomycin resistant *Staphylococcus aureus* (VRSA) arises from acquisition of the *vanA* operon via horizontal transfer that replaces D-alanyl-D-alanine with D-alanyl-D-lactate carboxyl termini[56,78-81] resulting in sudden high-level (minimum inhibitory concentration ≥16mg/L) resistance. Vancomycin intermediate *Staphylococcus aureus* (VISA), which lacks the *vanA* operon, are associated with low-level (minimum inhibitory concentration 2-8mg/L) developing resistance[52,56,184,185] produced from a variety of gene mutations, particularly in cell wall synthesis genes like two-component switches, *graSR*, *vraSR*, and *walKR*, and the over 40 cell wall "simulon" proteins they directly influence, including *mprF*, *arg*, and the *dltABCD* operon[55,56,99,100,186], with no mutations being consistent across isolates unlike *vanA* operon found in all VRSA strains[55,56]. VRSA clinical isolates are also MRSA, which occurs through acquiring a mutated transpeptidase (*mecA*)[21,172], and maintain high level resistance to both vancomycin and methicillin. Some of these isolates also develop linezolid resistance via acquisition of *lmrS* that encode a multi-drug efflux pump[49,128] or the *cfr* ribosomal methyltransferase[187].

While the mechanism of vancomycin resistance through the *vanA* operon is well characterized, mechanisms for VISA are not completely understood since it seems that the VISA phenotype can arise through independent and different mutations or mechanisms. For example, vancomycin and daptomycin resistances may arise either independently from different mechanisms or simultaneously through genes alterations in shared resistance producing mechanisms, such as *graSR*, *vraSR*, and *walKR*[56,101,129]. In

either case (daptomycin and vancomycin resistance individually or together) there are no specific mutations consistent across isolates[115,188,189]. Cell wall synthesis genes, particularly those regulated by *vraSR*, are implicated in resistances to oxacillin that lack *mecA*[74,75]. Despite this overlap in their associated genes, a phenotypic "see-saw" effect where methicillin resistance reduces when vancomycin resistance increases in VISA strains is sometimes observed clinically[56,104,190,191]. To better understand this complex network of genes potentially contributing to the development of antibiotic resistance, researchers are now considering a broader perspective based on pathway activity. There is an on-going effort to target individual molecular pathways to overcome antibiotic resistance[44,59-62], such as restoring vancomycin sensitivity in a VISA strain by inhibiting amino sugar and purine biosynthesis[59]. Having robust and comprehensive computational approaches that accurately identifies pathway changes on a global genome-wide scale in resistant and sensitive *S. aureus,* as I use in this work, could better direct such experimental efforts by revealing phenotypic association[44,192].

Biological pathway analysis is often used to assign functional membership to differentially expressed genes[67,160,165,193]. First, an appropriate, statistical cut-off (*e.g.*, T-test p-value) is used to select the most differentially expressed genes in a dataset between two phenotypes of interest[165]. Next, the group of selected genes (*i.e.*, gene set) is subjected to statistical techniques, such as Fisher's Exact Test (FET), which estimates the significance of enrichment (*i.e.*, a degree of overlap between a selected gene set and established pathways) through an exact p-value estimation method[157,158,160,165,194,195]. Pathway activity changes are defined by enrichment significance (*e.g.*, pathway enrichment with over-expressed gene set represents increased pathway activity). Even

though FET is well established and successfully applied, this approach is not suited to detect cellular processes where a group of genes in a specific pathway undergo subtle expression changes and miss statistical cut-offs by a small margin yet play a biologically important role[69,144,196]. To overcome this limitation, Subramanian, et al, at the Broad Institute developed Gene Set Enrichment Analysis (GSEA)[67,138], an approach widely utilized to examine molecular changes in oncology and other human disease mechanisms[67,138,197-200], but has not been used to examine antibiotic resistance in *S. aureus*. GSEA uses the differential expression levels of all genes in the dataset for gene ranking (*i.e.,* signature generation) to estimate enrichment based on a normalized running-sum statistic that represents the extent the query gene set is overrepresented (*i.e.*, high overlap) in the overall dataset. By considering all genes rather than just those that meet a statistical cut-off, GSEA is more sensitive in identifying overlooked gene groups[67]. Therefore, examining antibiotic resistance using a GSEA-based approach, particularly when expanding it to identify pathway activity changes directly from mRNA expression datasets for multiple pathways simultaneously, as my approach does here, I can get a pathway-centric view of resistance and its association with an observed phenotype.

Here I utilized GSEA to analyze publicly accessible mRNA expression data by defining pathways signatures (*i.e.,* pathway lists ranked by activity changes) to elucidate molecular changes associated with antibiotic resistance in *S. aureus* with the goal of identifying potential co-therapy targets that increase antibiotic susceptibility. Resistance mechanisms driven by known *vraS* or *graSR* mutations are reported, so I first used my pathway signature approach to detect pathways associated with known mutation-driven

resistance (*i.e.*, comparison of resistant and sensitive *S. aureus* under the same treatment condition)[56,71-76] since it is easier to see how differential gene expression in some pathways may be correlated to resistance, in addition to known and established mutation effects. I extended my analysis to identify known and novel pathways associated with antibiotic response (*i.e.*, comparison of *S. aureus* with and without antibiotic treatment, regardless of strain resistance level) and susceptibility (*i.e.*, difference in treatment response between resistant and sensitive strains) [77] to identify inducible mechanisms that could contribute to resistance. I first used my approach to examine vancomycin susceptibility, focusing on vancomycin because of its alarming treatment failure rate clinically[11,56]. I then extended my analysis to compare pathway activity changes associated with *vraS*-driven resistance to vancomycin, oxacillin, and linezolid susceptibilities and response in a sensitive strain specifically, to uncover novel activity changes associated with developing antibiotic resistance. One such pathway is lysine biosynthesis for which I experimentally demonstrated biological relevance via alterations in antibiotic sensitivity. I showed here that my approach can identify pathways as potential co-therapeutic targets. My results are immediately applicable for development of co-therapy options to overcome antibiotic resistance in *S. aureus*.

## 3.2.Results

### 3.2.1. Pathway Signature Approach Identified Pathway Activity Changes Associated with Antibiotic Resistance Driven by *vraS* and *graSR* Mutations

I began by using a dataset that compared a sensitive Δ*mutS* strain to the antibiotic resistant VC40 strain obtained from serial exposure of the Δ*mutS* strain to vancomycin (experimental details of this and all datasets used in this study are provided in

APPENDIX A) to define the VC40vsΔ*mutS* pathway signature (as described in Section 3.4.2), representing pathway activity changes resulting from *vraS* mutation contributing to antibiotic resistance. GSEA normalized enrichment score (NES), which measures the extent of gene enrichment in an individual pathway normalized to account for variations in pathway size[67], for pathways in the VC40vsΔ*mutS* pathway signature ranged from 1.79 to -2.09. From the VC40vsΔ*mutS* pathway signature, two pathway panels containing the 20 most differentially active pathways from the positive and negative tails of VC40vsΔ*mutS* (NES >1.24 and <-1.33 for up- and down-regulated pathways panels, respectively) were generated. I found pathways containing the genes associated with to *vraS*-driven resistance previously identified from single gene expression analysis[101], such as histidine biosynthesis (M00026: NES=1.79, GSEA p-value<0.001) from the up-regulated panel and amino-acyl tRNA biosynthesis (M00359: NES=-2.08, p-value<0.001; M00360: NES=-2.03, p-value=0.002) and succinate dehydrogenase (M00149: NES=-1.56, p-value=0.010) from the down-regulated panel (Table 4). My approach also identified several statistically significant pathways with no prior association to resistance, such as up-regulated lysine biosynthesis (M00016: NES=1.63, p-value=0.021; M00527: NES=1.69, p-value=0.011). I noticed that variations in pathway panel size (pathway panels sizes ranging from 15 to 25 pathways) and the use of VC40vsΔ*mutS* pathway signature to define mutation-driven resistance panels did not alter these results (APPENDIX B).

Table 4. *vraS*-driven Resistance Pathway Panels

| Panel | Signature | Module number |
|---|---|---|
| Up | VC40 vsΔ*mutS* | Histidine biosynthesis (**M00026**)*, Osmoprotectant transport system (M00209)*, Biotin biosynthesis BioW pathway (M00577)*, Lysine biosynthesis via diaminopimelic acid aminotransferase (M00527)*, Lysine biosynthesis via succinyl-diaminopimelic acid (M00016)*, Leucine biosynthesis (M00432), Biotin biosynthesis (M00123), D-Methionine transport system (M00238), Cationic antimicrobial peptide resistance VraFG transporter (**M00730**), Dissimilatory nitrate reduction (M00530), Putative peptide (M00583), Phosphonate (M00223), Betaine biosynthesis (M00555), Peptides/nickel (M00239), Cationic antimicrobial peptide (**M00732**), Arabinogalactan oligomer/maltooligosaccharide (M00491), Serine biosynthesis (**M00020**), VraS-VraR cell-wall peptidoglycan synthesis (**M00480**), Inosine monophosphate biosynthesis (M00048), Cytochrome D ubiquinol oxidase (M00153) |
| Down | VC40 vsΔ*mutS* | Amino-acyl tRNA biosynthesis prokaryotes (**M00360**)*, Amino-acyl tRNA biosynthesis eukaryotes (**M00359**)*, TCA cycle (M00009)*, ABC-2 type (M00254)*, Uridine monophosphate biosynthesis (M00051)*, Iron complex (M00240)*, Energy-coupling factor (M00582)*, Nickel complex (M00440)*, TCA first carbon oxidation (M00010)*, Spermidine/ putrescine transport system (M00299)*, Succinate dehydrogenase prokaryotes (**M00149**)*, ArlS-ArlR virulence regulation (M00716)*, TCA cycle second carbon oxidation (M00011), Acylglycerol degradation (M00098)*, Adenine ribonucleotide biosynthesis (M00049), Menaquinone biosynthesis (M00116), Molybdate transport system (M00189), DNA polymerase III complex, bacteria (M00260), Guanine ribonucleotide biosynthesis (M00050), Shikimate pathway (M00022) |

Modules listed in order of normalized enrichment score from most to least change in pathway activity. * represents Gene Set Enrichment Analysis derived p-value<0.05. Bold font indicates a pathway with genetic mutation association to *vraS*-driven resistance. Pathways that have a * but do not have bold font are pathways with no previous association with *vraS*-driven resistance identified from my pathway signature approach.

Next, I demonstrated the ability of my pathway signature approach to detect known antibiotic resistance mechanisms in another, non-overlapping datasets that examined resistance changes associated with mutations in *graSR*. Within this category, the first dataset compared sensitive strains HG001 (functioning *graSR*) and SG511

(truncated *graS*) to resistant HG001 and SG511 obtained from serial exposure to daptomycin. The second dataset compared a wildtype HG001 (WT, functioning *graS*) and its mutant strain with a deletion of entire *graSR* genes (Δ*graSR*). As is common with bacterial experiments, these datasets had a small sample size (<5 samples/condition)[201,202], so I was not surprised to observe complete separation (*i.e.*, no overlap) of individual samples, representing two distinct sample populations as detailed in APPENDIX C, when performing 1) principal component analysis[203-205] on all genes or pathways, 10 or 100 randomly selected genes, or 20 randomly selected pathways, and 2) leave one out cross validation using 1000 randomly selected pathway panels whose membership excluded pathways from my *vraS*-driven resistance panels ($r^2$=1.0). Despite this sample size limitation, I was able to define two pathway signatures: 1) HG001vsSG511 (GSEA NES ranging from 2.22 to -2.01), which embodies the difference in resistance mechanisms between strains with different *graSR* functions, and 2) WTvsΔ*graSR* (NES ranging from 2.34 to -2.19), which represents pathway activity changes associated with *graSR*-driven resistance mechanisms. When examining the most differentially active pathways in the HG001vsSG511 and WTvsΔ*graSR* pathway signatures, I again found pathways with single gene associations to *graSR*-driven resistance reported. For example, for the most differentially active pathways in the HG001vsSG511 pathway signature (Table 5), I detected increased KdpD-KdpE potassium transport (NES=1.80, GSEA p-value=0.002) and decreased SaeS-SaeR staphylococcal virulence regulation (NES=-1.66, p-value=0.002), C5 isoprenoid biosynthesis mevalonate pathway (NES=-1.80, GSEA p-value=0.002), and fatty acid biosynthesis initiation (NES=-1.63, GSEA p-value=0.018), pathways which had reported

single gene associations of ≥2-fold change in transcriptional levels[129]. For the most differentially active pathways in the WTvsΔ*graSR* pathway signature (Table 6), I found decreased GraS-GraR cationic antimicrobial peptide transport activity (NES=-1.45, p-value=0.007) as expected for a signature comparing strains known for their *graSR* genetic variations[76]. I also found several significant differentially active pathways with known *graSR*-driven resistance, as identified by a ≥1.8-fold change in transcriptional levels and a P-value (Z-test) $\leq 3.5\times10^{-4}$, such as cationic antimicrobial peptide resistance dltABCD operon (NES=-1.88, p-value<0.001), cationic antimicrobial peptide resistance lysyl-phosphatidylglycerol (L-PG) synthase MprF (NES=-1.56, p-value=0.002), LytS-LytR two-component regulatory system (NES=-1.46, p-value=0.006), and cationic antimicrobial peptide resistance VraFG transporter (NES=-1.59, p-value=0.002)[76]. Taken together, these results highlight the ability of my pathway signature approach to detect known resistance mechanisms.

Table 5. Most Differentially Active Pathways Representing the Difference in Resistance Mechanisms between Strains with Different *graS* Functions

| Panel | Signature | Module number |
|---|---|---|
| Up | HG001 vsSG511 | Oligopeptide (M00439)*, Dissimilatory nitrate reduction (M00530)*, Histidine biosynthesis (M00026)*, Lysine biosynthesis via diaminopimelic acid aminotransferase (M00527)*, Arbutin-like (M00268)*, Manganese/zinc (M00792)*, D-methionine transport (M00018)*, β-Lactam resistance Bla system (M00627)*, Arginine biosynthesis (M00844)*, Lysine biosynthesis succinyl-diaminopimelic acid (M00016)*, Glycolysis Embden-Meyerhof pathway (M00001)*, D-Methionine transport system (M00238)*, Guanine ribonucleotide biosynthesis (M00050)*, Urea cycle (M00029)*, Nucleotide sugar biosynthesis prokaryotes (M00362)*, KdpD-KdpE potassium transport (**M00454**)*, Glycolysis core module involving 3-carbon compounds (M00002)*, Reductive pentose phosphate cycle (M00166)*, Betaine biosynthesis (M00555)* |
| Down | HG001 vsSG511 | Iron complex (M00240)*, Mannitol-specific (M00274)*, AgrC-AgrA exoprotein synthesis (M00495)*, Biotin biosynthesis BioW pathway (M00577)*, Triacylglycerol biosynthesis (M00089)*, C5 isoprenoid biosynthesis mevalonate pathway (**M00095**)*, Pentose phosphate pathway archaea (M00580)*, Spermidine/ putrescine transport system (M00299)*, Biotin biosynthesis (M00123)*, Ribosome bacteria (M00178)*, F-type ATPase prokaryotes and chloroplasts (M00157)*, Inosine monophosphate biosynthesis (M00048)*, SaeS-SaeR staphylococcal virulence regulation (**M00468**)*, Putative ABC (M00211)*, Fatty acid biosynthesis initiation (**M00082**)*, Nickel complex (M00440)*, Zinc (M00242)*, ABC-2 type (M00254)*, Galactitol-specific (M00279) |

Modules listed in order of normalized enrichment score from most to least change in pathway activity. * represents Gene Set Enrichment Analysis derived p-value<0.05. Bold font indicates a pathway with genetic mutation association to the difference in resistance mechanisms between strains with different *graS* functions. Pathways that have a * but do not have bold font are pathways with no previous association with *graS*-driven resistance identified from my pathway signature approach.

Table 6. Most Differentially Active Pathways Representing *graS*-driven Resistance

| Panel | Signature | Module number |
|---|---|---|
| Up | WTvs Δ*graSR* | Lysine biosynthesis via succinyl-diaminopimelic acid (M00016)*, Lysine biosynthesis via diaminopimelic acid aminotransferase (M00527)*, Threonine biosynthesis (M00018)*, Riboflavin biosynthesis (M00125)*, Leucine biosynthesis (M00432)*, Histidine biosynthesis (M00026)*, Coenzyme A biosynthesis (M00120)*, Urea cycle (M00029)*, Nickel complex (M00440)*, Teichoic acid (M00251)*, Arginine biosynthesis (M00844)*, Isoleucine biosynthesis (M00570), PhoR-PhoB phosphate starvation response (M00434)*, Arbutin-like (M00268), Valine/isoleucine biosynthesis (M00019), Biotin biosynthesis BioW pathway (M00577), Trehalose-specific II component (M00270), BraS-BraR bacitracin transport (M00734), VraS-VraR cell-wall peptidoglycan synthesis (**M00480**), Phosphate (M00222) |
| Down | WTvs Δ*graSR* | Inosine monophosphate biosynthesis (M00048)*, Ribosome bacteria (M00178)*, Amino-acyl tRNA biosynthesis prokaryotes (M00360)*, Cationic antimicrobial peptide resistance dltABCD operon (**M00725**)*, Amino-acyl tRNA biosynthesis eukaryotes (M00359)*, RNA polymerase bacteria (M00183)*, Nucleotide sugar biosynthesis prokaryotes (M00362)*, Pyrimidine deoxyribonuleotide biosynthesis (M00053)*, Guanine ribonucleotide biosynthesis (M00050)*, Cytochrome aa3-600 menaquinol oxidase (M00416)*, Glutathione biosynthesis (M00188)*, Cationic antimicrobial peptide resistance VraFG transporter (**M00730**)*, Adenine ribonucleotide biosynthesis (M00049)*, Cationic antimicrobial peptide resistance lysyl-phosphatidylglycerol (L-PG) synthase MprF (**M00726**)*, Glycolysis core module involving three-carbon compounds (M00002)*, Manganese/zinc (M00792)*, LytS-LytR two-component regulatory system (**M00492**)*, Fatty acid biosynthesis initiation (M00082), GraS-GraR cationic antimicrobial peptide transport (**M00733**)*, TCA cycle (M00009) |

Modules listed in order of normalized enrichment score from most to least change in pathway activity. * represents Gene Set Enrichment Analysis derived p-value<0.05. Bold font indicates a pathway with genetic mutation association to *graS*-driven resistance. Pathways that have a * but do not have bold font are pathways with no previous association with *graS*-driven resistance identified from my pathway signature approach.

Since *graSR* and *vraSR* share control of expression for some genes like *mprF*[72,206,207], I examined the similarities and differences in pathway activities between my *vraS*-driven resistance panels and HG001vsSG511 and WTvsΔ*graSR* pathway

signatures. I found significant similarities between my up-regulated *vraS*-driven resistance panel and positive tails from both HG001vsSG511 and WTvsΔ*graSR* pathway signatures (Figure 4A). I was unable to find similarities for the down-regulated panel since the WTvsΔ*graSR* pathway signature was borderline significant, although the down-regulated panel in HG001vsSG511 is significantly enriched does not represent a true enrichment. To see how likely NES calculated for my panels could be achieved randomly, I re-ran the analysis with 1000 randomly generated 20-pathway panels and find statistical significance for the same three of four analyses (Figure 4B), confirming the borderline enrichment observed in the down-regulated panel. These results also showed enrichment obtained by my up-regulated panel were non-random.

Figure 4. Identification of Pathway Activity Change Similarities and Differences Associated with *vraS*- and *graSR*-driven Resistance

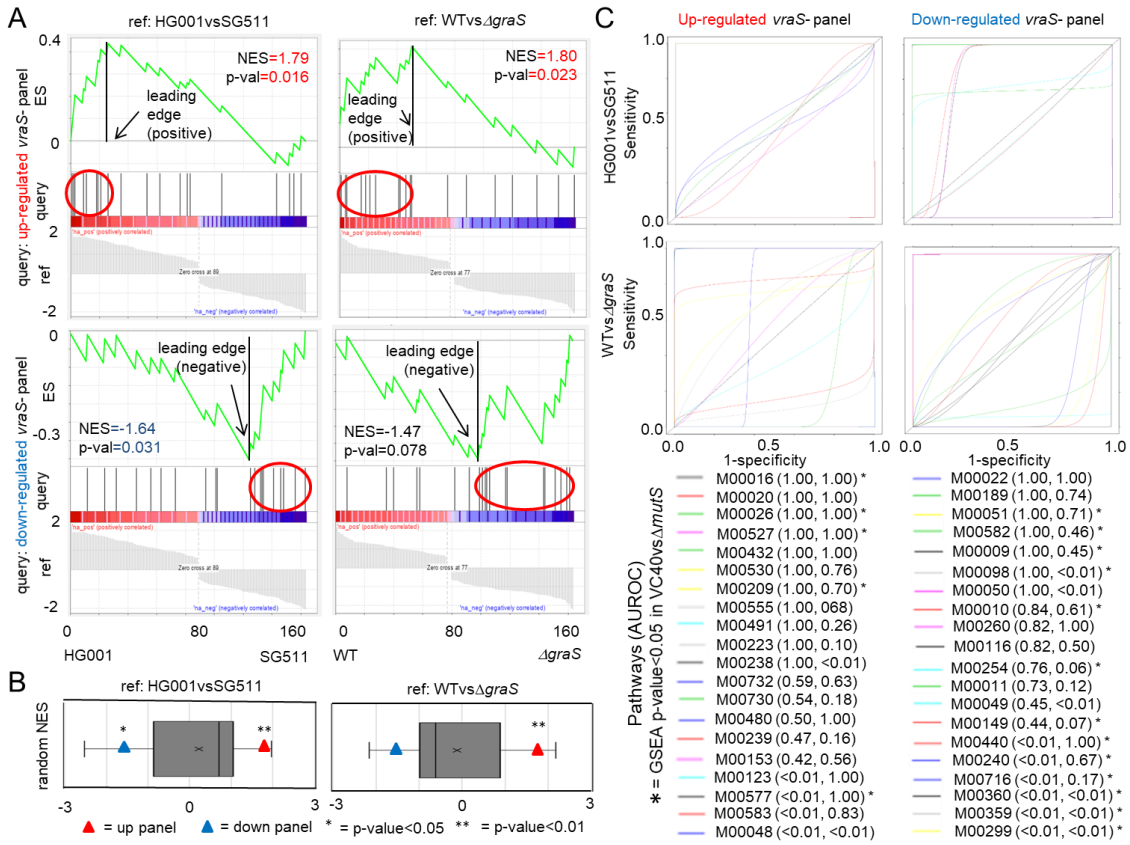


(A) Gene Set Enrichment Analysis (GSEA) show pathway activity change similarities and differences between *vraS*-driven resistance panels (queries) and the HG001vsSG511 and WTvsΔ*graSR* pathway signatures (references). (B) Box and whiskers plots of normalized enrichment score (NES) from 1000 randomly generated pathway panels (individual queries) compared to the HG001vsSG511 and WTvsΔ*graSR* pathway signatures (references) illustrate that the NES achieved by comparing reference pathway signatures to *vraS*-driven resistance panels used as query in (A) are among the best NES obtained randomly. (C) Receiver operator characteristic curve calculations quantify the ability of individual pathways to separate samples by resistance, revealing *vraS*-driven resistance pathways that contribute most to *graSR*-driven resistance. Stars indicate individual pathways with statistically significance in the VC40vsΔ*mutS* pathway signature. AUROC, area under the receiver operator characteristic; ES, enrichment score.

I examined individual pathway activity changes across resistance datasets by examining which pathways contribute most to GSEA calculating a panel's maximum enrichment (*i.e.*, leading-edge pathways, APPENDIX D) between *vraS*-driven resistance panels and HG001vsSG511 and WTvsΔ*graSR* pathway signatures. I found histidine

biosynthesis (M00026), which has an established association with *vraS*-driven resistance[101] and was significant in the VC40vsΔ*mutS* signature, was also significant in both HG001vsSG511 and WTvsΔ*graSR* pathway signatures (Table 7). Other panel pathways with observed associations to resistance were either 1) inconsistently significant across signatures, such as amino-acyl tRNA biosynthesis (M00359/M00360), and serine biosynthesis (M00020), or 2) not included in both leading-edges which occurs when a pathway has insufficient enrichment for it to contribute to achieving the pathway's maximum enrichment. For example, succinate dehydrogenase (M00149) was included in the HG001vsSG511 leading-edge (NES=-1.18, p-value=0.264), but not in the WTvsΔ*graSR* leading-edge (NES=-0.78, p-value=0.732). Lysine biosynthesis pathways, which were significant in VC40vsΔ*mutS*, were also significant in both HG001vsSG511 and WTvsΔ*graSR* pathway signatures.

Table 7. Shared Leading-edge Pathways Associated with *vraS*- and *graSR*-driven Resistance

| Panel | Module number | VC40vsΔ*mutS* | | HG001vsSG511 | | WTvsΔ*graS* | |
|---|---|---|---|---|---|---|---|
| | | NES | p-val | NES | p-val | NES | p-val |
| Up | Lysine biosynthesis via succinyl-diaminopimelic acid (M00016) | 1.63 | 0.021 | 1.92 | <0.001 | 2.24 | <0.001 |
| | Serine biosynthesis (**M00020**) | 1.30 | 0.064 | 1.47 | 0.006 | 1.05 | 0.442 |
| | Histidine biosynthesis (**M00026**) | 1.79 | <0.001 | 2.16 | <0.001 | 1.79 | 0.002 |
| | Leucine biosynthesis (M00432) | 1.45 | 0.074 | 1.72 | 0.004 | 1.80 | <0.001 |

| Panel | Module number | VC40vsΔ*mutS* | | HG001vsSG511 | | WTvsΔ*graS* | |
|---|---|---|---|---|---|---|---|
| | | NES | p-val | NES | p-val | NES | p-val |
| Up | Lysine biosynthesis via diaminopimelic acid aminotransferase (M00527) | 1.69 | 0.011 | 2.14 | <0.001 | 2.17 | <0.001 |
| | Dissimilatory nitrate reduction (M00530) | 1.34 | 0.136 | 2.21 | <0.001 | 0.95 | 0.507 |
| | Betaine biosynthesis (M00555) | 1.36 | 0.088 | 1.76 | <0.001 | 0.97 | 0.587 |
| Down | TCA cycle second carbon oxidation (M00011) | -1.49 | 0.052 | -1.15 | 0.271 | -1.43 | 0.068 |
| | Adenine ribonucleotide biosynthesis (M00049) | -1.49 | 0.053 | -1.17 | 0.272 | -1.59 | 0.005 |
| | ABC-2 type (M00254) | -1.79 | 0.004 | -1.52 | 0.019 | -1.04 | 0.401 |
| | Spermidine/ putrescine transport system (M00299) | -1.56 | 0.035 | -1.76 | 0.004 | -0.98 | 0.531 |
| | Amino-acyl tRNA biosynthesis eukaryotes (**M00359**) | -2.08 | <0.001 | -1.29 | 0.104 | -1.83 | 0.002 |
| | Amino-acyl tRNA biosynthesis prokaryotes (**M00360**) | -2.03 | 0.002 | -1.26 | 0.118 | -1.93 | 0.002 |

Leading-edge pathways identified through Gene Set Enrichment Analysis (GSEA) on *vraS*-driven resistance panels (query) and HG001vsSG511 and WTvsΔ*graSR* signatures (references). NES, normalized enrichment score, p-val, GSEA p-value. Bold font indicates a pathway with known association to *vraS*- and *graSR*-driven antibiotic resistance.

Another way to examine individual pathway activity changes across *vraS*- and *graSR*-driven antibiotic resistance datasets is to calculate area under the receiver operator

characteristic (AUROC) curve[197,208]. I did this for each of the 20 pathways in *vraS*-driven resistance panels individually from NES generated from individual samples that made up HG001vsSG511 and WTvsΔ*graSR* to examine which pathways contribute most to resistance predictions (Figure 4C). I found known resistance pathways, such as histidine and serine biosynthesis (M00026 and M00020, respectively) from the up-regulated panel and amino-acyl tRNA biosynthesis (M00359/M00360) from the down-regulated panel, were among those best (*i.e.*, most consistent across datasets with the appropriate activity level, 1.00 and <0.01 for up- and down-regulated, respectively) able to separate samples by resistance levels. Lysine biosynthesis pathways (M00016 and M00527) were also among the best pathways with other known resistance pathways, indicating their potential involvement in resistance.

### 3.2.2. Pathway Signature Approach Detects Pathway Activity Changes Associated with Vancomycin Susceptibility

I extended analysis with my pathway signature approach to another dataset dealing with vancomycin susceptibility by repeating the analysis previously described for the *vraS*- and *graSR*-driven resistance signatures. To do this, I used a dataset that compared vancomycin treated and untreated samples of resistant strains (T8 and C1) and a sensitive strain (PA). Unfortunately, unlike strains used for the *vraS*- and *graSR*-driven resistance signatures, there was no additional information about the characteristics of T8, C1, and PA strains available. To generate vancomycin susceptibility pathway panels, I used data from T8 and PA strains since T8 had a higher resistance level compared to C1, to define the T8vsPA pathway signature, and used this signature to generate panels as previously described (GSEA NES ranging from 1.32 to 1.77 and -1.51 to -2.29 for up-

and down-regulated pathways panels, respectively, Table 8). My vancomycin susceptibility panels included several significantly enriched pathways with documented gene mutation or pathway activity change associations with the vancomycin resistance phenotype. For example, I saw significant up-regulation of the VraSR two component system (M00480, NES=1.44, p-value=0.017), which is generally associated with resistance[56], and borderline significance of the pentose phosphate pathways (M00004: NES=1.42, GSEA p-value=0.073; M00006: NES=1.38, p-value=0.035)[59,209]. I also observed significant down-regulation of energy production pathways[210-213], such TCA cycle (M00009: NES=-1.94, p-value<0.001; M00011:, NES=-1.99, p-value<0.001) and F-type ATPase (M00157, NES=-1.66, p-value=0.006), and translation processes[214,215], like ribosomes (M0178, NES=-2.02, p-value<0.001) and amino-acyl tRNA biosynthesis (M00359: NES=-2.28, p-value<0.001; M00360: NES=-2.29, p-value<0.001). Further, I detected statistically significant pathways without current associations to the vancomycin resistance phenotype, such as increases in amino acid biosynthesis and transport, specifically threonine and isoleucine biosynthesis and D-methionine transport (M00018: NES=1.54, p-value=0.036; M00570: NES=1.66, p-value=0.008; M00238: NES=1.49, p-value=0.046). While lysine biosynthesis pathways were included in the up-regulated vancomycin susceptibility panel, they did not reach statistical significance (M00016: NES=1.46, p-value=0.063; M00527: NES=1.43, p-value=0.074).

Table 8. Vancomycin Susceptibility Pathway Panels

| Panel | Signature | Module number |
|---|---|---|
| Up | T8vsPA | Uridine monophosphate biosynthesis (M00051)*, Osmoprotectant transport system (M00209)*, Pantothenate biosynthesis (M00119)*, Isoleucine biosynthesis (M00570)*, Threonine biosynthesis (M00018)*, D-Methionine transport system (M00238)*, Oligopeptide (M00439)*, Formaldehyde assimilation ribulose monophosphate (M00345)*, Lysine biosynthesis via succinyl-diaminopimelic acid (M00016), Energy-coupling factor (M00582), VraS-VraR cell-wall peptidoglycan synthesis (**M00480**)*, Lysine biosynthesis via diaminopimelic acid aminotransferase (M00527), Pentose phosphate cycle (**M00004**), Pentose phosphate pathway archaea (**M00580**), Pentose phosphate pathway, oxidative phase (**M00006**)*, Betaine biosynthesis (M00555)*, Glyoxylate cycle (M00012)*, Riboflavin biosynthesis (M00125), Putative ABC (M00211), Cationic antimicrobial peptide resistance VraFG transporter (**M00730**) |
| Down | T8vsPA | Amino-acyl tRNA biosynthesis prokaryotes (**M00360**)*, Amino-acyl tRNA biosynthesis eukaryotes (**M00359**)*, Dissimilatory nitrate reduction (M00530)*, Ribosome bacteria (**M00178**)*, TCA cycle second carbon oxidation (**M00011**)*, TCA cycle (**M00009**)*, Iron complex (M00240)*, Nickel complex (M00440)*, Siroheme biosynthesis (M00846)*, Cystine (M00234)*, Fructose-specific (M00273)*, F-type ATPase prokaryotes and chloroplasts (**M00157**)*, Putative peptide (M00583)*, Cytochrome aa3-600 menaquinol oxidase (M00416)*, Spermidine/ putrescine transport system (M00299)*, Succinate dehydrogenase prokaryotes (M00149)*, NreB-NreC dissimilatory nitrate/nitrite reduction (M00483)*, Glucose- specific (M00809)*, Cytochrome C oxidase (M00154)*, Urea cycle (M00029) |

Modules listed in order of normalized enrichment score from most to least change in pathway activity. * represents Gene Set Enrichment Analysis derived p-value<0.05. Bold font indicates a pathway with known association to vancomycin intermediate resistance. Pathways that have a * but do not have bold font are novel pathways associated with vancomycin intermediate resistance identified from my pathway signature approach.

Next, I examined the pathway activity changes captured by my vancomycin susceptibility panels in non-overlapping data. To do this, I defined the C1vsPA pathway signature (NES ranging from 1.91 to -2.21), which was then used as reference for GSEA against the vancomycin susceptibility panels. I found significant similarities between vancomycin susceptibility panels and the C1vsPA pathway signature (Figure 5A) that are

not randomly generated (Figure 5B). To see if my observed enrichment holds, I generated vancomycin susceptibility panels from C1vaPA, as done for T8vsPA,and used them for GSEA against the T8vsPA signature as reference, and did not find a substantial change (NES=3.30, GSEA p-value<0.001, and NES=-3.31, p-value<0.001; for up- and down-regulated panels, respectively), supporting the conclusion that both vancomycin susceptibility panels obtained with GSEA are truly enriched.

Figure 5. Identification of Pathway Activity Change Similarities and Differences Associated with Vancomycin Susceptibility

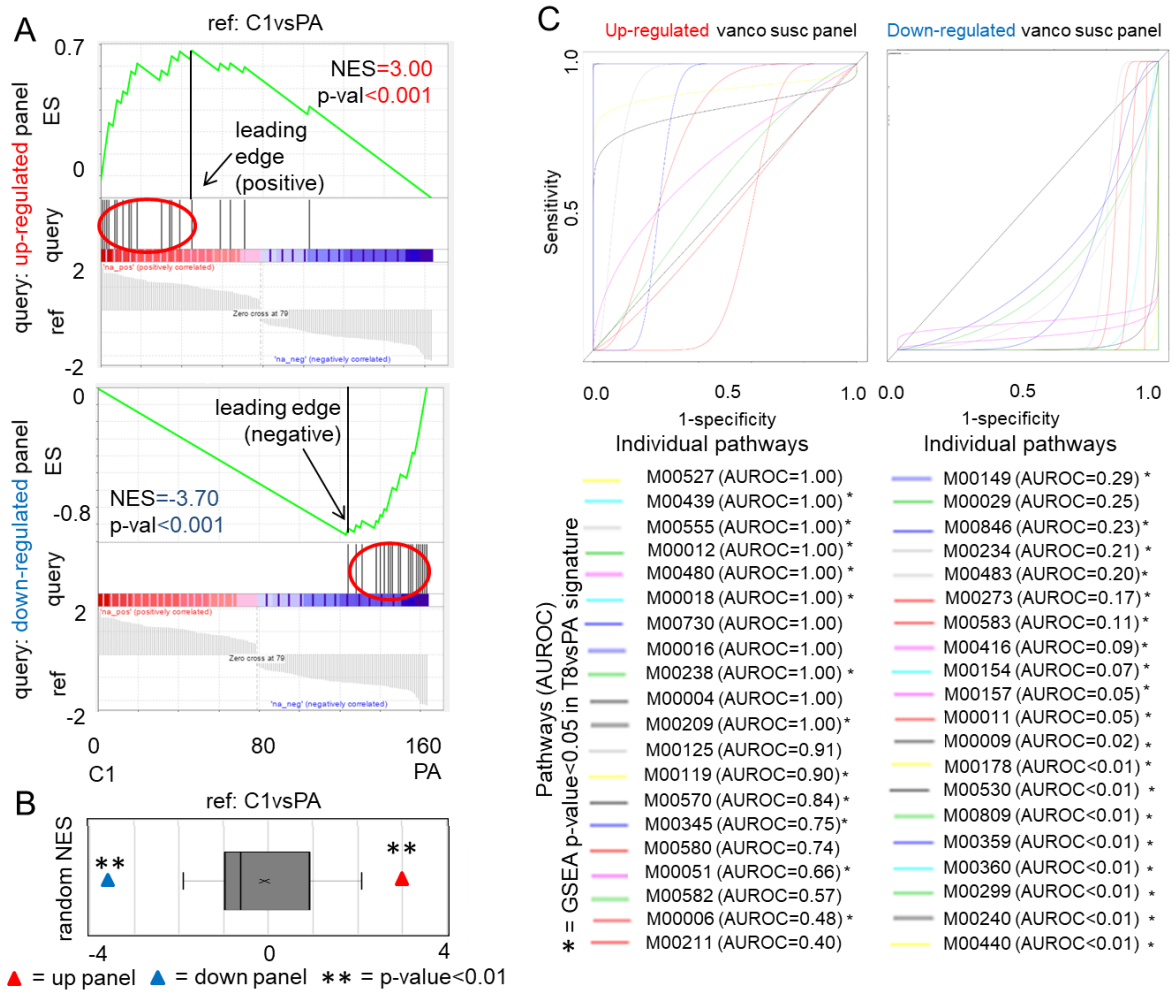


(A) Gene Set Enrichment Analysis (GSEA) show pathway activity change similarities between vancomycin (vanco) susceptibility (susc) panels (queries) and the C1vsPA pathway signature (reference). (B) Box and whiskers plots of normalized enrichment scores (NES) from 1000 randomly generated pathway panels (individual queries) compared to the C1vsPA pathway signature (reference) illustrate that the NES achieved by comparing reference pathway signatures to vancomycin susceptibility panels used as query in (A) are among the best NES obtained randomly. (C) Receiver operator characteristic curve calculations quantify the ability of individual pathways to separate samples by susceptibility, revealing pathways that contribute most to vancomycin susceptibility. Stars indicate individual pathways with statistically significance in the T8vsPA pathway signature. AUROC, area under the receiver operator characteristic; ES, enrichment score.

I then examined identified leading-edge pathways (APPENDIX D) and found several significantly enriched pathways shared across leading-edges with established genetic or pathway associations to the vancomycin resistance phenotype (Table 9). These pathways included up-regulated VraSR two component system and down-regulated TCA cycle, ribosomes, and amino-acyl tRNA biosynthesis. Further, I found significantly enriched pathways with no current observed association to vancomycin resistance that are shared between T8vsPA and C1vsPA (Table 9). These pathways included but are not limited to up-regulated threonine biosynthesis and D-methionine transport and down-regulated iron and nickel complex and nitrate reduction pathways. I also noted that even though lysine biosynthesis pathways (M00016 and M00527) were not statistically significant in the T8vsPA signature, these pathways achieved statistical significance in the C1vsPA signature (M00016: NES=1.85; M00527: NES=1.80, both p-value=0.002). Further, isoleucine biosynthesis (M00730), which was significant in the T8vsPAsignature, did not achieve statistical significance (NES=1.13, p-value=0.307).

Table 9. Significantly Enriched Leading-edge Pathways Associated with Vancomycin Susceptibility

| Panel | Module number | T8vsPA | | C1vsPA | |
|---|---|---|---|---|---|
| | | NES | p-val | NES | p-val |
| Up | Threonine biosynthesis (M00018) | 1.54 | 0.036 | 1.87 | 0.002 |
| | Osmoprotectant transport system (M00209) | 1.72 | 0.016 | 1.59 | 0.026 |
| | D-Methionine transport system (M00238) | 1.49 | 0.046 | 1.81 | 0.007 |
| | Oligopeptide (M00439) | 1.47 | 0.049 | 1.91 | <0.001 |
| | VraS-VraR cell-wall peptidoglycan synthesis (*M00480*) | 1.44 | 0.017 | 1.42 | 0.028 |
| Down | TCA cycle second carbon oxidation (*M00011*) | -1.99 | <0.001 | -1.57 | 0.024 |
| | Cytochrome C oxidase (M00154) | -1.51 | 0.015 | -1.43 | 0.039 |
| | Ribosome bacteria (*M00178*) | -2.02 | <0.001 | -1.86 | <0.001 |
| | Iron complex (M00240) | -1.79 | <0.001 | -2.21 | <0.001 |
| | Fructose-specific (M00273) | -1.70 | <0.001 | -1.63 | 0.009 |
| | Spermidine/ putrescine transport system (M00299) | -1.57 | 0.012 | -1.48 | 0.033 |
| | Amino-acyl tRNA biosynthesis eukaryotes (*M00359*) | -2.28 | <0.001 | -2.17 | <0.001 |
| | Amino-acyl tRNA biosynthesis prokaryotes (*M00360*) | -2.29 | <0.001 | -2.14 | <0.001 |
| | Nickel complex (M00440) | -1.78 | <0.001 | -1.94 | <0.001 |
| | NreB-NreC dissimilatory nitrate/nitrite reduction (M00483) | -1.52 | 0.038 | -1.47 | 0.041 |
| | Dissimilatory nitrate reduction (M00530) | -2.08 | <0.001 | -2.16 | <0.001 |
| | Glucose- specific (M00809) | -1.51 | 0.013 | -1.54 | <0.001 |

Statistically significant leading-edge pathways identified through Gene Set Enrichment Analysis (GSEA) on vancomycin susceptibility panels (query) and C1vsPA signatures (reference). NES, normalized enrichment score, p-val, GSEA p-value. Italics font indicates a pathway with known association to vancomycin intermediate resistance lacking the *vanA* operon.

To support my leading-edge findings, I calculated AUROC curves for each pathway individually and found known up-regulated VraSR two component system (M00480) and down-regulated translation processes (aminoacyl-tRNA biosynthesis,

M00359 and M00360, and ribosome, M00178) and energy production (TCA pathways, M00009 and M00011, and F-type ATPase, M00157) were among the best pathways to separate samples based on vancomycin susceptibility (Figure 5C). I also found amino acid pathways, threonine biosynthesis (M00018), D-methionine transport (M00238), and lysine biosynthesis (M00016 and M00527), separate samples well (AUROC=1.00), while isoleucine biosynthesis (M00570) did not (AUROC=0.84).

Next, I expanded my analysis to examine how individual strains respond to vancomycin treatment by comparing lists of significantly enriched pathways per each tail (APPENDIX E) from one of four pathway signatures between treated and untreated samples from the same strain (*e.g.*, PAfromT8treatvsPAfromT8unt). From this analysis, I identified several pathways with known genetic associations to the VISA phenotype, such as down-regulated TCA cycle, F-type ATPase, amino-acyl tRNA biosynthesis, and uridine biosynthesis (Table 10). I found no pathway shared across all four signatures when comparing statistically significant up-regulated pathways. The VraSR two component system (M00480) was observed in T8treat only though it is borderline significant in C1 (NES=1.36, GSEA p-value=0.067) but not in the PA strains ($0.98<NES<1.27$, p-value$>0.144$). I also found pathways without prior association to vancomycin resistance (Table 10), such as up-regulated threonine biosynthesis (M00018), D-methionine transport (M00238), and lysine biosynthesis (M00016 and M00527) in T8 and C1 but not in the PA strains. Interestingly, I found borderline significance in the other lysine biosynthesis pathway (M00527 T8: NES=1.39, p-value=0.075; C1: NES=1.63, p-value=0.013; PAfromT8: NES=1.21, p-value=0.245;

PAfromC1: NES=1.50, p-value=0.031). For the negative tail lists, only the vancomycin resistance (VanA, M00651) pathway was statistically significant in all signatures.

Table 10. Shared Significantly Enriched Pathways Associated with Vancomycin Response

| Panel | Module | T8 | | C1 | | PAfromT8 | | PAfromC1 | |
|---|---|---|---|---|---|---|---|---|---|
| | | NES | p-val | NES | p-val | NES | p-val | NES | p-val |
| Up | Lysine biosynthesis via succinyl-diaminopimelic acid (M00016) | 1.52 | 0.032 | 1.62 | 0.014 | 1.35 | 0.093 | 1.42 | 0.061 |
| | Threonine biosynthesis (M00018) | 1.74 | 0.003 | 1.82 | <0.001 | 1.41 | 0.093 | 1.30 | 0.138 |
| | Methionine transport system (M00238) | 1.78 | 0.003 | 1.66 | 0.006 | 1.24 | 0.213 | 1.27 | 0.160 |
| | Oligopeptide (M00439) | 1.91 | <0.001 | 1.74 | <0.001 | 1.22 | 0.233 | 1.11 | 0.348 |
| | Energy-coupling factor (M00582) | 1.72 | <0.001 | 1.75 | <0.001 | 1.11 | 0.331 | 1.49 | 0.051 |
| | Iron complex (M00240) | -1.12 | 0.292 | -1.88 | <0.001 | 1.71 | 0.006 | 1.81 | <0.001 |
| Down | TCA cycle second carbon oxidation (*M00011*) | -2.34 | <0.001 | -1.77 | 0.010 | -0.66 | 0.911 | 0.65 | 0.915 |
| | F-type ATPase prokaryotes and chloroplasts (*M00157*) | -1.61 | 0.036 | -1.71 | 0.029 | 1.46 | 0.041 | 1.00 | 0.479 |
| | Amino-acyl tRNA biosynthesis eukaryotes (*M00359*) | -2.28 | <0.001 | -2.49 | <0.001 | -0.69 | 0.920 | 1.05 | 0.439 |
| | Amino-acyl tRNA biosynthesis prokaryotes (*M00360*) | -2.39 | <0.001 | -2.51 | <0.001 | 0.61 | 0.957 | 1.13 | 0.322 |
| | NreB-NreC dissimilatory nitrate/nitrite reduction two-component regulatory system (M00483) | -1.53 | 0.024 | -1.68 | <0.001 | 0.90 | 0.659 | -1.04 | 0.412 |
| | Nickel complex (M00440) | -1.98 | <0.001 | -2.24 | <0.001 | 1.89 | <0.001 | 1.39 | 0.079 |
| | Dissimilatory nitrate reduction (M00530) | -2.33 | <0.001 | -2.44 | <0.001 | -0.80 | 0.734 | -0.93 | 0.558 |
| | Uridine monophosphate biosynthesis (*M00051*) | -1.39 | 0.134 | -1.45 | 0.098 | -1.93 | <0.001 | -2.18 | 0.003 |
| | Putative ABC transport system (M00211) | -0.73 | 0.758 | -1.26 | 0.208 | -1.87 | <0.001 | -1.76 | 0.006 |
| | ABC-2 type transport system (M00254) | -1.22 | 0.175 | -1.34 | 0.120 | -1.71 | 0.006 | -1.74 | 0.023 |

Modules achieving a Gene Set Enrichment Analysis (GSEA) derived p-value<0.05 in across either vancomycin resistant (T8 and C1) or sensitive (PAfromT8 and PAfromC1) strains, but not both. Italics font indicates a pathway with known association to vancomycin intermediate resistance lacking the *vanA* operon. NES, normalized enrichment score, p-val, GSEA p-value.

### 3.2.3. Comparison of *vraS*-driven Resistance Panels to Antibiotic Susceptibility and Response Pathway Signatures Identifies Top Pathway Candidates for Experimental Examination

Next, I extended this comparison to identify similar pathways between *vraS*-driven resistance panels and the most differentially active pathways associated with oxacillin (1422vs2798 and V3vs923) and linezolid (3577vs378, 5612vs378, 6939vs378, and 7210vs378) susceptibility and response in a sensitive strain[77] (HG001van, HG001fluc, and HG001line for vancomycin, flucloxacillin, and linezolid, respectively). By comparing *vraS*-driven resistance panels to vancomycin susceptibility and response pathway signatures, I noticed similarities to both pathway panels that are usually significant (Figure 6A) and not likely the result of random chance since their achieved NES are frequently significant compared to a random model distribution (Figure 6B). For oxacillin and linezolid, I saw a reversal in panel activity in sensitive strain signatures (HG001fluc and HG001line, Figure 6A), which I also observed partially in some susceptibility signatures, that are not due to random chance (Figure 6B).

Figure 6. Pathway Signature Comparison Reveal Similarities and Differences between *vraS*-driven Resistance Panel Activity and Pathway Activity Changes in Antibiotic Susceptibilities and Responses

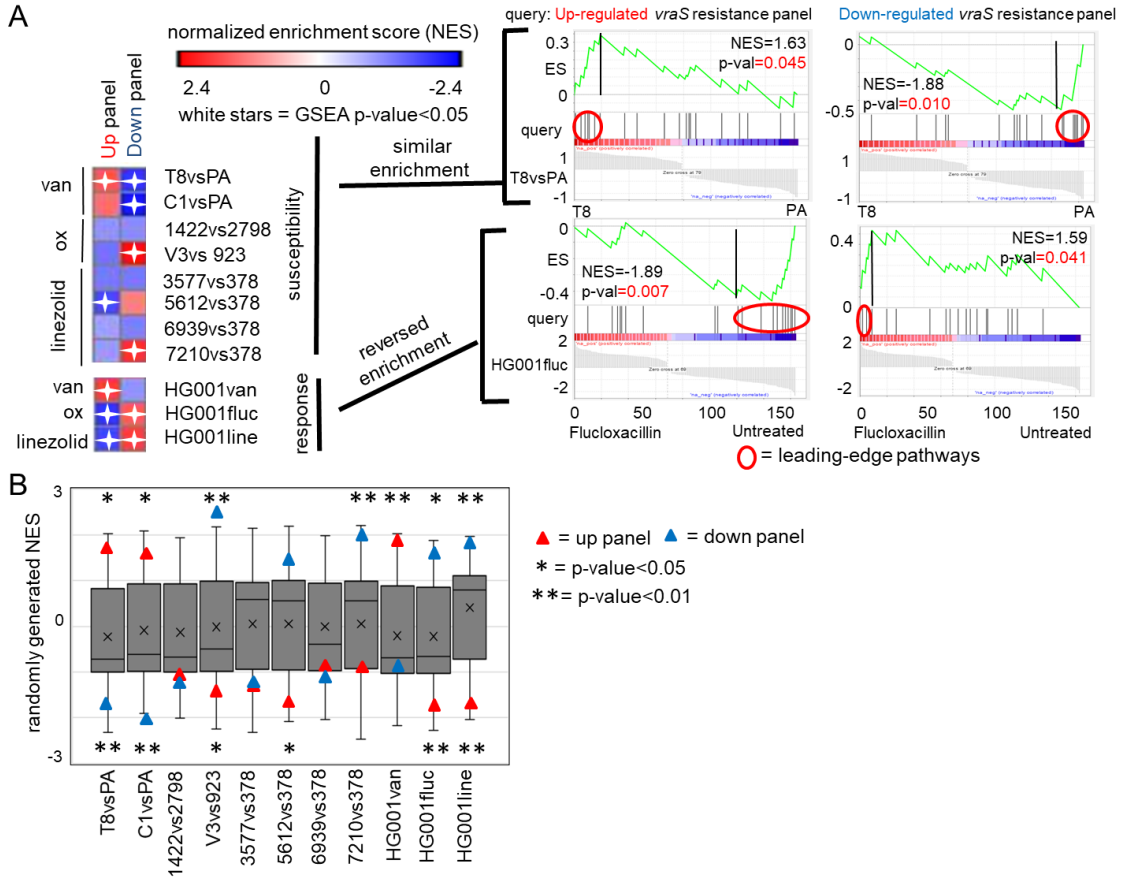


(A) Normalized enrichment score (NES) heat map (left) generated from comparing *vraS*-driven resistance panels (queries) to 11 pathway signatures representing vancomycin (van), oxacillin (ox), or linezolid susceptibility and response in a sensitive strain (references) for Gene Set Enrichment Analysis (GSEA) capture similarities and differences calculated via GSEA enrichment plots (right). (B) NES distribution from 1000 randomly generated pathway panels (individual queries) compared to the 11 pathway signatures (references) show how likely NES achieved by comparing reference pathway signatures to *vraS*-driven resistance panels are to be random.

Next, I looked at individual pathway data generated by GSEA across all 11 comparisons between the *vraS*-driven resistance panels and 11 susceptibility and response pathway signatures to identify pathways to target in future laboratory examinations. When considering these computational data to select candidate pathways

for future laboratory examinations, I gave priority to up-regulated panel pathways because of the reproducibility of their enrichment earlier in my analysis (Figure 4). APPENDIX D lists leading-edge pathways identified per GSEA comparison. Table 11 summarizes pathways shared across dataset leading edges for vancomycin susceptibilities and responses that may contribute to developing resistance, and Table 12 does the same for oxacillin. No shared pathways were found across linezolid susceptibilities and responses. Lysine biosynthesis pathways (M00527 and M00016) had the highest relative leading-edge frequency among up-regulated panel pathways with representation across antibiotics (Figure 7), and was easy to establish biological relevance experimentally. Based on this, I selected lysine biosynthesis for further experimental examination.

Table 11. Shared Leading-edge Pathways Associated with Vancomycin Susceptibility and Response

| Panel | Module number | T8vsPA | | C1vsPA | | HG001van | |
|---|---|---|---|---|---|---|---|
| | | NES | p-val | NES | p-val | NES | p-val |
| Up | Lysine biosynthesis via succinyl-diaminopimelic acid (M00016) | 1.46 | 0.063 | 1.85 | 0.002 | 1.15 | 0.285 |
| | Osmoprotectant transport system (M00209) | 1.72 | 0.016 | 1.59 | 0.026 | 1.64 | 0.027 |
| | VraS-VraR cell-wall peptidoglycan synthesis (**M00480**) | 1.44 | 0.017 | 1.42 | 0.028 | 1.40 | 0.057 |
| | Lysine biosynthesis via diaminopimelic acid aminotransferase (M00527) | 1.43 | 0.073 | 1.80 | 0.002 | 1.55 | 0.033 |
| | Betaine biosynthesis (M00555) | 1.38 | 0.038 | 1.35 | 0.099 | 1.37 | 0.086 |
| Down | Menaquinone biosynthesis (M00116) | -1.19 | 0.270 | -1.21 | 0.240 | -1.48 | 0.071 |
| | Succinate dehydrogenase prokaryotes (M00149) | -1.52 | 0.011 | -1.24 | 0.242 | -1.29 | 0.162 |

Shared leading-edge pathways identified by Gene Set Enrichment Analysis (GSEA) comparisons between *vraS*-driven resistance panels and vancomycin susceptibility (T8vsPA and C1vsPA) and response (HG001van) signatures. NES, normalized enrichment score, p-val, GSEA p-value. Bold font indicates a pathway with known association to vancomycin resistance.

Table 12. Shared Leading-edge Pathways Associated with Oxacillin Susceptibility and Flucloxacillin Response

| Panel | Module number | 1422vs2798 | | V3vs923 | | HG001fluc | |
|---|---|---|---|---|---|---|---|
| | | NES | p-val | NES | p-val | NES | p-val |
| Up | Lysine biosynthesis via succinyl-diaminopimelic acid (M00016) | -1.05 | 0.418 | -0.87 | 0.651 | -1.91 | <0.001 |
| | Inosine monophosphate biosynthesis (M00048) | -1.32 | 0.114 | -1.66 | 0.006 | -2.31 | <0.001 |
| | Lysine biosynthesis via diaminopimelic acid aminotransferase (M00527) | -1.19 | 0.290 | -0.67 | 0.872 | -1.66 | 0.022 |
| | Dissimilatory nitrate reduction (M00530) | -1.37 | 0.080 | -1.67 | 0.004 | -1.80 | 0.002 |
| | Putative peptide (M00583) | -1.18 | 0.285 | -0.91 | 0.649 | -1.47 | 0.019 |

Shared leading-edge pathways identified by Gene Set Enrichment Analysis (GSEA) comparisons between *vraS*-driven resistance panels and oxacillin susceptibility (1422vs2798 and V3vs923) and flucloxacillin response (HG001fluc) signatures. NES, normalized enrichment score, p-val, GSEA p-value. None of the pathways are already associated with oxacillin/flucloxacillin resistance.

Figure 7. Pathway Signature Comparison Identifies Top Pathway Candidates Across Antibiotic Susceptibilities and Responses

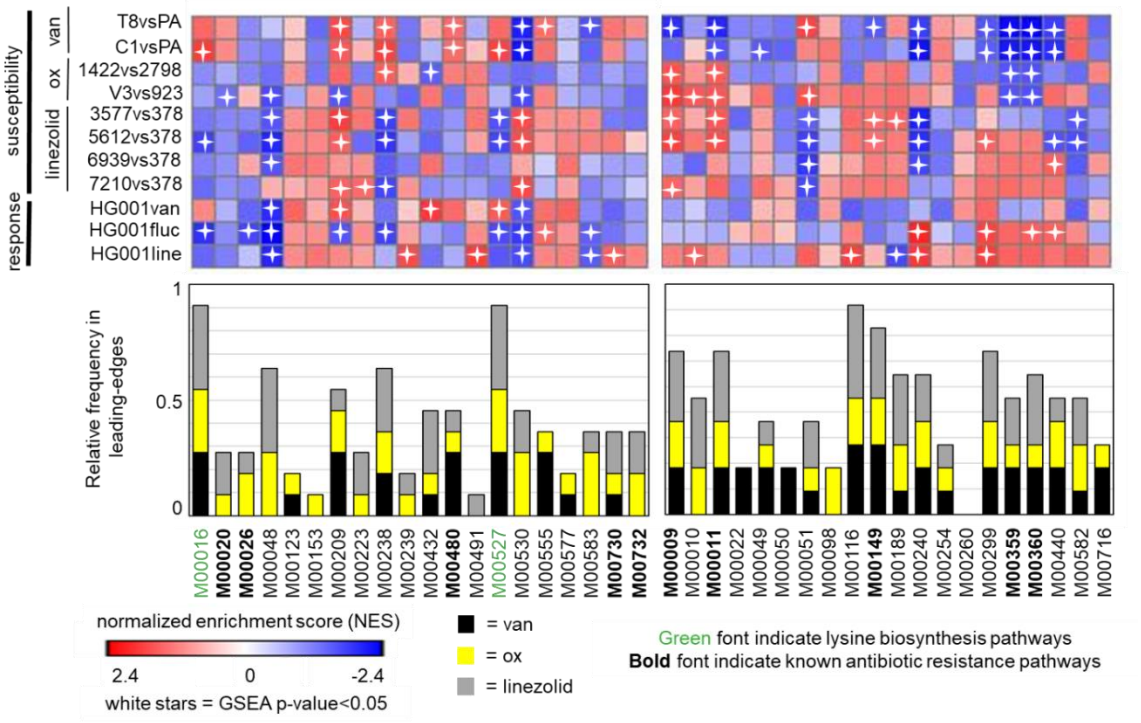


Gene Set Enrichment Analysis (GSEA) calculates normalized enrichment score (NES) and identifies leading-edge pathways between *vraS*-driven resistance panels (queries) and 11 antibiotic (vancomycin (van), oxacillin (ox), flucloxacillin, or linezolid treated and untreated) susceptibility or response pathway signatures (references) from which relative frequency of pathway in leading-edges across the 11 reference signatures were calculated, to determine which pathways may be best to target to overcome multiple antibiotic resistances.

### 3.2.4. Antibiotic Sensitivity Changes from Targeting Lysine Biosynthesis Provides Experimental Evidence to Support Computational Findings

My computational findings predicted that lysine biosynthesis activities might be involved in resistance to specific antibiotics, so I hypothesized that lysine biosynthesis plays some role in antibiotic sensitivity. To support this hypothesis, I examined whether manipulation of lysine biosynthetic pathway alters response of a sensitive strain towards vancomycin, oxacillin, or linezolid treatment. Aspartate kinase catalyzes the first step in the lysine biosynthesis pathway and aspartate kinase activity is inhibited by the final

product lysine by feedback inhibition (Figure 8A)[118]. Therefore, I conducted Kirby-Bauer disk diffusion experiments utilizing changes in the zone of inhibition (*i.e.*, distance of no growth from antibiotic disk) as an indicator of the effect of amino acid treatment on *S. aureus*'s sensitivity to individual antibiotics (vancomycin, oxacillin, or linezolid) as seen in Figure 8B. I observed a statistically significant (two-tailed Welch's T-test p-value<0.05) increase in sensitivity, as seen by increased zone of inhibition, for lysine compared to vehicle treated samples during vancomycin exposure (Figure 8C). I saw no change in vancomycin challenged, aspartate treated samples where I might expect to see increased resistance (*i.e.*, smaller average zone of inhibition). For oxacillin exposure, I observed significant increases in sensitivity for both lysine and aspartate treatment. For linezolid exposure, I noted a statistically significant increase in sensitivity in aspartate compared to vehicle treated samples and no change in sensitivity for lysine treated samples. For control purposes, I first repeated the disk diffusion experiment using phenylalanine treatment as a negative control, since the phenylalanine biosynthesis pathway (M00024) did not have statistically significant changes in activity for any dataset (data not shown) and I found no change in sensitivity to vancomycin, oxacillin, or linezolid (T-test p-value>0.204, Figure 8C) with phenylalanine treatment. Second, to confirm that there are no effects from using vehicle treated rather than no vehicle treatment (*i.e.*, tryptic soy agar only) samples for controls, I compared triplicate no treatment plates to vehicle treated plates and found no change in the average zone of inhibitions for any antibiotic (T-test p-value>0.492).

Figure 8. Lysine Biosynthesis from Aspartate is Involved in Vancomycin, Oxacillin, and Linezolid Sensitivity

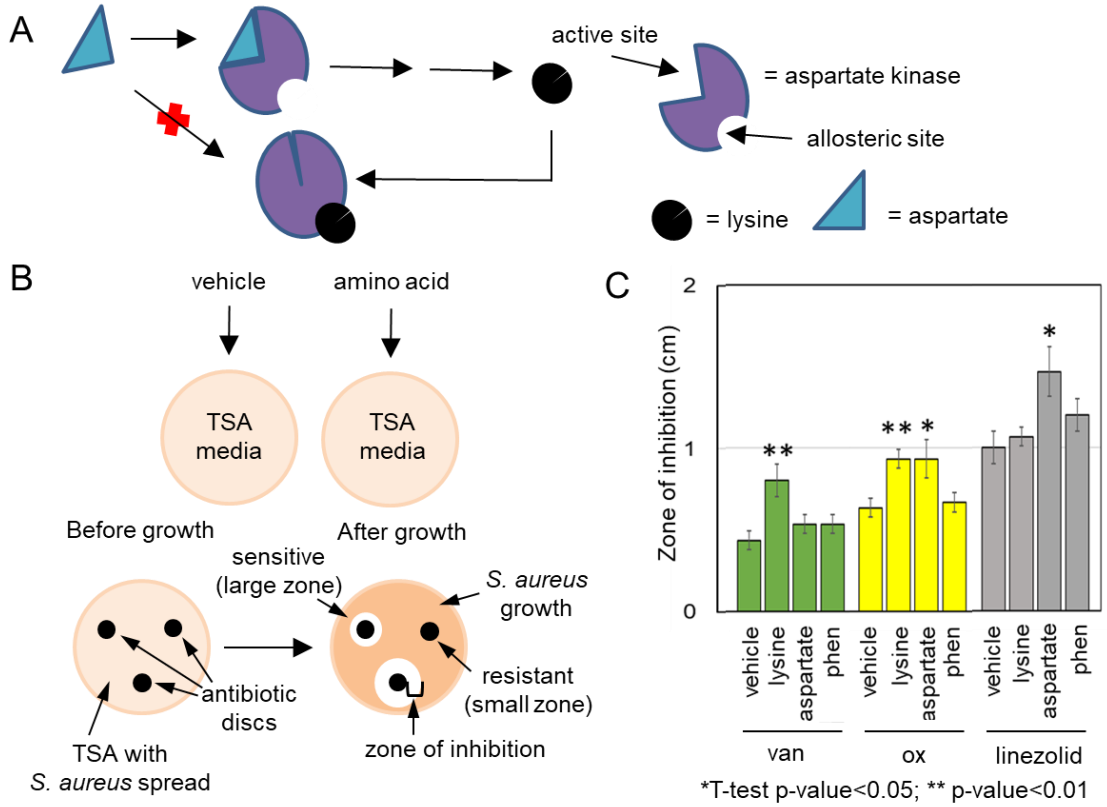


(A) Schematic of lysine biosynthesis from aspartate pathway where aspartate, the initial substrate for lysine biosynthesis, is modified by aspartate kinase for conversion into lysine, which inhibits aspartate kinase, reducing pathway activity under high concentrations of lysine and increasing activity under aspartate treatment. (B) Schematic of disk diffusion experiment where tryptic soy agar (TSA) plates are treated with vehicle (water) or 20mg/mL of amino acid (lysine, aspartate, or phenylalanine) then *S. aureus* is spread across each plate and antibiotic disks applied prior to incubation. After growth, zone of inhibition (*i.e.*, distance of no growth from edge of antibiotic disk to closest visible growth) measurements are taken for each disk to determine changes in sensitivity with larger zones representing more sensitivity. (C) Changes in the average zone of inhibition from triplicate cultures of the same *S. aureus* strain plated on TSA treated with vehicle (water) or 20 mg/mL of lysine, aspartate, or phenylalanine (as a negative control) then exposed to 30mcg vancomycin (van), 1mcg oxacillin (ox), or 30µg linezolid confirms biological relevance of lysine biosynthesis pathway in antibiotic sensitivity.

## 3.3.Discussion

### 3.3.1. Summary of Main Findings

Managing antibiotic resistant infections is a major ongoing clinical challenge[8,9,11,17-19]. My current understanding of resistance mechanisms is based on individual genes and pathway enrichment analysis based on statistical threshold that neglect genes with insufficient changes in expression. While these approaches have been successful in identifying resistance mechanisms in some infections, another approach might provide different perspectives on potential mechanisms of resistance for different antibiotic classes. Here, I used GSEA, a well-established computational tool that takes into account all changes including those normally do not satisfy arbitrary cutoff in traditional approach when calculating enrichment, to examine antibiotic resistance, and am the first to use GSEA on *S. aureus*. I am also the first to apply a computational approach using GSEA that defines and compares pathway signatures to detect activity changes associated with antibiotic resistance and susceptibility across spectra of antibiotic classes. I began this study by applying my pathway signature approach to identify pathways associated with *vraS*-driven resistance. It was shown that my approach was able to detect the pathways containing the known associations to resistance via single gene expression analysis (reported using >2 fold-change cutoff between VC40 and Δ*mutS*), such as up-regulated histidine biosynthesis[76,216-218] and down-regulated amino-acyl tRNA biosynthesis and succinate dehydrogenase[101], as one of the highly enriched pathways in my analyses (Table 4). I also identified pathways which had no previous association with antibiotic resistance, such as lysine biosynthesis pathways (Table 4). I was able to find my up-regulated resistance pathway panel in both *graSR*-driven

resistance pathway signatures (Figure 4A and Figure 4B). More specifically the up-regulation of histidine and lysine biosynthesis was consistently found to be significantly enriched (Table 7) and was one of the best able to separate samples by resistance levels (Figure 4C). When I repeated application of my approach to examine vancomycin susceptibility and response, I again detected several significantly enriched pathways that correspond to the pathways with documented gene mutations or pathway enrichment analyses associated with the vancomycin resistance (*i.e.*, VISA) phenotype (Table 9). These pathways included up-regulation of VraSR two component system and down-regulation of energy production pathways[210-213], for example F-type ATPase, and translation processes[214,215], such as amino-acyl tRNA biosynthesis, resulting in the slow growing phenotype reported in VISA strains clinically[56]. Among identified pathways with significant enrichment were pathways with no previous association with vancomycin resistance, such as up-regulated threonine biosynthesis and D-methionine transport (Table 9). Taken together, these results highlight the ability of my approach to detect pathways associated with antibiotic resistant phenotypes.

Next, I applied my pathway signature approach to several mRNA datasets examining resistance and/or response across different antibiotic classes to identify top pathway candidates affecting development of antibiotic resistance, which was the first analysis of its kind to the best of my knowledge. I then compared *vraS*-driven resistance panels to antibiotic (vancomycin, oxacillin, and linezolid) susceptibility and response signatures and revealed valuable insight into activity changes associated with the development of several antibiotic resistances. First, I found similarities that were usually significant between *vraS*-driven resistance panels and both vancomycin susceptibility and

response signatures (Figure 6). This is an indication of similar activity changes in the same pathways across signatures, as I observed for example in the osmoprotectant transport system (M00209), contribute to vancomycin resistance in Figure 7. Further in Figure 6, the up-regulated *vraS*-driven resistance panel resulted corresponding pathway activity changes in oxacillin and linezolid showed all 6 down regulated activities, representing a complete reversal (*i.e.*, enriched in the opposite tail, such as up-regulated panel enriched in negative tail). It also showed that the down regulated *vraS*-driven resistance panel exhibited only a half of oxacillin and linezolid susceptibility datasets showed up-regulated pathway activities, representing a 50% partial reversal. These results support previously reported findings of the occasional resistance "see-saw" between vancomycin and oxacillin or linezolid[56,190,191]. When comparing individual pathway activity changes in *vraS*-driven resistance panel pathways across antibiotic susceptibility and response signatures, my approach identified lysine biosynthesis as the top pathway candidate to target experimentally to alter antibiotic sensitivity (Figure 7). While lysine biosynthesis has not been previously implicated in antibiotic resistance directly, aspartate has been shown to play a role in biofilm formation for *S. aureus*[219] and biofilms are known for their antibiotic resistance[220-223]. Specifically, D- and L- isoforms of aspartate inhibited *S. aureus* biofilm formation in tissue culture plates[219]. Further, lysine biosynthesis may contribute to cell wall formation in several different ways. Lysine biosynthesis generates UDP-N-acetylmuramoyl-L-alanyl-γ-D-glutamyl-meso-2,6-diaminopimelate, a precursor for peptidoglycan biosynthesis. Lysine itself is part of the N-acetylmuramic acid pentapeptide that is used for cell wall cross-linkage. Although my pathway centric computational approach was successful in identifying a pathway that

may play a role in development of antibiotic resistance, the determination of exact mechanisms behind the involvement of lysine biosynthesis in antibiotic sensitivity is beyond the scope of my approach. However, it was clear from the high relative frequency in leading-edges across antibiotic susceptibility and response signatures that lysine biosynthesis was involved in antibiotic sensitivity somehow (Figure 7). Therefore, I hypothesized lysine biosynthesis would make a good target to alter antibiotic sensitivity and demonstrated this experimentally (Figure 8).

### 3.3.2. Implications, Limitations, and Other Considerations

My pathway signature approach provides insight into a different paradigm for generating antibiotic resistant phenotypes. Most resistance mechanisms identified to date focus around 1) an enzyme that inactivates the antibiotic, such as β-lactamase which cleaves β-lactam rings on penicillin and some of its derivatives[14,21], 2) a membrane transport that pumps the antibiotic out of the bacterial cell, like major facilitator superfamily multi-drug efflux proteins[49,128,224], or 3) a mutation that diminishes the binding of antibiotic agent such as altered transpeptidase from *mecA* as a MRSA mechanism[21,172]. Instead, my approach provides a broader view examining pathway activity changes that result from developing resistance. I demonstrated here that by taking this different perspective, novel targets to improve antibiotic sensitivity, such as lysine biosynthesis, can be detected.

While my computational approach can give a fresh perspective to antibiotic resistance mechanisms, my approach does not provide a complete understanding of how resistance develops. It is also true for our experimental study that showed while aspartate and lysine supplementation clearly affected antibiotic sensitivity whereas phenylalanine

supplementation had no effect, we cannot associate specific biological mechanisms with our findings. One possibility is that changes in pathway activity could lead to changes in amino acid concentrations leading to altered sensitivity. By using a single high dose of amino acid for my experiment, I assumed that regardless of variations in bioavailability across amino acids due to amino acid configuration (D- vs L-form), the bacterial cell would become saturated with either aspartate or lysine. While aspartate and/or lysine saturation would alter lysine biosynthesis pathway activity, it may also alter the activity of other pathways with shared enzymes. For example, threonine and methionine synthesis are also derived from an L-aspartate-4-semialdehyde produced in the aspartate to lysine biosynthesis pathway[225]. Aspartate kinase isozymes in *Escherichia coli* and *Corynebacterium pekinense* are inhibited by threonine and methionine[226,227] while there is no experimental evidence that aspartate kinase is inhibited by these amino acids in *S. aureus.* However, I noted increased threonine biosynthesis and D-Methionine transport pathway activities were prominent in vancomycin susceptibility, and D-Methionine transport was part of the HG001vsSG511 up-regulated panel leading-edge (Table 7). This might suggest that the resistance mechanism I identified from my computational analysis for vancomycin resistance maybe a previously unknown mechanism. It was experimentally shown that the SG511 strain, which was able to gain resistance equal to its HG001 counterpart despite having a truncated *graSR*, has different sets of up and down-regulated genes with little overlap[129]. Unfortunately, there were no threonine transport, lysine transport, or methionine biosynthesis pathways included in the KEGG pathways used in this work, so I was unable to better elucidate this resistance mechanism. However, in version 92.0 which was released on October 1, 2019, KEGG modules were

reorganized to focus on metabolism, adding in methionine biosynthesis (M00017) and removing transporter modules (*e.g.*, D-Methionine transport) and two-component system modules (*e.g.*, VraSR). This highlights the ever-changing nature of biological databases and the need for extensive analysis of databases used with my pathway signature approach since gene set properties, such as gene and pathway inclusion and overlap, substantially impact the detection ability of my approach.

My analysis also did not detect all pathways associated with antibiotic resistance that have been reported in the literature. For example, I noticed that the VraDE transporter (M00737), *vraS*driven resistance[101] and vancomycin resistance[56] was not selected as a part of pathway panels because it was not enriched enough (*i.e.*, not enough NES) although ABC transporter genes encoded by vraDE was reported to show high expression for *vraS*driven resistance[101] and vancomycin resistance[56] in microarray gene expression analyses. The observed lack of enrichment was not due to a lack of gene representation (*i.e.*, no genes) of the VraDE transporter pathway in either the KEGG knowledgebase (74 genes for M00737) or the VC40vsΔ*mutS* (7 genes) and T8vsPA (9 genes) gene signatures. Of the VraDE transport pathway genes represented in the VC40vsΔ*mutS* signature, I noted that no probes for *vraD* or *vraE* specifically were included in the dataset's platform. For the VraDE transport pathway genes represented in the T8vsPA and C1vsPA signatures, I noted that they did include probes for *vraD* or *vraE*. When looking at single gene expression for *vraD* or *vraE* from vancomycin susceptibility gene signatures, I found differential expression for *vraD* in response to vancomycin between resistant (T8 or C1) and sensitive (PA) strains was not significantly changed (C1 Welch's T-test p-value=0.092, T8 p-value=0.599) and *vraE* was significant

for C1 only (C1 p-value=0.033, T8 p-value=0.385). Further, I do not know why some pathways with known associations to antibiotic resistance in *S. aureus* via single gene expression analysis were not represented in *S. aureus* strains listed in the KEGG knowledgebase. An example is the WalKR two component system which is associated with vancomycin and daptomycin resistances[56,101], but was not included among *S. aureus* KEGG modules at the time of this work. While KEGG included some pathways regulated by WalKR, such as SaeS-SaeR staphylococcal virulence regulation (M00468), KEGG did not include all pathways reported to be regulated by WalKR, for example omitting autolysis or cell wall turnover pathways. If gene lists for missing pathways were available, they could have been incorporated into my analysis. Though annotation issues limited my achievable results, these issues did not prevent my pathway signature approach from detecting novel pathways, such as lysine biosynthesis, that were not previously detected using other computational methods. Therefore, I expect that my pathway signature approach's ability to detect enriched pathways will improve as genome and pathway knowledgebases are updated, since bacterial genomes commonly have annotation issues (*i.e.*, incomplete and inaccurate)[66,228,229] that reduce pathway database comprehensiveness (*i.e.*, fewer pathways and genes in each pathway)[64,230].

I also noted the vancomycin resistance (VanA, M00651) pathway was included among significant down-regulated pathways in all vancomycin response signatures from my vancomycin susceptibility dataset regardless of strain resistance. This finding is unexpected considering the *vanA* operon should be expressed more during vancomycin treatment[56]. To explain this, I examined individual gene expression for the *vanA* operon and found a small set of probes, including the one detecting *vanA* itself, detect expression

(APPENDIX A). I could not find any homologs close enough to these probe sequences to explain unintended hybridization to non-targeted proteins using Basic Local Alignment Search Tool (BLAST). Though I could not explain this finding, I noted that *vanA* expression should be detectable during vancomycin treatment if T8, C1, and/or PA use it as a resistance mechanism. This suggests that any resistance in these strains is derived from a different mechanism, which is not surprising if they are truly VISA strains.

### 3.3.3. Future Directions

This innovative project holds great potential to improve clinical treatment options for antibiotic resistant infections. For example, experimental development of therapeutics that target top pathway candidates, like lysine biosynthesis, identified here could improve antibiotic sensitivity in *S. aureus*. More *in vitro* experimental research is needed to better understand the meaning of my experimental results. Further experimental research could examine examining 1) antibiotic response over a time course and with range of amino acid doses (*i.e.*, titration), 2) kinetics of enzymes in the lysine pathway starting with aspartate kinase, and/or 3) binding affinity examination of strains with site specific mutagenesis of genes in the lysine biosynthesis pathway, is needed to elucidate the exact mechanism of involvement. These studies could involve site-specific mutagenesis (*i.e.*, creation of genetic mutants) where individual enzymes within lysine biosynthesis pathways could be altered using CRISPR-Cas9[231-233] and alterations in gene expression, pathway activity, biochemical levels, and phenotypic features like thickened cell walls and sensitivity measurements can be measured to establish the exact mechanism behind lysine biosynthesis involvement in antibiotic resistance. A good place to start based on my results in this work is with site-specific mutagenesis on the meso-2,6-

diaminoheptanedioate intermediate and seeing if this changes sensitivity to vancomycin since, according to KEGG, this intermediate in the lysine biosynthesis pathway can also be used for peptidoglycan biosynthesis, major cell wall component that is associated with increased cell wall thickening, characteristic of VISA strains clinically[56]. To evaluate the success lysine and aspartate co-treatment may have *in vivo,* further experiments beginning with animal models with resistant *S. aureus* infections are needed. For example, infection recovery studies using *in vivo* animal models, where animals are infected with *S. aureus,* either a sensitive or resistance strain, and some infected animals are provided lysine or aspartate supplementation along with their prescribed antibiotic (*e.g.*, lysine supplementation with vancomycin treatment). The expected outcome of these experiments, based on the results in this current investigation, should be that animals with lysine or aspartate supplementation would recover more rapidly than animals given antibiotics alone. Thus, providing evidence of our pathway signature approach's predictive ability. If further experimentation reveals specific lysine biosynthesis pathway genes involved in antibiotic resistance, targeted interventions could be developed based on their gene expression pattern. For example, if a lysine biosynthesis gene is overexpressed, it can be silenced using RNAi approaches while an under-expressed gene could become overexpressed with additional gene copies delivered via bacteriophage therapy. Regardless of how lysine biosynthesis is altered, human clinical trials would be needed before therapeutics that target lysine biosynthesis could be implemented on a global scale.

Though applied here to *S. aureus* only, my pathway signature approach is directly applicable to other antibiotic resistant infections, potentially producing valuable

therapeutic directions that could revolutionize the management of deadly infectious diseases in this era of evolving antibiotic resistance. Thus, I recommend immediate application of my approach to examine antibiotic resistance in clinically relevant infections caused by organisms reported by the Center for Disease Control and Prevention as major public threats , such as *Acinetobacter spp.*, *Mycobacterium tuberculosis,* and *Clostridium difficile*[11]. Regardless of the intended application, a thorough review of available pathway knowledge bases specific to the application is needed to ensure optimal pathway signature creation since knowledgebases vary and are continually updated. Consideration should be given to gene coverage, gene overlap, pathway inclusion, and strain/tissue variation. This is especially important when applying this approach to examining other antibiotic resistant infections as knowledgebases may differ in their contents across bacterial species[230]. The pathway knowledgebase selection process, along with the creation of pathway signatures themselves can be daunting and time-consuming, particularly for biologists without user-friendly software. While my pathway signature approach could be used by laboratory and clinical biologists directly after conducting a mRNA expression study as part of or in addition to RNA-seq analysis software, such as Rockhopper[234,235], the approach can also be used by computational biologists for data mining as done in this dissertation. I therefore recommend development of publicly available software, either in collaboration with or in parallel to what is available for human disease at the Broad Institute in the MSigDB[152]. Accomplishing this will require development of user-friendly software for pathway signature generation, and ongoing semi-automated expansion and maintenance of a multi-knowledgebase catalog of pathway sets across biological life. Further, use of

pathway signatures could be developed into a diagnostic tool to identify resistance clinically. While my study here ran into sample size limitations, if a dataset were generated with enough mRNA expression data to produce a successful cross-validation model, an average multi-variable logistic equation could be generated to predict resistances. If computing power were improved to be able to examine genome-wide expression of a patient's sample without the immobile, expensive chip technology prominent today, the logistic equation could become the basis for improved diagnostic methods for antibiotic resistant infections. Taken together, this work could potentially lead to the development of new clinical advancements, both in drug development and diagnostics, to treat *S. aureus* infections. These future directions have the potential to revolutionize how humanity detects, predicts, and interprets pathway activity from mRNA expression in several areas throughout microbial science and significantly enhances understanding of cellular biology. Antibiotic resistant infections continue to be a foremost medical challenge. My work here addresses this challenge by 1) introducing a computational approach which define pathway signatures to characterize molecular changes associated with mutation-driven resistance and vancomycin, oxacillin, and linezolid susceptibilities and responses in *S. aureus*, and 2) using that approach to identify known and novel pathways that can be targeted to improve antibiotic sensitivity in *S. aureus*. Further, I lysine biosynthesis is specifically observed to affect vancomycin, oxacillin, and linezolid sensitivity, suggesting it could become a useful co-therapy target to treat resistant infections clinically. Examining the antibiotic resistance mechanisms that involve lysine biosynthesis may lead to the development of new co-therapeutic options to preclude or overcome antibiotic resistance.

## 3.4.Methods

### 3.4.1. mRNA Expression Resources

I used GSEA to define pathway signatures (*i.e.*, ranked lists of pathways by changes in activity based on differential mRNA expression) from Kyoto Encyclopedia of Genes and Genomes (KEGG) *S. aureus* pathways (APPENDIX F) and mRNA expression data (Table 13) as illustrated in Figure 9. More details on all Gene Expression Omnibus (GEO) datasets are found in APPENDIX A.

Figure 9. Schematic Overview of Approach

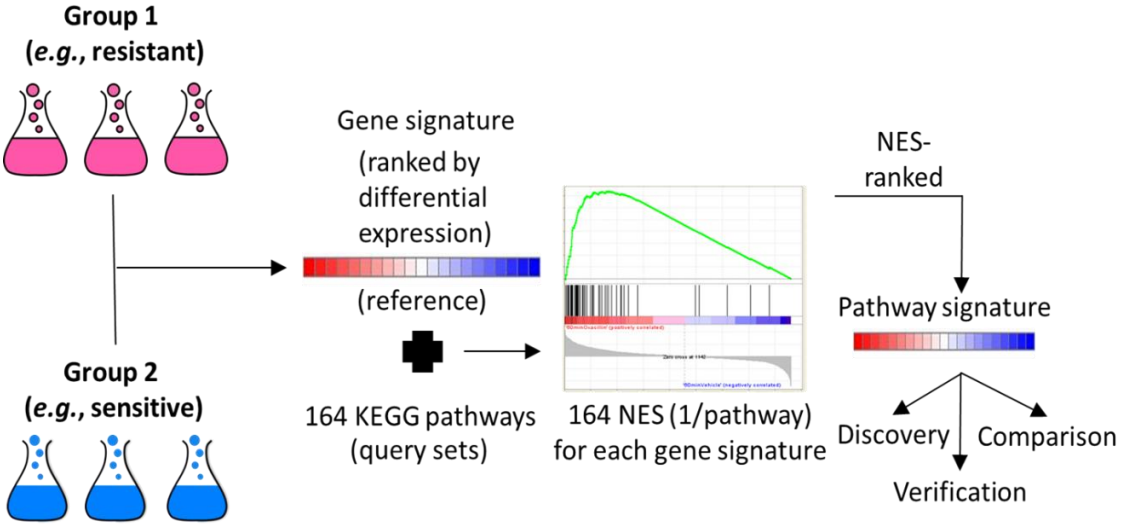


Gene signatures are ranked lists of genes from high (red) to low (blue) differential mRNA expression between Group 1 and Group 2 based on an appropriate statistical method, such as T-score. Gene signatures are used as references for Gene Set Enrichment Analysis (GSEA) against 164 Kyoto Encyclopedia of Genes and Genomes (KEGG) *S. aureus* pathways (APPENDIX F) as individual query sets to generate 164 normalized enrichment score (NES), one per pathway, representing the extent of enrichment. Pathways with the most differential activity change have NES furthest away from zero (white). Pathway signatures (*i.e.*, pathway lists ranked by NES from high (red) to low (blue) differential activity between Group 1 and Group 2) are used in this study for three purposes: 1) discovery of pathway activity changes between two experimental groups, 2) verification of discovered findings, and 3) comparison to other pathway signatures.

Table 13. *S. aureus* Datasets Utilized for this Study

| T | Use | Dataset | Description | Group 1 | Group 2 | S | Ranking |
|---|---|---|---|---|---|---|---|
| None | D | GSE46887[101] | Triplicate untreated cultures of resistant (vanco and daptomycin) VC40[1] (VraSR mutation) and sensitive Δ*mutS* logged with DNA pool[2] | VC40 | Δ*mutS* | 6 | T-test |
| | V | GSE50842[129] | Duplicate untreated cultures of resistant (vanco and daptomycin) progeny of both HG001 (GraSR) and SG511[3] (truncated GraSR) logged to their respective sensitive ancestor strains[2] | HG001 | SG511 | 4 | FC |
| | V | GSE26016[76] | Unlogged triplicate HG001 (WT) and Δ*graSR* cultures[4] | WT | Δ*graSR* | 6 | T-test |
| Vanco | D, C | GSE26400 | Triplicate replicates of vanco untreated or treated (4mM PA, 16mM C1, 32mM T8) samples of vanco resistant C1 or T8 logged to its respective PA sample by treatment[5] over a time course[6] | T8 | PA | 6 | T-test |
| | V, C | | | C1 | PA | 6 | T-test |
| Oxacillin | C | GSE26282 | Triplicate replicates of untreated or oxacillin treated resistant samples with 2798 logged to 1422 by treatment[5] over a time course[6] | 1422 | 2798 | 6 | T-test |
| | C | GSE26258 | Five replicates of oxacillin treated or untreated samples of oxacillin resistant V3 and 923 logged by treatment[5] | V3 | 923 | 10 | T-test |
| Linezolid | C | GSE26358 | Duplicate replicates of linezolid untreated or treated samples of resistant 3577, 5612, 6939, or 7210 logged to sensitive 378 by treatment[5] over a time course[6] | 3577 | 378 | 4 | FC |
| | C | | | 5612 | 378 | 4 | FC |
| | C | | | 6939 | 378 | 4 | FC |
| | C | | | 7210 | 378 | 4 | FC |
| Many | C | GSE70040 [77] | Unlogged cultures[6] of antibiotic sensitive strain HG001 either vanco, fluc, or linezolid treated or untreated over a time course[7] | Vanco | Untreated[8] | 18 | T-test |
| | C | | | Fluc | Untreated[8] | 18 | T-test |
| | C | | | Linezolid | Untreated[8] | 18 | T-test |

C, comparison of pathway signature to pathway panels defined in discovery dataset; D, discovery dataset used to define pathway panels used for comparison to all other datasets; FC, fold change; fluc, flucloxacillin; S, number of samples used; T, treatment (datasets with treated samples also have untreated samples); V, verification of discovery findings; vanco, vancomycin; WT, wild-type.

[1] Background strain NCTC8325

[2] Values were used as provided by Gene Expression Omnibus

[3] HG001 is a derivative (a *rsbU*+ variant) of strain NCTC 8325[77]

[4] Samples were z-scored across all samples for normalization
[5] Example log by treatment as provided by Gene Expression Omnibus: log2(T8 treated/PA treated), log2(T8 untreated/PA untreated). Example re-log by strain as used in this study: log2(T8 treated/T8 untreated), log2(PA treated/PA untreated).
[6] 60min samples were used
[7] Samples grown to exponential phase in tryptic soy broth were used for this study
[8] Same 15 untreated samples used

To identify molecular changes associated with antibiotic resistance I searched the GEO repository[236,237] on June 17 and December 29, 2019. From this I found nine datasets for use in my study (Table 13). I began by exploring mutation-driven resistance as produced by known or established *vraSR* or *graSR* mutations using three datasets (GSE46887[101] GSE50842[129], and GSE26016[76]) that compared gene expression between resistant (higher *vraSR* or *graSR* function) and sensitive (lower *vraSR* or *graSR* function) strains under the same treatment conditions. GEO provided expression data for GSE46887 and GSE50842 samples as log10 ratios of resistant strains to either a genomic DNA pool or sensitive strains, respectively, representing strain differences that reveal resistance mechanisms in individual strains, so I converted these ratios to log2 ratios for consistency across data used in this study. GEO provided expression data for GSE26016 as unlogged intensities so I z-scored across all samples so that all data is normalized prior to use.

I then examined activity changes in *S. aureus* under antibiotic treatment conditions (*i.e.*, response). To do this, I first used four datasets (GSE26400, GSE26258, GSE26282, and GSE26358) that examined gene expression between treated and untreated samples of strains with varying resistance levels. GEO provided expression data for these datasets as log2 ratios of high resistant to low resistant strains (*e.g.*, T8 treated/PA treated, T8 untreated/PA untreated). Fortunately, GEO also provided unlogged intensities for these datasets, so I used intensities to calculate log2 ratios of treated versus untreated for each strain separately (*e.g.*, T8 treated/T8 untreated, PA treated/PA untreated), revealing response mechanisms for individual strains, for consistency across data used in this study. Further, I used one dataset (GSE70040[77]) to explore antibiotic

response in a sensitive strain. For this dataset, GEO provided unlogged intensities so I z-scored across all samples for normalization prior to use. For all datasets, if a locus tag had multiple platform probes, I selected the probe with the highest coefficient of variation to represent that locus tag to remove locus tag replicates in gene signatures. Individual dataset overviews with experimental information including strain, platform, and media and normalization details are provided in APPENDIX A.

### 3.4.2. Signature Definition and Generation

From the datasets found in GEO, I defined gene signatures (*i.e.*, locus tag lists ranked by differential gene expression as defined by appropriate statistic, Figure 9). Probes for each platform are converted to locus tags (*e.g.*, SAR1563) when necessary using GEO provided platform annotation files. Justification for my use of locus tags is found in APPENDIX B. If multiple probes have the same locus tag, I used the one with the highest coefficient of variation across all dataset samples and remove locus tag replicates in gene signatures. Using gene signatures individually, I defined pathway signatures by comparing a gene signature to each one of 164 KEGG (version 87.0, APPENDIX F)[194,195] pathways using GSEA, javaGSEA Desktop Application version 3.0 from Broad Institute, to calculate NES from 1000 locus tag permutations by which I rank the 164 pathways (Figure 9). Rationale for my use of KEGG is located in APPENDIX B. I purposely selected only KEGG pathways with at least 10 locus tags, a requirement for accurate GSEA calculations, gathered across any one of the 10 fully sequenced *S. aureus* strains available with varying methicillin and vancomycin sensitivities used to design platform probes for datasets used in this study: sensitive to methicillin and vancomycin (MSSA476, NCTC8325), MRSA strains sensitive to vancomycin (COL, N315, MW2,

Newman, MRSA252, USA300_TCH1516, and USA300FPR3757), and MRSA/VISA (Mu50), to maximize my approach's detection potential.

### 3.4.3. Defining Pathway Panels

To detect pathway activity changes associated with antibiotic resistance, I defined two *vraS*-driven resistance panels (Table 4) by selecting the 20 most up- and down-regulated pathways (*i.e.*, best NES) from the VC40vsΔ*mutS* pathway signature. I used the same selection process on the T8vsPA pathway signature to define two vancomycin susceptibility panels (Table 8) to detect pathway activity changes associated with vancomycin susceptibility.

### 3.4.4. Comparison Across Pathway Signatures

To verify the accuracy of pathway panel predictions, I first performed GSEA between *vraS*-driven resistance panels and HG001vsSG511 and WTvsΔ*graSR* pathway signatures. I repeated this process using vancomycin susceptibility panels and the C1vsPA pathway signature. Random modelling is done by using 1000 randomly selected pathway panels consisting of 20 pathways each selected from the 164 KEGG pathways used to generate pathway signatures as queries for GSEA against HG001vsSG511, WTvsΔ*graSR*, and C1vsPA as reference signatures, generating a null distribution of NES, to which I compared achieved NES for each reference pathway signature and count the number of equal or better NES to estimate significance (*i.e.*, distribution p-value). I also utilized ROC curve analysis[197,238] for individual pathway panels via easyROC, version 1.3 to quantify the ability of each pathway panel to separate samples by resistance level through AUROC curve calculation[197,208,238,239].

To compare pathway signatures, I used *vraS*-driven resistance panels as query sets for GSEA to individual antibiotic susceptibility (vancomycin: T8vsPA and C1vsPA; oxacillin: 1422vs2798 and V3vs923; and linezolid: 3577vs378, 5612vs378, 6939vs378, and 7210vs378) and response (HG001van, HG001fluc, and HG001line for vancomycin, flucloxacillin, and linezolid, respectively) pathway signatures as references. Heat maps were generated by GENE-E[240].

3.4.5. Disk Diffusion Validation of Computational Predictions

To establish biological relevance of predictions made by my pathway signature approach, I performed Kirby-Bauer disk diffusion tests to observe sensitivity changes between vehicle (water) and amino acid (lysine, aspartate, or phenylalanine) treatment during antibiotic exposure. I prepare amino acid (DL-Aspartic Acid, L-Lysine, or DL-Phenylalanine powder acquired from Carolina #843600 resuspended in sterile water, then filter sterilized) solutions and applied equal amounts of either sterile water or amino acid solution (final concentration on plate at 20mg/mL) separately to a pre-manufactured tryptic soy agar (TSA, Carolina #822022) plate. Next, I applied equal amounts of *S. aureus* (Carolina # 155554A) from one of triplicate overnight TSB cultures to each plate (*i.e.*, technical replicates) and allowed to dry before applying 30mcg (*i.e.*, μg) vancomycin (Carolina #843600), 1mcg oxacillin (Carolina #806278), and 30μg linezolid (Fisher #BD231761) disks and incubated overnight at 37°C with standard atmospheric conditions.

# CHAPTER 4

# CONCLUSION

In prior chapters, I described *S. aureus* as a causative agent of potentially life-threatening infections and discussed how modern medicine relies on antibiotic therapies, like vancomycin, oxacillin, and linezolid, to cure *S. aureus* infections. I provided an overview of the global antibiotic resistance problem menacing humanity, increasing mortality from once curable infections. Unfortunately, gene level examination alone has been only partially effective in identifying antibiotic resistance mechanisms, so I decided to take a broader perspective by examining pathway activity. To do this, I discussed the rationale and steps for a pathway signature approach that identified pathways with the most differential activity from mRNA expression data and applied it to elucidate pathway activity changes associated with mutation-driven resistance and vancomycin susceptibility. I then compared pathway activity changes associated with mutation-driven resistance to changes associated with vancomycin, oxacillin, or linezolid susceptibilities and responses to identify top pathway candidates for further laboratory characterization. I used this analysis to select lysine biosynthesis and demonstrated the biological relevance of this prediction to improve antibiotic sensitivity using disk diffusion. In this chapter, I summarized the importance and share future directions for my work.

This work was the first to use Gene Set Enrichment Analysis (GSEA), a well-established computational tool that does not neglect genes with insignificant changes when calculating enrichment, to examine antibiotic resistance in *Staphylococcus aureus* (*S. aureus*). Further, I was the first to apply a new computational approach using GSEA that defines and compares pathway signatures to detect activity changes associated with

antibiotic resistance that is immediately applicable to examine activity changes associated with resistance in other bacterial pathogens. This has the potential of providing valuable computational predictions to expedite the development of co-therapy options to overcome or preclude antibiotic resistance. By applying my pathway signature approach to multiple resistance studies across different antibiotic classes to identify pathways affecting development of antibiotic resistance, I established a precedence for this type of analysis in the field of microbiology. I am already applying my pathway signature approach to identify potential co-therapeutic targets associated with antibiotic resistance in several other pathogens, such as *Pseudomonas aeruginosa*, *Escherichia coli*, and *Streptococcal* species. My innovative computational approach can also be applied to other microbial questions outside of antibiotic resistance that require combining mRNA expression and biological pathway activity analyses. For example, I am starting to apply my approach to analyze mRNA expression differences between bacterial strains in cow lumen to identify pathway targets to reduce methane production, a known greenhouse gas and climate change contributor. Finally, my computational approach uncovered several top pathway candidates as potential co-therapeutic targets, such as lysine biosynthesis, to overcome antibiotic resistance in *S. aureus*. I successfully verified the biological relevance for lysine biosynthesis experimentally. With more experimental work, co-therapies targeting lysine biosynthesis and/or other top pathway candidates identified here can be developed and have the potential to save thousands of lives from antibiotic resistant infections. When the gravity of the potential of my results in *S. aureus* presented here is compounded by the breath of microbial work using my approach currently ongoing and proposed for the future, the impact of this dissertation work is truly exciting.

# REFERENCES


1. Govindarajan R, Duraiyan J, Kaliyappan K, Palanisamy M. Microarray and its applications. *J Pharm Bioallied Sci.* 2012;4(Suppl 2):S310-312.
2. Jaksik R, Iwanaszko M, Rzeszowska-Wolny J, Kimmel M. Microarray experiments and factors which affect their reliability. *Biol Direct.* 2015;10:46.
3. Madigan MT, Bender KS, Buckley DH, Sattley WM, Stahl DA. *Brock biology of microorganisms.* Fifteenth edition. ed. Ny, Ny: Pearson; 2018.
4. Sender R, Fuchs S, Milo R. Are We Really Vastly Outnumbered? Revisiting the Ratio of Bacterial to Host Cells in Humans. *Cell.* 2016;164(3):337-340.
5. Thorpe KE, Joski P, Johnston KJ. Antibiotic-Resistant Infection Treatment Costs Have Doubled Since 2002, Now Exceeding $2 Billion Annually. *Health Aff (Millwood).* 2018;37(4):662-669.
6. Health NIo. Understanding emerging and re-emerging infectious diseases. *Biological sciences curriculum study NIH Curriculum Supplement Series National Institutes of Health, Bethesda, MD.* 2007.
7. Price LB, Hungate BA, Koch BJ, Davis GS, Liu CM. Colonizing opportunistic pathogens (COPs): The beasts in all of us. *PLoS Pathog.* 2017;13(8):e1006369.
8. Woolhouse M, Waugh C, Perry MR, Nair H. Global disease burden due to antibiotic resistance - state of the evidence. *J Glob Health.* 2016;6(1):010306.
9. Nathan C, Cars O. Antibiotic resistance--problems, progress, and prospects. *N Engl J Med.* 2014;371(19):1761-1763.
10. Chiavazzo E, Isaia M, Mammola S, et al. Cave spiders choose optimal environmental factors with respect to the generated entropy when laying their cocoon. *Sci Rep.* 2015;5:7611.
11. Ventola CL. The antibiotic resistance crisis: part 1: causes and threats. *P T.* 2015;40(4):277-283.
12. Van Boeckel TP, Gandra S, Ashok A, et al. Global antibiotic consumption 2000 to 2010: an analysis of national pharmaceutical sales data. *Lancet Infect Dis.* 2014;14(8):742-750.
13. Kapoor G, Saigal S, Elongavan A. Action and resistance mechanisms of antibiotics: A guide for clinicians. *J Anaesthesiol Clin Pharmacol.* 2017;33(3):300-305.
14. Pantosti A, Sanchini A, Monaco M. Mechanisms of antibiotic resistance in Staphylococcus aureus. *Future Microbiol.* 2007;2(3):323-334.
15. Velkov T, Roberts KD, Nation RL, Thompson PE, Li J. Pharmacology of polymyxins: new insights into an 'old' class of antibiotics. *Future Microbiol.* 2013;8(6):711-724.
16. Rossolini GM, Arena F, Pecile P, Pollini S. Update on the antibiotic resistance crisis. *Curr Opin Pharmacol.* 2014;18:56-60.
17. Woolhouse M, Farrar J. Policy: An intergovernmental panel on antimicrobial resistance. *Nature.* 2014;509(7502):555-557.
18. Laxminarayan R, Matsoso P, Pant S, et al. Access to effective antimicrobials: a worldwide challenge. *Lancet.* 2016;387(10014):168-175.
19. Munita JM, Arias CA. Mechanisms of Antibiotic Resistance. *Microbiol Spectr.* 2016;4(2).
20. Golkar Z, Bagasra O, Pace DG. Bacteriophage therapy: a potential solution for the antibiotic resistance crisis. *J Infect Dev Ctries.* 2014;8(2):129-136.
21. Peacock SJ, Paterson GK. Mechanisms of Methicillin Resistance in Staphylococcus aureus. *Annu Rev Biochem.* 2015;84:577-601.

22. Grundmann H, Aires-de-Sousa M, Boyce J, Tiemersma E. Emergence and resurgence of meticillin-resistant Staphylococcus aureus as a public-health threat. *Lancet.* 2006;368(9538):874-885.
23. de Kraker ME, Stewardson AJ, Harbarth S. Will 10 Million People Die a Year due to Antimicrobial Resistance by 2050? *PLoS Med.* 2016;13(11):e1002184.
24. Ippolito G, Leone S, Lauria FN, Nicastri E, Wenzel RP. Methicillin-resistant Staphylococcus aureus: the superbug. *Int J Infect Dis.* 2010;14 Suppl 4:S7-11.
25. Cosgrove SE, Qi Y, Kaye KS, Harbarth S, Karchmer AW, Carmeli Y. The impact of methicillin resistance in Staphylococcus aureus bacteremia on patient outcomes: mortality, length of stay, and hospital charges. *Infect Control Hosp Epidemiol.* 2005;26(2):166-174.
26. Bartlett JG, Gilbert DN, Spellberg B. Seven ways to preserve the miracle of antibiotics. *Clin Infect Dis.* 2013;56(10):1445-1450.
27. Gould IM, Reilly J, Bunyan D, Walker A. Costs of healthcare-associated methicillin-resistant Staphylococcus aureus and its control. *Clin Microbiol Infect.* 2010;16(12):1721-1728.
28. Gould IM. Costs of hospital-acquired methicillin-resistant Staphylococcus aureus (MRSA) and its control. *Int J Antimicrob Agents.* 2006;28(5):379-384.
29. Kopp BJ, Nix DE, Armstrong EP. Clinical and economic analysis of methicillin-susceptible and -resistant Staphylococcus aureus infections. *Ann Pharmacother.* 2004;38(9):1377-1382.
30. Holden MT, Feil EJ, Lindsay JA, et al. Complete genomes of two clinical Staphylococcus aureus strains: evidence for the rapid evolution of virulence and drug resistance. *Proc Natl Acad Sci U S A.* 2004;101(26):9786-9791.
31. Jensen SO, Lyon BR. Genetics of antimicrobial resistance in Staphylococcus aureus. *Future Microbiol.* 2009;4(5):565-582.
32. Skinner D, Keefer CS. Significance of bacteremia caused by staphylococcus aureus: A study of one hundred and twenty-two cases and a review of the literature concerned with experimental infection in animals. *Archives of Internal Medicine.* 1941;68(5):851-875.
33. Charles HR, Thelma M. Resistance of Staphylococcus aureus to the Action of Penicillin. *Proceedings of the Society for Experimental Biology and Medicine.* 1942;51(3):386-389.
34. Jevons MP. "Celbenin" - resistant Staphylococci. *British Medical Journal.* 1961;1(5219):124-125.
35. del Rio A, Cervera C, Moreno A, Moreillon P, Miro JM. Patients at risk of complications of Staphylococcus aureus bloodstream infection. *Clin Infect Dis.* 2009;48 Suppl 4:S246-253.
36. Fluit AC, Jones ME, Schmitz FJ, Acar J, Gupta R, Verhoef J. Antimicrobial susceptibility and frequency of occurrence of clinical blood isolates in Europe from the SENTRY antimicrobial surveillance program, 1997 and 1998. *Clin Infect Dis.* 2000;30(3):454-460.
37. Brisse S, Milatovic D, Fluit AC, et al. Molecular surveillance of European quinolone-resistant clinical isolates of Pseudomonas aeruginosa and Acinetobacter spp. using automated ribotyping. *J Clin Microbiol.* 2000;38(10):3636-3645.
38. Dantes R, Mu Y, Belflower R, et al. National burden of invasive methicillin-resistant Staphylococcus aureus infections, United States, 2011. *JAMA Intern Med.* 2013;173(21):1970-1978.
39. Rodvold KA, McConeghy KW. Methicillin-resistant Staphylococcus aureus therapy: past, present, and future. *Clin Infect Dis.* 2014;58 Suppl 1:S20-27.
40. Stryjewski ME, Corey GR. Methicillin-resistant Staphylococcus aureus: an evolving pathogen. *Clin Infect Dis.* 2014;58 Suppl 1:S10-19.

41. Livermore DM. Has the era of untreatable infections arrived? *J Antimicrob Chemother.* 2009;64 Suppl 1:i29-36.
42. Laxminarayan R, Bhutta ZA. Antimicrobial resistance-a threat to neonate survival. *Lancet Glob Health.* 2016;4(10):e676-677.
43. Chen L, Todd R, Kiehlbauch J, Walters M, Kallen A. Notes from the Field: Pan-Resistant New Delhi Metallo-Beta-Lactamase-Producing Klebsiella pneumoniae-Washoe County, Nevada, 2016. *MMWR Morbidity and mortality weekly report.* 2017;66(1):33-33.
44. Petchiappan A, Chatterji D. Antibiotic Resistance: Current Perspectives. *ACS Omega.* 2017;2(10):7400-7409.
45. Gardete S, Tomasz A. Mechanisms of vancomycin resistance in Staphylococcus aureus. *J Clin Invest.* 2014;124(7):2836-2840.
46. Dinesh N, Sharma S, Balganesh M. Involvement of efflux pumps in the resistance to peptidoglycan synthesis inhibitors in Mycobacterium tuberculosis. *Antimicrob Agents Chemother.* 2013;57(4):1941-1943.
47. Chopra I, Roberts M. Tetracycline antibiotics: mode of action, applications, molecular biology, and epidemiology of bacterial resistance. *Microbiol Mol Biol Rev.* 2001;65(2):232-260 ; second page, table of contents.
48. Hooper DC, Jacoby GA. Mechanisms of drug resistance: quinolone resistance. *Ann N Y Acad Sci.* 2015;1354:12-31.
49. Floyd JL, Smith KP, Kumar SH, Floyd JT, Varela MF. LmrS is a multidrug efflux pump of the major facilitator superfamily from Staphylococcus aureus. *Antimicrob Agents Chemother.* 2010;54(12):5406-5412.
50. Schumacher A, Trittler R, Bohnert JA, Kummerer K, Pages JM, Kern WV. Intracellular accumulation of linezolid in Escherichia coli, Citrobacter freundii and Enterobacter aerogenes: role of enhanced efflux pump activity and inactivation. *J Antimicrob Chemother.* 2007;59(6):1261-1264.
51. Nikaido H. Multidrug resistance in bacteria. *Annu Rev Biochem.* 2009;78:119-146.
52. Quiles-Melero I, Gomez-Gil R, Romero-Gomez MP, et al. Mechanisms of linezolid resistance among Staphylococci in a tertiary hospital. *J Clin Microbiol.* 2013;51(3):998-1001.
53. Tran TT, Munita JM, Arias CA. Mechanisms of drug resistance: daptomycin resistance. *Ann N Y Acad Sci.* 2015;1354:32-53.
54. Foster TJ. Antibiotic resistance in Staphylococcus aureus. Current status and future prospects. *FEMS Microbiol Rev.* 2017;41(3):430-449.
55. Bosi E, Monk JM, Aziz RK, Fondi M, Nizet V, Palsson BO. Comparative genome-scale modelling of Staphylococcus aureus strains identifies strain-specific metabolic capabilities linked to pathogenicity. *Proc Natl Acad Sci U S A.* 2016;113(26):E3801-3809.
56. McGuinness WA, Malachowa N, DeLeo FR. Vancomycin Resistance in Staphylococcus aureus. *Yale J Biol Med.* 2017;90(2):269-281.
57. Stinear TP, Holt KE, Chua K, et al. Adaptive change inferred from genomic population analysis of the ST93 epidemic clone of community-associated methicillin-resistant Staphylococcus aureus. *Genome Biol Evol.* 2014;6(2):366-378.
58. Hiramatsu K, Katayama Y, Matsuo M, et al. Multi-drug-resistant Staphylococcus aureus and future chemotherapy. *J Infect Chemother.* 2014;20(10):593-601.
59. Gardner SG, Marshall DD, Daum RS, Powers R, Somerville GA. Metabolic Mitigation of Staphylococcus aureus Vancomycin Intermediate-Level Susceptibility. *Antimicrob Agents Chemother.* 2018;62(1).

60. Peng B, Su YB, Li H, et al. Exogenous alanine and/or glucose plus kanamycin kills antibiotic-resistant bacteria. *Cell Metab.* 2015;21(2):249-262.
61. Su YB, Peng B, Li H, et al. Pyruvate cycle increases aminoglycoside efficacy and provides respiratory energy in bacteria. *Proc Natl Acad Sci U S A.* 2018;115(7):E1578-E1587.
62. Vilcheze C, Hartman T, Weinrick B, et al. Enhanced respiration prevents drug tolerance and drug resistance in Mycobacterium tuberculosis. *Proc Natl Acad Sci U S A.* 2017;114(17):4495-4500.
63. Wadi L, Meyer M, Weiser J, Stein LD, Reimand J. Impact of outdated gene annotations on pathway enrichment analysis. *Nat Methods.* 2016;13(9):705-706.
64. Khatri P, Sirota M, Butte AJ. Ten years of pathway analysis: current approaches and outstanding challenges. *PLoS Comput Biol.* 2012;8(2):e1002375.
65. de Leeuw CA, Neale BM, Heskes T, Posthuma D. The statistical properties of gene-set analysis. *Nat Rev Genet.* 2016;17(6):353-364.
66. Goad B, Harris LK. Identification and prioritization of macrolide resistance genes with hypothetical annotation in Streptococcus pneumoniae. *Bioinformation.* 2018;14(9):488-498.
67. Subramanian A, Tamayo P, Mootha VK, et al. Gene set enrichment analysis: a knowledge-based approach for interpreting genome-wide expression profiles. *Proc Natl Acad Sci U S A.* 2005;102(43):15545-15550.
68. Tintle NL, Sitarik A, Boerema B, Young K, Best AA, Dejongh M. Evaluating the consistency of gene sets used in the analysis of bacterial gene expression data. *BMC Bioinformatics.* 2012;13:193.
69. Tintle NL, Best AA, DeJongh M, et al. Gene set analyses for interpreting microarray experiments on prokaryotic organisms. *BMC Bioinformatics.* 2008;9:469.
70. Michael CA, Dominey-Howes D, Labbate M. The antimicrobial resistance crisis: causes, consequences, and management. *Front Public Health.* 2014;2:145.
71. Taglialegna A, Varela MC, Rosato RR, Rosato AE. VraSR and Virulence Trait Modulation during Daptomycin Resistance in Methicillin-Resistant Staphylococcus aureus Infection. *mSphere.* 2019;4(1).
72. Mehta S, Cuirolo AX, Plata KB, et al. VraSR two-component regulatory system contributes to mprF-mediated decreased susceptibility to daptomycin in in vivo-selected clinical strains of methicillin-resistant Staphylococcus aureus. *Antimicrob Agents Chemother.* 2012;56(1):92-102.
73. Kuroda M, Kuroda H, Oshima T, Takeuchi F, Mori H, Hiramatsu K. Two-component system VraSR positively modulates the regulation of cell-wall biosynthesis pathway in Staphylococcus aureus. *Mol Microbiol.* 2003;49(3):807-821.
74. Gardete S, Wu SW, Gill S, Tomasz A. Role of VraSR in antibiotic resistance and antibiotic-induced stress response in Staphylococcus aureus. *Antimicrob Agents Chemother.* 2006;50(10):3424-3434.
75. Boyle-Vavra S, Yin S, Jo DS, Montgomery CP, Daum RS. VraT/YvqF is required for methicillin resistance and activation of the VraSR regulon in Staphylococcus aureus. *Antimicrob Agents Chemother.* 2013;57(1):83-95.
76. Falord M, Mader U, Hiron A, Debarbouille M, Msadek T. Investigation of the Staphylococcus aureus GraSR regulon reveals novel links to virulence, stress response and cell wall signal transduction pathways. *PLoS One.* 2011;6(7):e21323.
77. Mader U, Nicolas P, Depke M, et al. Staphylococcus aureus Transcriptome Architecture: From Laboratory to Infection-Mimicking Conditions. *PLoS Genet.* 2016;12(4):e1005962.

78. Blaskovich MAT, Hansford KA, Butler MS, Jia Z, Mark AE, Cooper MA. Developments in Glycopeptide Antibiotics. *ACS Infect Dis.* 2018;4(5):715-735.
79. Limbago BM, Kallen AJ, Zhu W, Eggers P, McDougal LK, Albrecht VS. Report of the 13th vancomycin-resistant Staphylococcus aureus isolate from the United States. *J Clin Microbiol.* 2014;52(3):998-1002.
80. Walters MS, Eggers P, Albrecht V, et al. Vancomycin-Resistant Staphylococcus aureus-Delaware, 2015. *MMWR Morbidity and mortality weekly report.* 2015;64(37):1056-1056.
81. Perichon B, Courvalin P. VanA-type vancomycin-resistant Staphylococcus aureus. *Antimicrob Agents Chemother.* 2009;53(11):4580-4587.
82. Capriotti T. Resistant 'superbugs' create need for novel antibiotics. *Dermatol Nurs.* 2007;19(1):65-70.
83. Nikolaidis I, Favini-Stabile S, Dessen A. Resistance to antibiotics targeted to the bacterial cell wall. *Protein Sci.* 2014;23(3):243-259.
84. Baltz RH. Daptomycin: mechanisms of action and resistance, and biosynthetic engineering. *Curr Opin Chem Biol.* 2009;13(2):144-151.
85. Taylor SD, Palmer M. The action mechanism of daptomycin. *Bioorg Med Chem.* 2016;24(24):6253-6268.
86. Miller WR, Bayer AS, Arias CA. Mechanism of Action and Resistance to Daptomycin in Staphylococcus aureus and Enterococci. *Cold Spring Harb Perspect Med.* 2016;6(11).
87. Tian Y, Li T, Zhu Y, Wang B, Zou X, Li M. Mechanisms of linezolid resistance in staphylococci and enterococci isolated from two teaching hospitals in Shanghai, China. *BMC Microbiol.* 2014;14:292.
88. Swaney SM, Aoki H, Ganoza MC, Shinabarger DL. The oxazolidinone linezolid inhibits initiation of protein synthesis in bacteria. *Antimicrob Agents Chemother.* 1998;42(12):3251-3255.
89. Lambert T. Antibiotics that affect the ribosome. *Rev Sci Tech.* 2012;31(1):57-64.
90. Thati V, Shivannavar CT, Gaddad SM. Vancomycin resistance among methicillin resistant Staphylococcus aureus isolates from intensive care units of tertiary care hospitals in Hyderabad. *Indian J Med Res.* 2011;134(5):704-708.
91. Walters MS, Eggers P, Albrecht V, et al. Vancomycin-Resistant Staphylococcus aureus - Delaware, 2015. *MMWR Morb Mortal Wkly Rep.* 2015;64(37):1056.
92. Weigelt JA. *MRSA, Second Edition.* CRC Press; 2016.
93. Nelson JL, Rice KC, Slater SR, et al. Vancomycin-intermediate Staphylococcus aureus strains have impaired acetate catabolism: implications for polysaccharide intercellular adhesin synthesis and autolysis. *Antimicrob Agents Chemother.* 2007;51(2):616-622.
94. Cui L, Ma X, Sato K, et al. Cell wall thickening is a common feature of vancomycin resistance in Staphylococcus aureus. *J Clin Microbiol.* 2003;41(1):5-14.
95. Sieradzki K, Tomasz A. Inhibition of cell wall turnover and autolysis by vancomycin in a highly vancomycin-resistant mutant of Staphylococcus aureus. *J Bacteriol.* 1997;179(8):2557-2566.
96. Lowy FD. Antimicrobial resistance: the example of Staphylococcus aureus. *J Clin Invest.* 2003;111(9):1265-1273.
97. Cui L, Iwamoto A, Lian JQ, et al. Novel mechanism of antibiotic resistance originating in vancomycin-intermediate Staphylococcus aureus. *Antimicrob Agents Chemother.* 2006;50(2):428-438.
98. Kim W, Hendricks GL, Tori K, Fuchs BB, Mylonakis E. Strategies against methicillin-resistant Staphylococcus aureus persisters. *Future Med Chem.* 2018;10(7):779-794.

99. Howden BP, Davies JK, Johnson PD, Stinear TP, Grayson ML. Reduced vancomycin susceptibility in Staphylococcus aureus, including vancomycin-intermediate and heterogeneous vancomycin-intermediate strains: resistance mechanisms, laboratory detection, and clinical implications. *Clin Microbiol Rev.* 2010;23(1):99-139.
100. Bonev BB, Brown NM. *Bacterial Resistance to Antibiotics: From Molecules to Man.* Wiley; 2019.
101. Berscheid A, Francois P, Strittmatter A, et al. Generation of a vancomycin-intermediate Staphylococcus aureus (VISA) strain by two amino acid exchanges in VraS. *J Antimicrob Chemother.* 2014;69(12):3190-3198.
102. Meehl M, Herbert S, Gotz F, Cheung A. Interaction of the GraRS two-component system with the VraFG ABC transporter to support vancomycin-intermediate resistance in Staphylococcus aureus. *Antimicrob Agents Chemother.* 2007;51(8):2679-2689.
103. Crossley KB, Jefferson KK, Archer GL, Fowler VG. *Staphylococci in human disease.* John Wiley & Sons; 2009.
104. Chen FJ, Lauderdale TL, Lee CH, et al. Effect of a Point Mutation in mprF on Susceptibility to Daptomycin, Vancomycin, and Oxacillin in an MRSA Clinical Strain. *Front Microbiol.* 2018;9:1086.
105. Howden BP, Stinear TP, Allen DL, Johnson PD, Ward PB, Davies JK. Genomic analysis reveals a point mutation in the two-component sensor gene graS that leads to intermediate vancomycin resistance in clinical Staphylococcus aureus. *Antimicrob Agents Chemother.* 2008;52(10):3755-3762.
106. McAleese F, Wu SW, Sieradzki K, et al. Overexpression of genes of the cell wall stimulon in clinical isolates of Staphylococcus aureus exhibiting vancomycin-intermediate- S. aureus-type resistance to vancomycin. *J Bacteriol.* 2006;188(3):1120-1133.
107. Alexander EL, Gardete S, Bar HY, Wells MT, Tomasz A, Rhee KY. Intermediate-type vancomycin resistance (VISA) in genetically-distinct Staphylococcus aureus isolates is linked to specific, reversible metabolic alterations. *PLoS One.* 2014;9(5):e97137.
108. Chen CJ, Lin MH, Shu JC, Lu JJ. Reduced susceptibility to vancomycin in isogenic Staphylococcus aureus strains of sequence type 59: tracking evolution and identifying mutations by whole-genome sequencing. *J Antimicrob Chemother.* 2014;69(2):349-354.
109. Mwangi MM, Wu SW, Zhou Y, et al. Tracking the in vivo evolution of multidrug resistance in Staphylococcus aureus by whole-genome sequencing. *Proc Natl Acad Sci U S A.* 2007;104(22):9451-9456.
110. Cui L, Isii T, Fukuda M, et al. An RpoB mutation confers dual heteroresistance to daptomycin and vancomycin in Staphylococcus aureus. *Antimicrob Agents Chemother.* 2010;54(12):5222-5233.
111. Matsuo M, Hishinuma T, Katayama Y, Cui L, Kapi M, Hiramatsu K. Mutation of RNA polymerase beta subunit (rpoB) promotes hVISA-to-VISA phenotypic conversion of strain Mu3. *Antimicrob Agents Chemother.* 2011;55(9):4188-4195.
112. Watanabe Y, Cui L, Katayama Y, Kozue K, Hiramatsu K. Impact of rpoB mutations on reduced vancomycin susceptibility in Staphylococcus aureus. *J Clin Microbiol.* 2011;49(7):2680-2684.
113. Herbert S, Bera A, Nerz C, et al. Molecular basis of resistance to muramidase and cationic antimicrobial peptide activity of lysozyme in staphylococci. *PLoS Pathog.* 2007;3(7):e102.
114. Draper LA, Cotter PD, Hill C, Ross RP. Lantibiotic resistance. *Microbiol Mol Biol Rev.* 2015;79(2):171-191.

115. Sabat AJ, Tinelli M, Grundmann H, et al. Daptomycin Resistant Staphylococcus aureus Clinical Strain With Novel Non-synonymous Mutations in the mprF and vraS Genes: A New Insight Into Daptomycin Resistance. *Front Microbiol.* 2018;9:2705.
116. Barros EM, Martin MJ, Selleck EM, Lebreton F, Sampaio JLM, Gilmore MS. Daptomycin Resistance and Tolerance Due to Loss of Function in Staphylococcus aureus dsp1 and asp23. *Antimicrob Agents Chemother.* 2019;63(1).
117. Vestergaard M, Nohr-Meldgaard K, Bojer MS, et al. Inhibition of the ATP Synthase Eliminates the Intrinsic Resistance of Staphylococcus aureus towards Polymyxins. *mBio.* 2017;8(5).
118. Pogue JM, Ortwine JK, Kaye KS. Clinical considerations for optimal use of the polymyxins: A focus on agent selection and dosing. *Clin Microbiol Infect.* 2017;23(4):229-233.
119. Falagas ME, Kasiakou SK. Toxicity of polymyxins: a systematic review of the evidence from old and recent studies. *Crit Care.* 2006;10(1):R27.
120. Trimble MJ, Mlynarcik P, Kolar M, Hancock RE. Polymyxin: Alternative Mechanisms of Action and Resistance. *Cold Spring Harb Perspect Med.* 2016;6(10).
121. de Almeida LM, de Araujo MR, Sacramento AG, et al. Linezolid resistance in Brazilian Staphylococcus hominis strains is associated with L3 and 23S rRNA ribosomal mutations. *Antimicrob Agents Chemother.* 2013;57(8):4082-4083.
122. Locke JB, Hilgers M, Shaw KJ. Mutations in ribosomal protein L3 are associated with oxazolidinone resistance in staphylococci of clinical origin. *Antimicrob Agents Chemother.* 2009;53(12):5275-5278.
123. Locke JB, Hilgers M, Shaw KJ. Novel ribosomal mutations in Staphylococcus aureus strains identified through selection with the oxazolidinones linezolid and torezolid (TR-700). *Antimicrob Agents Chemother.* 2009;53(12):5265-5274.
124. Marshall SH, Donskey CJ, Hutton-Thomas R, Salata RA, Rice LB. Gene dosage and linezolid resistance in Enterococcus faecium and Enterococcus faecalis. *Antimicrob Agents Chemother.* 2002;46(10):3334-3336.
125. Besier S, Ludwig A, Zander J, Brade V, Wichelhaus TA. Linezolid resistance in Staphylococcus aureus: gene dosage effect, stability, fitness costs, and cross-resistances. *Antimicrob Agents Chemother.* 2008;52(4):1570-1572.
126. Kehrenberg C, Schwarz S, Jacobsen L, Hansen LH, Vester B. A new mechanism for chloramphenicol, florfenicol and clindamycin resistance: methylation of 23S ribosomal RNA at A2503. *Mol Microbiol.* 2005;57(4):1064-1073.
127. Long KS, Poehlsgaard J, Kehrenberg C, Schwarz S, Vester B. The Cfr rRNA methyltransferase confers resistance to Phenicols, Lincosamides, Oxazolidinones, Pleuromutilins, and Streptogramin A antibiotics. *Antimicrob Agents Chemother.* 2006;50(7):2500-2505.
128. Costa SS, Viveiros M, Amaral L, Couto I. Multidrug Efflux Pumps in Staphylococcus aureus: an Update. *Open Microbiol J.* 2013;7:59-71.
129. Muller A, Grein F, Otto A, et al. Differential daptomycin resistance development in Staphylococcus aureus strains with active and mutated gra regulatory systems. *Int J Med Microbiol.* 2018;308(3):335-348.
130. Bratlie MS, Johansen J, Drablos F. Relationship between operon preference and functional properties of persistent genes in bacterial genomes. *BMC Genomics.* 2010;11:71.
131. Du W, Cao Z, Wang Y, Blanzieri E, Zhang C, Liang Y. Operon prediction by Markov clustering. *Int J Data Min Bioinform.* 2014;9(4):424-443.

132. Subramanian D, Natarajan J. RNA-seq analysis reveals resistome genes and signalling pathway associated with vancomycin-intermediate Staphylococcus aureus. *Indian J Med Microbiol.* 2019;37(2):173-185.
133. Choe D, Szubin R, Dahesh S, et al. Genome-scale analysis of Methicillin-resistant Staphylococcus aureus USA300 reveals a tradeoff between pathogenesis and drug resistance. *Sci Rep.* 2018;8(1):2215.
134. Liu J, Yang L, Hou Y, et al. Transcriptomics Study on Staphylococcus aureus Biofilm Under Low Concentration of Ampicillin. *Front Microbiol.* 2018;9:2413.
135. Wu S, Liu Y, Zhang H, Lei L. The Pathogenicity and Transcriptome Analysis of Methicillin-Resistant Staphylococcus aureus in Response to Water Extract of Galla chinensis. *Evid Based Complement Alternat Med.* 2019;2019:3276156.
136. Hua R, Xia Y, Wu W, Yan J, Yang M. Whole transcriptome analysis reveals potential novel mechanisms of low-level linezolid resistance in Enterococcus faecalis. *Gene.* 2018;647:143-149.
137. Goad B, Harris LK. Identification and prioritization of macrolideresistance genes with hypothetical annotation inStreptococcus pneumoniae. *Bioinformation.* 2018;14(9):488-498.
138. Mootha VK, Lindgren CM, Eriksson KF, et al. PGC-1alpha-responsive genes involved in oxidative phosphorylation are coordinately downregulated in human diabetes. *Nat Genet.* 2003;34(3):267-273.
139. Mitrofanova A, Aytes A, Zou M, Shen MM, Abate-Shen C, Califano A. Predicting Drug Response in Human Prostate Cancer from Preclinical Analysis of In Vivo Mouse Models. *Cell Rep.* 2015;12(12):2060-2071.
140. Zhang W, Zeng Z, Zhou Y, et al. Identification of aberrant cell cycle regulation in Epstein-Barr virus-associated nasopharyngeal carcinoma by cDNA microarray and gene set enrichment analysis. *Acta Biochim Biophys Sin (Shanghai).* 2009;41(5):414-428.
141. Kato H, Karube K, Yamamoto K, et al. Gene expression profiling of Epstein-Barr virus-positive diffuse large B-cell lymphoma of the elderly reveals alterations of characteristic oncogenetic pathways. *Cancer Sci.* 2014;105(5):537-544.
142. Khatri P, Draghici S. Ontological analysis of gene expression data: current tools, limitations, and open problems. *Bioinformatics.* 2005;21(18):3587-3595.
143. Man MZ, Wang X, Wang Y. POWER_SAGE: comparing statistical tests for SAGE experiments. *Bioinformatics.* 2000;16(11):953-959.
144. Irizarry RA, Wang C, Zhou Y, Speed TP. Gene set enrichment analysis made simple. *Stat Methods Med Res.* 2009;18(6):565-575.
145. Schwartz JM, Gaugain C, Nacher JC, de Daruvar A, Kanehisa M. Observing metabolic functions at the genome scale. *Genome Biol.* 2007;8(6):R123.
146. Efron B, Tibshirani R. On testing the significance of sets of genes. *Ann Appl Stat.* 2007;1(1):107-129.
147. Dinu I, Potter JD, Mueller T, et al. Improving gene set analysis of microarray data by SAM-GS. *BMC Bioinformatics.* 2007;8:242.
148. Yoon S, Kim SY, Nam D. Improving Gene-Set Enrichment Analysis of RNA-Seq Data with Small Replicates. *PLoS One.* 2016;11(11):e0165919.
149. Yan X, Sun F. Testing gene set enrichment for subset of genes: Sub-GSE. *BMC Bioinformatics.* 2008;9:362.
150. Kim HY. Statistical notes for clinical researchers: Chi-squared test and Fisher's exact test. *Restor Dent Endod.* 2017;42(2):152-155.

151. Abatangelo L, Maglietta R, Distaso A, et al. Comparative study of gene set enrichment methods. *BMC Bioinformatics.* 2009;10:275.
152. Liberzon A, Subramanian A, Pinchback R, Thorvaldsdottir H, Tamayo P, Mesirov JP. Molecular signatures database (MSigDB) 3.0. *Bioinformatics.* 2011;27(12):1739-1740.
153. Liberzon A, Birger C, Thorvaldsdottir H, Ghandi M, Mesirov JP, Tamayo P. The Molecular Signatures Database (MSigDB) hallmark gene set collection. *Cell Syst.* 2015;1(6):417-425.
154. Liberzon A. A description of the Molecular Signatures Database (MSigDB) Web site. *Methods Mol Biol.* 2014;1150:153-160.
155. Fabregat A, Jupe S, Matthews L, et al. The Reactome Pathway Knowledgebase. *Nucleic Acids Res.* 2018;46(D1):D649-D655.
156. Croft D, Mundo AF, Haw R, et al. The Reactome pathway knowledgebase. *Nucleic Acids Res.* 2014;42(Database issue):D472-477.
157. The Gene Ontology C. Expansion of the Gene Ontology knowledgebase and resources. *Nucleic Acids Res.* 2017;45(D1):D331-D338.
158. Ashburner M, Ball CA, Blake JA, et al. Gene ontology: tool for the unification of biology. The Gene Ontology Consortium. *Nat Genet.* 2000;25(1):25-29.
159. Zhulin IB. Databases for Microbiologists. *J Bacteriol.* 2015;197(15):2458-2467.
160. Mi H, Huang X, Muruganujan A, et al. PANTHER version 11: expanded annotation data from Gene Ontology and Reactome pathways, and data analysis tool enhancements. *Nucleic Acids Res.* 2017;45(D1):D183-D189.
161. Altman T, Travers M, Kothari A, Caspi R, Karp PD. A systematic comparison of the MetaCyc and KEGG pathway databases. *BMC Bioinformatics.* 2013;14:112.
162. Kanehisa M, Sato Y, Kawashima M, Furumichi M, Tanabe M. KEGG as a reference resource for gene and protein annotation. *Nucleic Acids Res.* 2016;44(D1):D457-462.
163. Kanehisa M, Goto S, Sato Y, Furumichi M, Tanabe M. KEGG for integration and interpretation of large-scale molecular data sets. *Nucleic Acids Res.* 2012;40(Database issue):D109-114.
164. Kanehisa M, Araki M, Goto S, et al. KEGG for linking genomes to life and the environment. *Nucleic Acids Res.* 2008;36(Database issue):D480-484.
165. Huang da W, Sherman BT, Lempicki RA. Bioinformatics enrichment tools: paths toward the comprehensive functional analysis of large gene lists. *Nucleic Acids Res.* 2009;37(1):1-13.
166. Huang da W, Sherman BT, Lempicki RA. Systematic and integrative analysis of large gene lists using DAVID bioinformatics resources. *Nat Protoc.* 2009;4(1):44-57.
167. Overbeek R, Begley T, Butler RM, et al. The subsystems approach to genome annotation and its use in the project to annotate 1000 genomes. *Nucleic Acids Res.* 2005;33(17):5691-5702.
168. Gillespie JJ, Wattam AR, Cammer SA, et al. PATRIC: the comprehensive bacterial bioinformatics resource with a focus on human pathogenic species. *Infect Immun.* 2011;79(11):4286-4298.
169. Overbeek R, Olson R, Pusch GD, et al. The SEED and the Rapid Annotation of microbial genomes using Subsystems Technology (RAST). *Nucleic Acids Res.* 2014;42(Database issue):D206-214.
170. Greene JM, Collins F, Lefkowitz EJ, et al. National Institute of Allergy and Infectious Diseases bioinformatics resource centers: new assets for pathogen informatics. *Infect Immun.* 2007;75(7):3212-3219.

171. Kuroda M, Ohta T, Uchiyama I, et al. Whole genome sequencing of meticillin-resistant Staphylococcus aureus. *Lancet.* 2001;357(9264):1225-1240.
172. Munita JM, Bayer AS, Arias CA. Evolving resistance among Gram-positive pathogens. *Clin Infect Dis.* 2015;61 Suppl 2:S48-57.
173. Loomba PS, Taneja J, Mishra B. Methicillin and Vancomycin Resistant S. aureus in Hospitalized Patients. *J Glob Infect Dis.* 2010;2(3):275-283.
174. Rasmussen RV, Fowler VG, Jr., Skov R, Bruun NE. Future challenges and treatment of Staphylococcus aureus bacteremia with emphasis on MRSA. *Future Microbiol.* 2011;6(1):43-56.
175. Chaiwongkarjohn S, Pramyothin P, Suwantarat N, et al. A report on the first case of vancomycin-intermediate Staphylococcus aureus (VISA) in Hawai'i. *Hawaii Med J.* 2011;70(11):233-236.
176. Moravvej Z, Estaji F, Askari E, Solhjou K, Naderi Nasab M, Saadat S. Update on the global number of vancomycin-resistant Staphylococcus aureus (VRSA) strains. *Int J Antimicrob Agents.* 2013;42(4):370-371.
177. Endimiani A, Blackford M, Dasenbrook EC, et al. Emergence of linezolid-resistant Staphylococcus aureus after prolonged treatment of cystic fibrosis patients in Cleveland, Ohio. *Antimicrob Agents Chemother.* 2011;55(4):1684-1692.
178. Liu C, Bayer A, Cosgrove SE, et al. Clinical practice guidelines by the infectious diseases society of america for the treatment of methicillin-resistant Staphylococcus aureus infections in adults and children: executive summary. *Clin Infect Dis.* 2011;52(3):285-292.
179. Gu B, Kelesidis T, Tsiodras S, Hindler J, Humphries RM. The emerging problem of linezolid-resistant Staphylococcus. *J Antimicrob Chemother.* 2013;68(1):4-11.
180. Sanchez Garcia M, De la Torre MA, Morales G, et al. Clinical outbreak of linezolid-resistant Staphylococcus aureus in an intensive care unit. *JAMA.* 2010;303(22):2260-2264.
181. Bhattacharya PK. Emergence of antibiotic-resistant bacterial strains, methicillin-resistant Staphylococcus aureus, extended spectrum beta lactamases, and multi-drug resistance is a problem similar to global warming. *Rev Soc Bras Med Trop.* 2014;47(6):815-816.
182. Magiorakos AP, Srinivasan A, Carey RB, et al. Multidrug-resistant, extensively drug-resistant and pandrug-resistant bacteria: an international expert proposal for interim standard definitions for acquired resistance. *Clin Microbiol Infect.* 2012;18(3):268-281.
183. Flamm RK, Mendes RE, Hogan PA, Streit JM, Ross JE, Jones RN. Linezolid Surveillance Results for the United States (LEADER Surveillance Program 2014). *Antimicrob Agents Chemother.* 2016;60(4):2273-2280.
184. Zhang S, Sun X, Chang W, Dai Y, Ma X. Systematic Review and Meta-Analysis of the Epidemiology of Vancomycin-Intermediate and Heterogeneous Vancomycin-Intermediate Staphylococcus aureus Isolates. *PLoS One.* 2015;10(8):e0136082.
185. Liu C, Bayer A, Cosgrove SE, et al. Clinical practice guidelines by the infectious diseases society of america for the treatment of methicillin-resistant Staphylococcus aureus infections in adults and children. *Clin Infect Dis.* 2011;52(3):e18-55.
186. Hu Q, Peng H, Rao X. Molecular Events for Promotion of Vancomycin Resistance in Vancomycin Intermediate Staphylococcus aureus. *Front Microbiol.* 2016;7:1601.
187. Azhar A, Rasool S, Haque A, et al. Detection of high levels of resistance to linezolid and vancomycin in Staphylococcus aureus. *J Med Microbiol.* 2017;66(9):1328-1331.
188. Roch M, Gagetti P, Davis J, et al. Daptomycin Resistance in Clinical MRSA Strains Is Associated with a High Biological Fitness Cost. *Front Microbiol.* 2017;8:2303.

189. Ma Z, Lasek-Nesselquist E, Lu J, et al. Characterization of genetic changes associated with daptomycin nonsusceptibility in Staphylococcus aureus. *PLoS One.* 2018;13(6):e0198366.
190. Ortwine JK, Werth BJ, Sakoulas G, Rybak MJ. Reduced glycopeptide and lipopeptide susceptibility in Staphylococcus aureus and the "seesaw effect": Taking advantage of the back door left open? *Drug Resist Updat.* 2013;16(3-5):73-79.
191. Barber KE, Ireland CE, Bukavyn N, Rybak MJ. Observation of "seesaw effect" with vancomycin, teicoplanin, daptomycin and ceftaroline in 150 unique MRSA strains. *Infect Dis Ther.* 2014;3(1):35-43.
192. Mazharul Islam M, Thomas VC, Van Beek M, et al. An integrated computational and experimental study to investigate Staphylococcus aureus metabolism. *NPJ Syst Biol Appl.* 2020;6(1):3.
193. Madigan MT, Martinko JM, Dunlap PV, Clark DP. Brock biology of microorganisms 12th edn. *Int Microbiol.* 2008;11:65-73.
194. Wixon J, Kell D. The Kyoto encyclopedia of genes and genomes--KEGG. *Yeast.* 2000;17(1):48-55.
195. Kanehisa M, Goto S. KEGG: kyoto encyclopedia of genes and genomes. *Nucleic Acids Res.* 2000;28(1):27-30.
196. Tilford CA, Siemers NO. Gene set enrichment analysis. *Methods Mol Biol.* 2009;563:99-121.
197. Panja S, Hayati S, Epsi NJ, Parrott JS, Mitrofanova A. Integrative (epi) Genomic Analysis to Predict Response to Androgen-Deprivation Therapy in Prostate Cancer. *EBioMedicine.* 2018;31:110-121.
198. Murohashi M, Hinohara K, Kuroda M, et al. Gene set enrichment analysis provides insight into novel signalling pathways in breast cancer stem cells. *Br J Cancer.* 2010;102(1):206-212.
199. Cai B, Jiang X. Revealing Biological Pathways Implicated in Lung Cancer from TCGA Gene Expression Data Using Gene Set Enrichment Analysis. *Cancer Inform.* 2014;13(Suppl 1):113-121.
200. Livshits A, Git A, Fuks G, Caldas C, Domany E. Pathway-based personalized analysis of breast cancer expression data. *Mol Oncol.* 2015;9(7):1471-1483.
201. Altekruse SF, Elvinger F, Wang Y, Ye K. A model to estimate the optimal sample size for microbiological surveys. *Appl Environ Microbiol.* 2003;69(10):6174-6178.
202. Mandal S. Emerging Statistical Methodologies in the Field of Microbiome Studies. In: *Handbook of Statistics.* Vol 37. Elsevier; 2017:37-52.
203. Mansournia MA, Geroldinger A, Greenland S, Heinze G. Separation in Logistic Regression: Causes, Consequences, and Control. *Am J Epidemiol.* 2018;187(4):864-870.
204. van Smeden M, de Groot JA, Moons KG, et al. No rationale for 1 variable per 10 events criterion for binary logistic regression analysis. *BMC Med Res Methodol.* 2016;16(1):163.
205. Sinkovec H, Geroldinger A, Heinze G. Bring More Data!-A Good Advice? Removing Separation in Logistic Regression by Increasing Sample Size. *Int J Environ Res Public Health.* 2019;16(23).
206. Yang SJ, Bayer AS, Mishra NN, et al. The Staphylococcus aureus two-component regulatory system, GraRS, senses and confers resistance to selected cationic antimicrobial peptides. *Infect Immun.* 2012;80(1):74-81.
207. Falord M, Karimova G, Hiron A, Msadek T. GraXSR proteins interact with the VraFG ABC transporter to form a five-component system required for cationic antimicrobial peptide

sensing and resistance in Staphylococcus aureus. *Antimicrob Agents Chemother.* 2012;56(2):1047-1058.
208. Hanley JA, McNeil BJ. The meaning and use of the area under a receiver operating characteristic (ROC) curve. *Radiology.* 1982;143(1):29-36.
209. Ayar-Kayali H. Pentose phosphate pathway flux analysis for glycopeptide antibiotic vancomycin production during glucose-limited cultivation of Amycolatopsis orientalis. *Prep Biochem Biotechnol.* 2011;41(1):94-105.
210. Thomas VC, Kinkead LC, Janssen A, et al. A dysfunctional tricarboxylic acid cycle enhances fitness of Staphylococcus epidermidis during beta-lactam stress. *MBio.* 2013;4(4).
211. Wang Y, Bojer MS, George SE, et al. Inactivation of TCA cycle enhances Staphylococcus aureus persister cell formation in stationary phase. *Sci Rep.* 2018;8(1):10849.
212. Gaupp R, Lei S, Reed JM, et al. Staphylococcus aureus metabolic adaptations during the transition from a daptomycin susceptibility phenotype to a daptomycin nonsusceptibility phenotype. *Antimicrob Agents Chemother.* 2015;59(7):4226-4238.
213. Onyango LA, Alreshidi MM. Adaptive Metabolism in Staphylococci: Survival and Persistence in Environmental and Clinical Settings. *J Pathog.* 2018;2018:1092632.
214. Gefen O, Gabay C, Mumcuoglu M, Engel G, Balaban NQ. Single-cell protein induction dynamics reveals a period of vulnerability to antibiotics in persister bacteria. *Proc Natl Acad Sci U S A.* 2008;105(16):6145-6149.
215. Wood TK, Knabel SJ, Kwan BW. Bacterial persister cell formation and dormancy. *Appl Environ Microbiol.* 2013;79(23):7116-7121.
216. Belcheva A, Golemi-Kotra D. A close-up view of the VraSR two-component system. A mediator of Staphylococcus aureus response to cell wall damage. *J Biol Chem.* 2008;283(18):12354-12364.
217. Kato Y, Suzuki T, Ida T, Maebashi K. Genetic changes associated with glycopeptide resistance in Staphylococcus aureus: predominance of amino acid substitutions in YvqF/VraSR. *J Antimicrob Chemother.* 2010;65(1):37-45.
218. Muzamal U, Gomez D, Kapadia F, Golemi-Kotra D. Diversity of two-component systems: insights into the signal transduction mechanism by the Staphylococcus aureus two-component system GraSR. *F1000Res.* 2014;3:252.
219. Yang H, Wang M, Yu J, Wei H. Aspartate inhibits Staphylococcus aureus biofilm formation. *FEMS Microbiol Lett.* 2015;362(7).
220. McCarthy H, Rudkin JK, Black NS, Gallagher L, O'Neill E, O'Gara JP. Methicillin resistance and the biofilm phenotype in Staphylococcus aureus. *Front Cell Infect Microbiol.* 2015;5:1.
221. Ciofu O, Tolker-Nielsen T. Tolerance and Resistance of Pseudomonas aeruginosa Biofilms to Antimicrobial Agents-How P. aeruginosa Can Escape Antibiotics. *Front Microbiol.* 2019;10:913.
222. Preda VG, Sandulescu O. Communication is the key: biofilms, quorum sensing, formation and prevention. *Discoveries (Craiova).* 2019;7(3):e100.
223. Zhang K, Du Y, Si Z, et al. Enantiomeric glycosylated cationic block co-beta-peptides eradicate Staphylococcus aureus biofilms and antibiotic-tolerant persisters. *Nat Commun.* 2019;10(1):4792.
224. Marklevitz J, Harris LK. Prediction driven functional annotation of hypothetical proteins in the major facilitator superfamily of S. aureus NCTC 8325. *Bioinformation.* 2016;12(4):254-262.
225. Shimizu K. 1 - Main metabolism. In: Shimizu K, ed. *Bacterial Cellular Metabolic Systems.* Woodhead Publishing; 2013:1-54.

226. Min W, Li H, Li H, Liu C, Liu J. Characterization of Aspartate Kinase from Corynebacterium pekinense and the Critical Site of Arg169. *Int J Mol Sci.* 2015;16(12):28270-28284.
227. Ogawa-Miyata Y, Kojima H, Sano K. Mutation analysis of the feedback inhibition site of aspartokinase III of Escherichia coli K-12 and its use in L-threonine production. *Biosci Biotechnol Biochem.* 2001;65(5):1149-1154.
228. Ijaq J, Chandrasekharan M, Poddar R, Bethi N, Sundararajan VS. Annotation and curation of uncharacterized proteins- challenges. *Front Genet.* 2015;6:119.
229. School K, Marklevitz J, W KS, L KH. Predictive characterization of hypothetical proteins in Staphylococcus aureus NCTC 8325. *Bioinformation.* 2016;12(3):209-220.
230. Soh D, Dong D, Guo Y, Wong L. Consistency, comprehensiveness, and compatibility of pathway databases. *BMC Bioinformatics.* 2010;11:449.
231. Lander ES. The Heroes of CRISPR. *Cell.* 2016;164(1-2):18-28.
232. Hsu PD, Lander ES, Zhang F. Development and applications of CRISPR-Cas9 for genome engineering. *Cell.* 2014;157(6):1262-1278.
233. Gupta RM, Musunuru K. Expanding the genetic editing tool kit: ZFNs, TALENs, and CRISPR-Cas9. *J Clin Invest.* 2014;124(10):4154-4161.
234. McClure R, Balasubramanian D, Sun Y, et al. Computational analysis of bacterial RNA-Seq data. *Nucleic Acids Res.* 2013;41(14):e140.
235. Tjaden B. De novo assembly of bacterial transcriptomes from RNA-seq data. *Genome Biol.* 2015;16:1.
236. Edgar R, Domrachev M, Lash AE. Gene Expression Omnibus: NCBI gene expression and hybridization array data repository. *Nucleic Acids Res.* 2002;30(1):207-210.
237. Barrett T, Wilhite SE, Ledoux P, et al. NCBI GEO: archive for functional genomics data sets--update. *Nucleic Acids Res.* 2013;41(Database issue):D991-995.
238. Hajian-Tilaki K. Receiver Operating Characteristic (ROC) Curve Analysis for Medical Diagnostic Test Evaluation. *Caspian J Intern Med.* 2013;4(2):627-635.
239. Goksuluk D, Korkmaz S, Zararsiz G, Karaagaoglu AE. easyROC: an interactive web-tool for ROC curve analysis using R language environment. *R Journal.* 2016;8(213):e30.
240. Gould J. GENE-E. https://software.broadinstitute.org/GENE-E/, 2017.
241. Charbonnier Y, Gettler B, Francois P, et al. A generic approach for the design of whole-genome oligoarrays, validated for genomotyping, deletion mapping and gene expression analysis on Staphylococcus aureus. *BMC Genomics.* 2005;6:95.
242. Koessler T, Francois P, Charbonnier Y, et al. Use of oligoarrays for characterization of community-onset methicillin-resistant Staphylococcus aureus. *J Clin Microbiol.* 2006;44(3):1040-1048.
243. Aligholi M, Emaneini M, Jabalameli F, Shahsavan S, Dabiri H, Sedaght H. Emergence of high-level vancomycin-resistant Staphylococcus aureus in the Imam Khomeini Hospital in Tehran. *Med Princ Pract.* 2008;17(5):432-434.
244. Stapleton PD, Taylor PW. Methicillin resistance in Staphylococcus aureus: mechanisms and modulation. *Sci Prog.* 2002;85(Pt 1):57-72.
245. Altschul SF, Madden TL, Schaffer AA, et al. Gapped BLAST and PSI-BLAST: a new generation of protein database search programs. *Nucleic Acids Res.* 1997;25(17):3389-3402.
246. Mohan R, Venugopal S. Computational structural and functional analysis of hypothetical proteins of Staphylococcus aureus. *Bioinformation.* 2012;8(15):722-728.

247. Wattam AR, Davis JJ, Assaf R, et al. Improvements to PATRIC, the all-bacterial Bioinformatics Database and Analysis Resource Center. *Nucleic Acids Res.* 2017;45(D1):D535-D542.

APPENDIX A. Overview of mRNA Expression Resources

Here, we detail the mRNA expression datasets provided by the Gene Expression Omnibus (GEO) used in this study. We first use three datasets (GSE46887, GSE50842, and GSE26016) containing untreated samples of antibiotic resistant and sensitive *S. aureus* strains to identify pathway activity changes based on mRNA expression resulting in antibiotic resistance from established mutations in *vraSR* or *graSR*[53,56,75].

GSE46887 contained triplicate untreated samples of an antibiotic sensitive strain (NCTC 8325) with a *mutS* (mismatch repair gene) deletion mutation (Δ*mutS*) to its antibiotic resistant progeny strain (VC40) that was generated from 30 serial passages of Δ*mutS* with increasing vancomycin exposure, grown in brain heart infusion broth to exponential growth phase before mRNA collection (samples (S)=6)[101]. Among other mutations, VC40 had two VraSR mutations (L114S and D242G) that resulted in high level vancomycin resistance (MIC ≥48 mg/L) and low level daptomycin resistance (MIC=4 mg/L) with oxacillin sensitivity (MIC=1mg/L) and was not tested for linezolid resistance as determined through genetic reconstitution of the NCTC8325 genome (*i.e.*, same mutations introduced to sensitive NCTC8325 resulting in increased vancomycin (MIC≥3mg/L) and daptomycin (MIC= 2mg/L) resistance)[101]. Samples were profiled on Agilent-021782 Custom *S. aureus* V6 Array (GEO accession GPL10537) to measure mRNA expression. This non-commercial, validated microarray platform[241,242] had 10807 60-mer oligonucleotide probes specific to *S. aureus* covering >95% of ORFs annotated in *S. aureus* strains of varying methicillin and vancomycin sensitivities: sensitive to methicillin and vancomycin (MSSA476 and NCTC8325), MRSA strains sensitive to vancomycin (COL, N315, MW2, MRSA252, and USA300FPR3757), and

MRSA/VISA (Mu50), according to the published paper for this dataset[101]. However, we note that GEO provided 7266 probes containing 6888 unique probes (non-overlapping gene coverage, *i.e.*, different probes targeting same gene) from other strains, some of which we verified from performing Basic Local Alignment Search Tool (BLAST) on probe nucleotide sequences (Table A-1). Further, we note that this platform does not include probes for the *vanA* operon, indicating we cannot assess the mechanism of vancomycin resistance in VC40, though the fact VC40 was generated from repeated increasing exposure to vancomycin indicates it is a VISA strain. We also notice that the VraS (SAOUHSC_02099) probe does not cover the regions where single polymorphism mutations in VraS were documented in VC40, making it impossible to distinguish between WT and mutant expression. GEO provided mRNA expression data for GSE46887 as log10(sample/gDNA pool) values. We convert these log10 ratios to log2 ratios for consistency across data used in this study.

Table A-1. Platform coverage

| Strain | GPL10537 | GPL7137 | GPL10597 | GPL5879 | GPL20586 |
|---|---|---|---|---|---|
| NCTC8325 | 2655[1] | 352 | 0 | 0 | 2836 |
| COL | 0 | 904 | 240 | 1335 | 0 |
| N315 | 0 | 2437 | 88 | 87 | 0 |
| Mu50 | 0 | 560 | 1462 | 1490 | 0 |
| MW2 | 0 | 172 | 83 | 106 | 0 |
| USA300 | 419 | 902 | 1262 | 0 | 0 |
| MRSA252 | 0 | 744 | 720 | 745 | 0 |
| MSSA476 | 0 | 432 | 634 | 649 | 0 |
| UAMS-1 | 491 | 0 | 0 | 0 | 0 |
| Newman | 726 | 1 | 0 | 0 | 0 |
| JH-1 | 0 | 3 | 0 | 0 | 0 |
| JH-9 | 0 | 24 | 0 | 0 | 0 |
| SAW1 | 2114 | 0 | 0 | 0 | 0 |
| Plasmids | 0 | 67 | 23 | 9 | 0 |
| Tiling region | 222 | 0 | 0 | 0 | 1192 |
| Obsolete | 0 | 0 | 75 | 125 | 0 |
| Control | 261 | 0 | 500 | 510 | 0 |
| Total tags | 6888 | 6598 | 5087 | 5056 | 4028 |

[1] Stain 564 was used, which is a derivative of strain NCTC 8325.

GSE50842 contained duplicate untreated samples (S=4) of wildtype (antibiotic sensitive) HG001 (normal GraSR) and SG511 (truncated GraSR) strains, both *rsbU*$^{+}$ (phosphoserine phosphatase that positively regulates RNA polymerase $\sigma^{B}$ activity during stress-response) derivatives of NCTC8235, and their antibiotic resistant progeny after four months of incrementally increasing daptomycin exposure grown in Mueller Hinton broth until exponential phase[129]. Antibiotic resistant progeny had intermediate vancomycin resistance (MIC=4mg/L), high daptomycin resistance (MIC=31mg/L) and were noted to be more susceptible to oxacillin and linezolid (MIC not reported)[129]. Samples were profiled on the customized commercial platform Agilent-017903 *S. aureus* V5 Bis 15K, basic version, array (GEO accession GPL7137), which had 6608 60-mer oligonucleotide probes with 6598 unique locus tags from various strains (Table A-1).

GEO or Agilent did not provide sequences for probes for this platform, so it is not possible to assess how the *graSR* mutation may impact gene expression in this dataset. Further, this platform does not include probes for the *vanA* operon, indicating we cannot assess the mechanism of vancomycin resistance in resistant HG001 and SG511, though given their low level resistance (MIC=4mg/L) they are unlikely to use the *vanA* operon, which is associated with immediate high level resistance (MIC≥16mg/L)[56]. GEO provided mRNA expression data for GSE50842 as log10(resistant progeny/sensitive wild type in same strain) values. We convert these log10 ratios to log2 ratios for consistency across data used in this study.

GSE26016 contained triplicate samples (S=6) of wildtype HG001 (WT) and its mutant strain with a *graSR* entire gene (*i.e.*, coding sequence) deletion (Δ*graSR*) grown to mid-exponential phase in tryptic soy broth (TSB) containing 50mg/L colistin for *graSR* induction[76]. Only resistance to colistin, another cell membrane disruptor with similar structure to daptomycin, was established for GSE26016 strains[76]. The WT strain was colistin resistance (MIC=700mg/L) while the Δ*graSR* strain was colistin sensitive (MIC=100mg/L), and resistance in the (Δ*graS*) mutant was completely restored (MIC=700mg/L) via genetic reconstitution[76]. GEO provided this mRNA expression data was provided as unlogged median-normalized gene-level intensities so we z-score across all samples so that all data is normalized prior to use. Samples were profiled on the same platform used for GSE46887 which has a probe to detect *graSR* expression. We note that, while around 2-fold higher than WT, the experiment was able to detect *graSR* expression in the Δ*graSR* mutant.

To examine molecular changes associated with vancomycin, oxacillin, or linezolid susceptibilities individually, we used four datasets (GSE26400, GSE26282, GSE26358, and GSE26258) that contained untreated and antibiotic treated samples of strains with varying resistance levels. Three datasets (GSE26400, GSE26282, and GSE26358) compared untreated and antibiotic (vancomycin, oxacillin, or linezolid, respectively) treated *S. aureus* strains grown in TSB over a time course (30min, 60min, 90min, and 120min post-inoculation into treated media for early exponential, mid-exponential, late exponential, and early stationary growth phases, respectively). GSE26400 contained triplicate samples of untreated and vancomycin treated strains (S=3 per each treatment condition, S=6 samples total per time point, S=48 total), with T8 (32mM vancomycin) and C1 (16mM vancomycin), and PA (4mM vancomycin). GSE26282 contained triplicate samples of untreated and oxacillin treatment strains 1422 and 2798 to characterize a new methicillin resistant isolate lacking *mecA* (S=24). GSE26358 contained duplicate samples of untreated (S=32) and linezolid (S=31) treatment for four linezolid resistant strains: 3577 (S=16), 5612 (S=16), 6939 (S=15), and 7210 (S=16), compared to the linezolid sensitive strain 378. All samples for GSE26400, GSE26282, and GSE26358 were profiled on J. Craig Venter Institute (JCVI) *S. aureus* 16K v9 array designed primarily based on strain USA300 (GEO accession GPL10597). This non-commercial set contains 5087 probes of 70-mer oligonucleotides (Table A-1), including 4368 unique genes with 88 unique genes having multiple probes (P=232 with overlapping gene coverage). Plasmid derived probes for this platform came from pLW043, the plasmid containing Tn1546 transposon with the van operon. GEO values were provided as both log2 ratios of differing strains of the same treatment condition

(*e.g.*, T8treated/PAtreated and T8untreated/PAuntreated) and their associated integrated intensity values.GSE26258 studies oxacillin resistance by examining five replicates grown in tryptic soy broth (TSB) of oxacillin treated and untreated samples of VC30 and 923 (S=10), profiled on JCVI PFGRC *S. aureus* 22K v6 array designed primarily based on strain COL (GEO accession GPL5879). This non-commercial platform with 5056 70-mer probes with 4783 unique probes. GEO provided probe sequences for this platform. GEO values were provided as both integrated intensity values and log2 ratios of differing treatments and strains (*e.g.*, 923treated/923untreated and V3untreated/923untreated). For these datasets, we use intensities to calculate log2 ratios of treated versus untreated for each strain separately (*e.g.*, T8 treated/T8 untreated, PA treated/PA untreated), revealing response mechanisms for individual strains, for consistency across data used in this study.

One limitation to using these antibiotic susceptibility datasets is that they have not undergone proper peer review and there is a lack of information consistency on how data was generated experimentally. For example, there are no available MIC data for strains from GSE26400 (PA, C1, T8), GSE26358 (3577, 5612, 6939, 7210, and 378), GSE26258 (VC30 and 923), and GSE26282 (1422 and 2798), so we cannot confirm the level of resistance for samples used in my work. Therefore, we assume that antibiotic concentrations used were close to MICs for each strain but cannot confirm this assumption. Antibiotic concentrations used to generate mRNA expression data were not provided for samples from GSE26282, GSE26258, or GSE26358. In GSE26400, the concentration was reported at mM rather than the clinical standard of mg/L[92]. Conversion of 16mM to mg/L would be over 23,000mg/L, around 4300% of the highest MIC reported (512mg/L)[243], therefore we believe the mM to be a GEO typographical error

indicating C1 and T8 are high-level vancomycin resistant strains. Unfortunately, we attempted to communicate with the depositors of these datasets several times to clarify this confusion but did not receive any reply. Also, we do not know the details of how the experiment was performed, so it is possible parallel PA cultures were used to standardize C1 and T8 intensities (*e.g.*, T8treated/PAtreated) since these were performed as two separate runs that may have occurred simultaneously. However, it is also possible that the PAfromT8 strain may have mutations not present in the PAfromC1 strain which could occur if the two runs were performed at different times. For this reason, we treat PAfromT8 and PAfromC1 as separate strains for this work. Finally, we do not know mechanisms, such as *vanA*, used by these strains to produce an antibiotic resistance phenotype, and sequenced genomes are not available for strains used in these studies. Probe sequences were available for these datasets though, so we used them to attempt to determine resistance mechanisms. We first select probe sequences for genes in operons with well-established associations to vancomycin resistance (VRSA, *vanA* operon)[56] and methicillin resistance (MRSA, *mecA* operon)[14,244]. We also included the *bla* operon which has been associated methicillin resistance in the absence of the *mecA* operon[14,244]. We verify gene identify using these probe sequences using BLAST. Since GEO provided values as log ratios of differing strains of the same treatment condition (*e.g.*, T8treated/PAtreated) with each raw intensity used for ratio calculations, we examine provided raw intensity values to better understand resistance mechanisms used by these strains (APPENDIX A). While we confirm that oxacillin samples (1422 and 2798) do not have *mecA* expression, we notice for vancomycin resistant samples (T8, C1, and PA) that *vanA* operon gene expression can sometimes be detected in untreated

samples but not in treated samples (*e.g.*, VRA0037, VRA0038, VRA0039, VRA0040, VRA0041, VRA0042, and VRA0043 for *vraR*, *vraS*, *vraH*, *vraA*, *vraX*, *vraY*, and *vraZ*, respectively), the opposite of what would be expected in a VRSA strain since the *vanA* operon has been shown to be constitutively or inducible expressed suggesting that detection should occur in vancomycin treated samples[56]. We fail to find another gene with sequence homology to these probes that might explain this expression pattern using BLAST. While these limitations can complicate conclusions drawn from this work, they are not significant enough to preclude the use of these datasets to examine antibiotic resistance in *S. aureus*.

Figure A-1. Gene Expression Examination for Known Resistance Operons Provides Insight into Potential Resistance Mechanisms

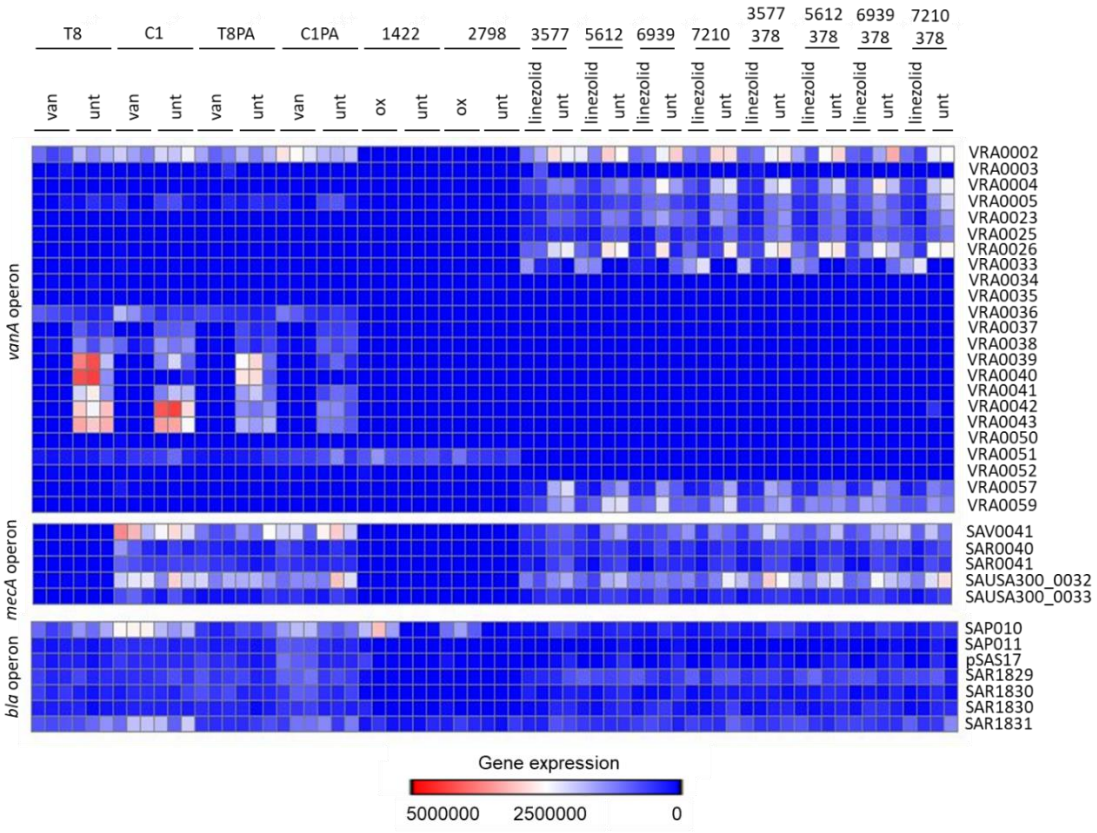


Gene expression heat map of raw intensity values for probes from GPL10597 for well-characterized resistance operons, *vanA* for VRSA and *mecA* and *bla* for MRSA.

To examine vancomycin, oxacillin, or linezolid responses in a sensitive strain, we use data from antibiotic sensitive HG001 samples at GEO accession GSE70040[77]. This dataset contained 156 samples of over 40 experimental conditions including treatment with no antibiotic, 0.63mg/L vancomycin, 0.02mg/L flucloxacillin (like oxacillin), and 0.10mg/L linezolid in TSB collected during both exponential phase and four hours after entrance into stationary phase, post-inoculation into treated media. Samples were profiled on gene level BaSysBio *S. aureus* T1 385K array 080604_SA_JH_Tiling (GEO accession GPL20586) on probes corresponding to a unique gene or complementary strand nucleotide sequence though exact probe sequences used for the platform are not provided (Table A-1). We note that this platform does not include probes for the *vanA* operon. GEO reported mRNA expression as quantile-normalized gene-level intensity values so we z-scored across all samples for normalization prior to use.

APPENDIX B. Justification Supplemental

**Justification for use of 20 pathways per panel and VC40vsΔ*mutS* pathway signature to define *vraS*-driven resistance panels**

We begin by using mutation-driven resistance pathway signatures,VC40vsΔ*mutS*, HG001vsSG511, and WTvsΔ*graS*, for further analysis to justify the use of 20 pathways per panel in my study, which captures approximately 25% of the 164 *S. aureus* pathways from KEGG, 12.5% per tail. To do this, we define *vraS*-driven resistance pathway panels from the VC40vsΔ*mutS* pathway signature as done in my study for the 20 pathway panels, except with 10, 13, 15, 18, 22, 25, 28, and 30 pathways per panel instead. We compare these new pathway panels as query against HG001vsSG511 and WTvsΔ*graSR* pathway signatures as reference using GSEA. From this analysis, we note that using panels containing 13 to 25 pathways do not substantially change similarities uncovered by GSEA when compared to verification signatures, while 28 and 30 panel pathways no longer detected similarities in WTvsΔ*graSR* and 10 panel pathways loses detection for the up-regulated panel and HG001vsSG511 (Figure B-1). We note that use of 15 and 25 pathways per panel detect enrichment in the down-regulated panel for the signature that 18, 20, and 22 pathways per panel does not detect. We will re-address this issue momentarily.

Figure B-1. Using 20 Pathways per Panel Does Not Affect Pathway Panel Enrichment Results

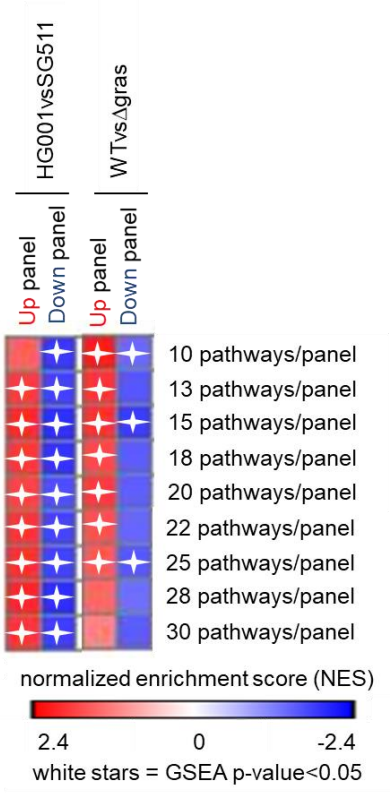


Heat map of normalized enrichment scores (NES) achieved from Gene Set Enrichment Analysis (GSEA) of verification signatures HG001vsSG511 and WTvsΔ*graSR* (references) and various sized pathway panels defined from VC40vsΔ*mutS* illustrates the use of 20 pathways/panel does not substantially alter obtained results.

As justification for my use of the VC40vsΔ*mutS* pathway signature to define *vraS*-driven resistance panels in my study, we examine how results may change if panels are derived from other datasets. To do this, we define *graSR*-driven pathway panels from HG001vsSG511 and WTvsΔ*graSR* in the same manner performed to derive the *vraS*-driven resistance panels used in my study. We use the *graSR*-driven pathway panels as queries for GSEA versus the VC40vsΔ*mutS* pathway signature as reference. We do not find a substantial change for up-regulated panels, despite variations in pathway panel size

(Figure B-2), supporting the conclusion that my up-regulated pathway panel is truly enriched. We lose enrichment in my down-regulated panel which confirms what was observed when pathway panels are defined from the VC40vsΔ*mutS* pathway signature. We also note that using 15 or 25 pathways per panel lost enrichment in one of the two up-regulated panels (Figure B-2), supporting my decision to select 20 pathways per panel rather than 15 or 25 pathways per panel for use in the remainder of this study. We finally note that lysine biosynthesis pathways (M00016 and M00527) are the only pathways shared across leading-edges when we define panels from HG001vsSG511 (NES>1.91, p-value<0.001) and WTvsΔ*graSR* (NES>2.16, p-value<0.001), showing my overall findings regarding lysine biosynthesis are not lost when *graSR*-driven resistance panels are used.

Figure B-2. Using Verification Signatures to Derive Pathway Panels Does Not Affect Pathway Panel Enrichment Results

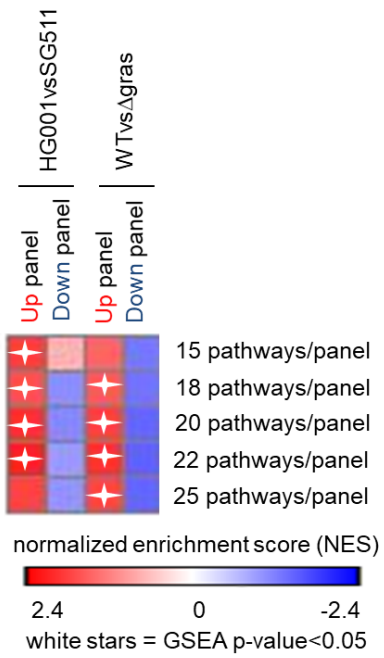


Heat map of normalized enrichment scores (NES) achieved from GSEA of VC40vs*ΔmutS* signature (reference) and various sized pathway panels defined from HG001vsSG511 and WTvsΔ*graSR* signatures confirms true enrichment of up-regulated pathway panels not seen in down-regulated pathway panels.

**Justification for use of locus tags**

We use locus tags (*e.g.*, SAUSA300_2200) rather than gene symbols (*e.g.*, *rpsS*) to increase gene signature lengths and ensure pathway query set sizes are greater than 10 since multiple locus tags can map to the same gene symbol (*e.g.*, locus tags SAOUHSC_02989 and SAOUHSC_02491 from *S. aureus* NCTC 8325 have *secY* as their gene symbol in NCBI Genome), and longer gene signatures and query sets above 10 items allow GSEA to calculate more robust NES for pathway signature generation[65,67]. While using locus tags increases the length of gene signatures, it does not improve

genome annotation since we notice in the platform used to profile most datasets used in this work (GPL10597) that a substantial number (26.8%) of probes have hypothetical annotation (*i.e.*, no gene symbol and description) when probes are converted to gene symbols using NCBI databases and Position-Specific Iterative Basic Local Alignment Search Tool (PSI-BLAST)[245], and find similar percentages when examining genome annotation across the seven *S. aureus* strains of varying methicillin and vancomycin sensitivities GPL10597 probes were designed to target, which is a common finding among bacterial genomes[229,246]. Unfortunately, lack of complete genome annotation weakens the detection ability of any gene expression and pathway enrichment analyses, including the approach used here, due to incomplete pathway database information.

**Justification for use of KEGG**

To address pathway database completeness, we evaluate several knowledgebases, including Molecular Signatures Database (MSigDB) version 6.2[67,152], Reactome version 67[155], Gene Ontology version 12.0[68,157,158], and Pathosystems Resource Integration Center (PATRIC) version 3.5.7[168,247], for gene, pathway, and strain inclusion, all important considerations when selecting a pathway database[65]. We find these knowledgebases differ substantially in gene coverage (G=2458, G=730, G=657, and G=0 for KEGG, GO, PATRIC, and Reactome, respectively), when we compare the number of unique locus tags for the 12 *S. aureus* species with targeted genes on platforms used for datasets in this work. KEGG and PATRIC both have locus tags and gene symbols available whereas GO only has gene symbols, which limited my ability to use GO. Further, we find KEGG had 326 pathways specific to *S. aureus* with 53 strains with varying resistances represented while PATRIC had 94 pathways with one strain represented. Therefore, we use KEGG

for this work since it has the largest number of genes, pathways, and represented *S. aureus* genomes between knowledgebases at the time of this study, though we acknowledge that knowledgebases are constantly updated as biological understanding advances so we recommend a thorough knowledgebase analysis be done prior to any use of my pathway signature approach.

APPENDIX C. Complete Separation Data

Compared to human trials, bacterial experiments frequently have a small sample size (<5 samples/condition)[201,202], which can lead to complete separation during random model validation methods (*i.e.*, principal component analysis (PCA) and logistic regression analysis)[203-205]. For example, we observe complete separation in both *graSR*-driven resistance datasets when unlogged or raw intensity gene expression values, for GSE50842 and GSE26016 respectively, are used for individual samples in PCA on 10 or 100 randomly selected genes or when all dataset genes are selected (Figure C-1). We also find complete sample separation when using NES from 10 or 20 randomly selected pathways for PCA (data not shown). This separation is confirmed via leave one out cross validation (LOOCV) where we achieve 98% complete sample separation ($r^2$=1.0) from 1000 randomly selected 20-pathway panels whose membership excluded pathways from my *vraS*-driven resistance panels in both datasets. For this reason, we use a GSEA-based pathway signature comparison approach with a random modeling component to verify my *vraS*-driven and vancomycin susceptibility panels.

Figure C-1. Principal Component Analysis of Randomly Selected Genes

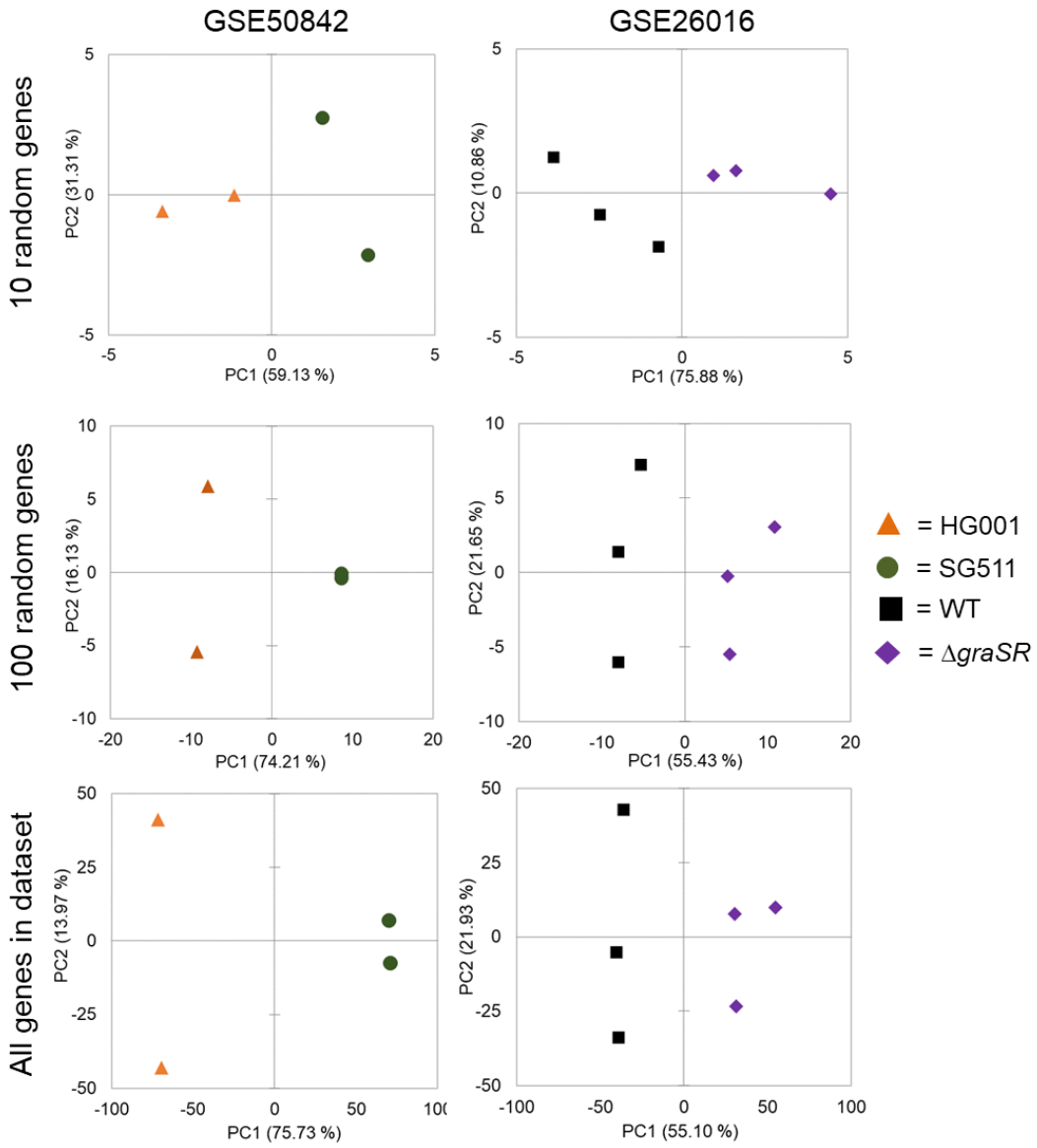


Principal component analysis (PCA) shows complete separation of GSE50842 and GSE26016 samples regardless of number of genes selected, suggesting these datasets separate naturally and would not be good for traditional random model validation methods (*i.e.*, principal component analysis (PCA) and logistic regression analysis).

Figure C-2. Principal Component Analysis of Randomly Selected Pathways

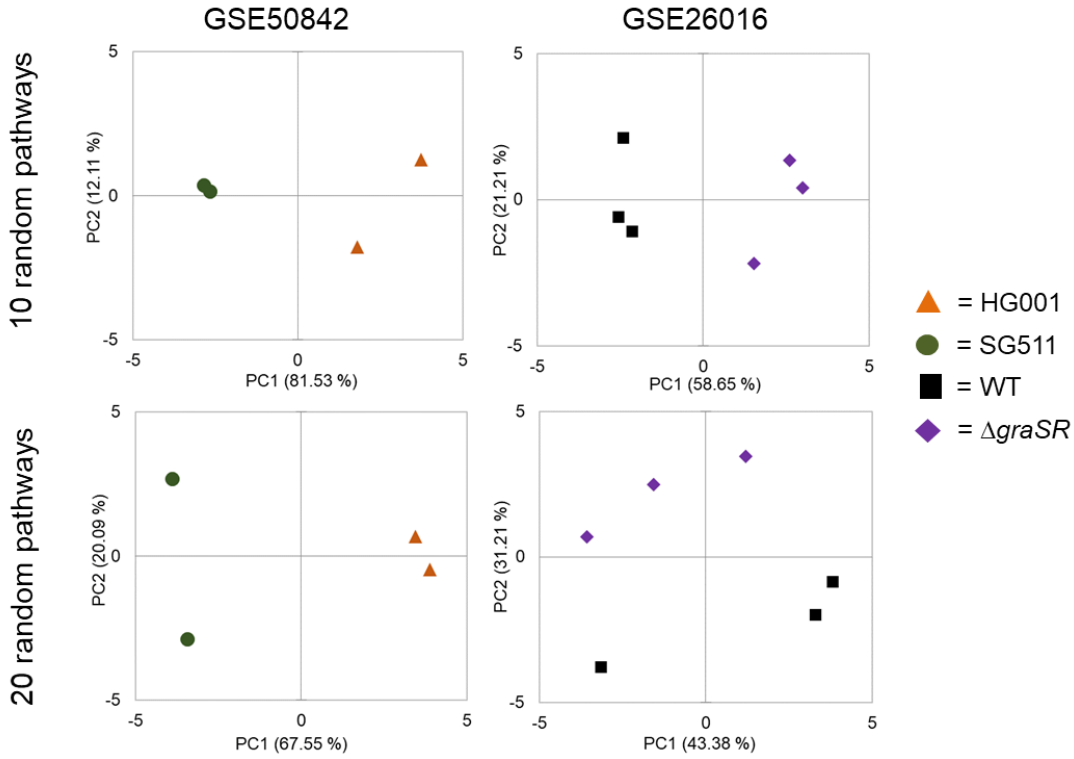


Principal component analysis (PCA) shows complete separation of GSE50842 and GSE26016 samples regardless of number of pathways selected, suggesting these datasets separate naturally and would not be good for traditional random model validation methods (*i.e.*, principal component analysis (PCA) and logistic regression analysis).

To assess if use of a dataset with more samples could introduce enough variation in gene expression to make PCA and logistic regression analysis work, we compare raw intensities for GSE26016 sample populations and find differences in variance (WT: 172.9; Δ*graSR*: 147.0) between WT and Δ*graSR* (Table C-1). When looking at individual sample distributions, we note overlap of sample means and ranges, suggesting that more samples has the potential to produce enough variation though more work is needed to determine how many samples is enough. Experimental generation of a mRNA expression

dataset with enough samples for successful logistic regression analysis with random modeling could improve random modeling results using PCA and LOOCV.

Table C-1. Individual Sample Statistics for GSE26016 Show Overlap Between WT and Δ*graSR* Samples

| | WT | | | Δ*graSR* | | |
|---|---|---|---|---|---|---|
| GSM | 638321 | 638322 | 638323 | 638324 | 638325 | 638326 |
| Mean | 5.89 | 5.36 | 5.95 | 5.11 | 6.21 | 5.54 |
| Range min | 0.19 | 0.14 | 0.14 | 0.13 | 0.13 | 0.12 |
| Range max | 113.19 | 71.70 | 82.85 | 78.34 | 76.05 | 72.98 |

GSM refers to sample identification label in Gene Expression Omnibus (*e.g.*, GSM638321).

APPENDIX D. Leading-edge Pathway Tables

Table D-1 is derived from Gene Set Enrichment Analysis (GSEA) using *vraS*-driven resistance panels defined from the VC40vsΔ*mutS* signature (query) and HG001vsSG511 and WTvsΔ*graSR* resistance signatures (references).

Table D-2 is derived from GSEA using vancomycin susceptibility (*i.e.*, difference in response between resistant and sensitive strains) panels defined from the T8vsPA susceptibility signature (query) and C1vsPA susceptibility signature (reference).

Table D-3 is derived from GSEA using *vraS*-driven resistance panels (query) and T8vsPA and C1vsPA vancomycin susceptibility signatures (references).

Table D-4 is derived from GSEA using *vraS*-driven resistance panels (query) and 1422vs2798 and V3vs923 oxacillin susceptibility signatures (references).

Table D-5 is derived from GSEA using *vraS*-driven resistance panels (query) and 3577vs378, 5612vs378, 6939vs378, and 7210vs378 linezolid susceptibility signatures (references).

Table D-6 is derived from GSEA using *vraS*-driven resistance panels (query) and HG001van, HG001fluc, and HG001line response signatures in a sensitive strain for vancomycin, flucloxacillin (like oxacillin), and linezolid responses, respectively (references).

Table D-1. Leading-edge Pathways Associated with *vraS*- and *graSR*-driven Resistance

| Panel | Signature | Module number |
|---|---|---|
| Up | HG001vs SG511 | Dissimilatory nitrate reduction (M00530)*, Lysine biosynthesis via diaminopimelic acid aminotransferase (M00527)*, Histidine biosynthesis (**M00026**)*, Lysine biosynthesis via succinyl-diaminopimelic acid (M00016)*, D-Methionine transport system (M00238)*, Betaine biosynthesis (M00555)*, Arabinogalactan oligomer/maltooligosaccharide (M00491)*, Leucine biosynthesis (M00432)*, Phosphonate (M00223)*, Serine biosynthesis (**M00020**)* |
| | WTvs Δ*graS* | Lysine biosynthesis via succinyl-diaminopimelic acid (M00016)*, Lysine biosynthesis via diaminopimelic acid aminotransferase (M00527)*, Leucine biosynthesis (M00432)*, Histidine biosynthesis (**M00026**)*, Biotin biosynthesis BioW pathway (M00577), VraS-VraR cell-wall peptidoglycan synthesis (**M00480**), Biotin biosynthesis (M00123), Putative peptide (M00583), Osmoprotectant transport system (M00209), Serine biosynthesis (**M00020**), Cationic antimicrobial peptide (**M00732**), Betaine biosynthesis (M00555), Dissimilatory nitrate reduction (M00530) |
| Down | HG001vs SG511 | Iron complex (M00240)*, Spermidine/ putrescine transport system (M00299)*, Nickel complex (M00440)*, ABC-2 type (M00254)*, ArlS-ArlR virulence regulation (M00716), Menaquinone biosynthesis (M00116), Amino-acyl tRNA biosynthesis eukaryotes (**M00359**), Amino-acyl tRNA biosynthesis prokaryotes (**M00360**), Adenine ribonucleotide biosynthesis (M00049), TCA cycle second carbon oxidation (M00011) |
| | WTvs Δ*graS* | Amino-acyl tRNA biosynthesis prokaryotes (**M00360**)*, Amino-acyl tRNA biosynthesis eukaryotes (**M00359**)*, Guanine ribonucleotide biosynthesis (M00050)*, Adenine ribonucleotide biosynthesis (M00049)*, TCA cycle (M00009), TCA cycle second carbon oxidation (M00011), Succinate dehydrogenase prokaryotes (**M00149**), Acylglycerol degradation (M00098), ABC-2 type (M00254), Uridine monophosphate biosynthesis (M00051), TCA first carbon oxidation (M00010), Energy-coupling factor (M00582), Spermidine/ putrescine transport system (M00299) |

Modules listed in order of normalized enrichment score from most to least change in pathway activity. * represents Gene Set Enrichment Analysis derived p-value<0.05. HG001vsSG511 signature represents the difference in resistance between strains with *graSR* mutations. WTvsΔ*graSR* signature approximates *graS*-driven resistance. Bold font indicates a pathway with known association to antibiotic resistance (*vraSR* or *graSR*-

driven). Pathways that have a * but do not have bold font are novel pathways associated with antibiotic resistance identified from my pathway signature approach.

Table D-2. Leading-edge Pathways Associated with Vancomycin Susceptibility in *S. aureus*

| Panel | Signature | Module number |
|---|---|---|
| Up | C1vsPA | Oligopeptide (M00439)*, Threonine biosynthesis (M00018)*, Lysine biosynthesis via succinyl-diaminopimelic acid (M00016)*, D-Methionine transport system (M00238)*, Lysine biosynthesis via diaminopimelic acid aminotransferase (M00527)*, Riboflavin biosynthesis (M00125)*, Osmoprotectant transport system (M00209)*, Energy-coupling factor (M00582), VraS-VraR cell-wall peptidoglycan synthesis (*M00480*)*, Pantothenate biosynthesis (M00119), Betaine biosynthesis (M00555), Isoleucine biosynthesis (M00570), Formaldehyde assimilation ribulose monophosphate (M00345), Uridine monophosphate biosynthesis (M00051), Cationic antimicrobial peptide resistance VraFG transporter (*M00730*), Glyoxylate cycle (M00012) |
| Down | C1vsPA | Iron complex (M00240)*, Amino-acyl tRNA biosynthesis prokaryotes (*M00360*)*, Dissimilatory nitrate reduction (M00530)*, Amino-acyl tRNA biosynthesis eukaryotes (*M00359*)*, Nickel complex (M00440)*, Ribosome bacteria (*M00178*)*, Fructose-specific (M00273)*, TCA cycle second carbon oxidation (*M00011*)*, Glucose- specific (M00809)*, Spermidine/ putrescine transport system (M00299)*, NreB-NreC dissimilatory nitrate/nitrite reduction (M00483)*, Putative peptide (M00583), Cytochrome C oxidase (M00154)*, TCA cycle (*M00009*), F-type ATPase prokaryotes and chloroplasts (*M00157*), Urea cycle (M00029), Siroheme biosynthesis (M00846), Cytochrome aa3-600 menaquinol oxidase (M00416), Succinate dehydrogenase prokaryotes (M00149), Cystine (M00234) |

Modules listed in order of normalized enrichment score from most to least change in pathway activity. * represents Gene Set Enrichment Analysis derived p-value<0.05. Italics font indicates a pathway with known association to vancomycin intermediate resistance lacking the *vanA* operon. Pathways that have a * but do not have bold font are novel pathways associated with vancomycin intermediate resistance identified from my pathway signature approach.

Table D-3 Leading-edge Pathways Associated with *vraS*-driven Resistance and Vancomycin Susceptibility in *S. aureus*

| Panel | Signature | Module number |
|---|---|---|
| Up | T8 vs PA | Osmoprotectant transport system (M00209)*, D-Methionine transport system (M00238)*, Lysine biosynthesis via succinyl-diaminopimelic acid (M00016), VraS-VraR cell-wall peptidoglycan synthesis (***M00480***)*, Lysine biosynthesis via diaminopimelic acid aminotransferase (M00527), Betaine biosynthesis (M00555)*, Cationic antimicrobial peptide resistance VraFG transporter (***M00730***) |
| | C1 vs PA | Lysine biosynthesis via succinyl-diaminopimelic acid (M00016)*, D-Methionine transport system (M00238)*, Lysine biosynthesis via diaminopimelic acid aminotransferase (M00527)*, Osmoprotectant transport system (M00209)*, VraS-VraR cell-wall peptidoglycan synthesis (***M00480***)*, Betaine biosynthesis (M00555) |
| Down | T8 vs PA | Amino-acyl tRNA biosynthesis prokaryotes (***M00360***)*, Amino-acyl tRNA biosynthesis eukaryotes (***M00359***)*, TCA cycle second carbon oxidation (*M00011*)*, TCA cycle (*M00009*)*, Iron complex (M00240)*, Nickel complex (M00440)*, Spermidine/ putrescine transport system (M00299)*, Succinate dehydrogenase prokaryotes (**M00149**)*, ArlS-ArlR two-component regulatory system (M00716), Guanine ribonucleotide biosynthesis (*M00050*), Menaquinone biosynthesis (M00116), Adenine ribonucleotide biosynthesis (*M00049*), Shikimate pathway (M00022) |
| | C1 vs PA | Iron complex (M00240)*, Amino-acyl tRNA biosynthesis prokaryotes (***M00360***)*, Amino-acyl tRNA biosynthesis eukaryotes (***M00359***)*, Nickel complex (M00440)*, TCA cycle second carbon oxidation (*M00011*)*, Adenine ribonucleotide biosynthesis (*M00049*)*, Spermidine/ putrescine transport system (M00299)*, Guanine ribonucleotide biosynthesis (*M00050*), TCA cycle (*M00009*), Succinate dehydrogenase prokaryotes (**M00149**), ArlS-ArlR virulence regulation (M00716), Menaquinone biosynthesis (M00116) |

Modules listed in order of normalized enrichment score from most to least change in pathway activity. * represents Gene Set Enrichment Analysis derived p-value<0.05. Bold font indicates a pathway with known association to *vraS*-driven antibiotic resistance. Italics font indicates a pathway with known association to vancomycin intermediate resistance lacking the *vanA* operon. Pathways that have a * but do not have bold font are novel pathways associated with vancomycin intermediate resistance identified from my pathway signature approach.

Table D-4. Leading-edge Pathways Associated with *vraS*-driven Resistance and Oxacillin Susceptibility in *S. aureus*

| Panel | Signature | Module number |
|---|---|---|
| Up | 1422vs2798 | Leucine biosynthesis (M00432)*, Dissimilatory nitrate reduction (M00530), Inosine monophosphate biosynthesis (*M00048*), Cytochrome D ubiquinol oxidase (M00153), Betaine biosynthesis (M00555), Phosphonate (M00223), Putative peptide (M00583), Lysine biosynthesis via diaminopimelic acid aminotransferase (M00527), Histidine biosynthesis (**M00026**), Lysine biosynthesis via succinyl-diaminopimelic acid (M00016), Cationic antimicrobial peptide (***M00732***) |
| | V3vs923 | Dissimilatory nitrate reduction (M00530)*, Inosine monophosphate biosynthesis (*M00048*)*, Osmoprotectant transport system (M00209)*, Peptides/nickel (M00239), Cationic antimicrobial peptide (***M00732***), Serine biosynthesis (**M00020**), VraS-VraR cell-wall peptidoglycan synthesis (***M00480***), D-Methionine transport system (M00238), Cationic antimicrobial peptide resistance VraFG transporter (***M00730***), Putative peptide (M00583), Lysine biosynthesis via succinyl-diaminopimelic acid (M00016), Biotin biosynthesis (M00123), Biotin biosynthesis BioW pathway (M00577), Lysine biosynthesis via diaminopimelic acid aminotransferase (M00527) |
| Down | 1422vs2798 | TCA cycle (*M00009*)*, TCA cycle second carbon oxidation (*M00011*)*, Molybdate transport system (M00189), Succinate dehydrogenase prokaryotes (**M00149**), ArlS-ArlR virulence regulation (M00716), Acylglycerol degradation (M00098), TCA first carbon oxidation (*M00010*), ABC-2 type transport system (M00254) |
| | V3vs923 | TCA cycle (*M00009*)*, Uridine monophosphate biosynthesis (*M00051*)*, TCA cycle second carbon oxidation (*M00011*)*, TCA first carbon oxidation (*M00010*)*, Nickel complex (M00440), Molybdate transport system (M00189), Menaquinone biosynthesis (M00116), Adenine ribonucleotide biosynthesis (*M00049*), Succinate dehydrogenase prokaryotes (**M00149**), Acylglycerol degradation (M00098), Iron complex (M00240), Spermidine/ putrescine transport system (M00299), Energy-coupling factor (M00582) |

Modules listed in order of normalized enrichment score from most to least change in pathway activity. * represents Gene Set Enrichment Analysis derived p-value<0.05. Bold font indicates a pathway with known association to *vraS*-driven antibiotic resistance. Italics font indicates a pathway with known association to vancomycin intermediate resistance lacking the *vanA* operon. Underlined pathways indicate as oxacillin resistance

association. Pathways that have a * but are not underlined are novel pathways associated with oxacillin intermediate resistance identified from my pathway signature approach.

Table D-5. Leading-edge Pathways Associated with *vraS*-driven Resistance and Linezolid Susceptibility in *S. aureus*

| Panel | Signature | Module number |
|---|---|---|
| Up | 3577vs378 | D-Methionine transport system (M00238)*, Lysine biosynthesis via diaminopimelic acid aminotransferase (M00527)*, Inosine monophosphate biosynthesis (*M00048*)*, Cationic antimicrobial peptide (***M00732***), Leucine biosynthesis (M00432), Lysine biosynthesis via succinyl-diaminopimelic acid (M00016), Cationic antimicrobial peptide resistance VraFG transporter (***M00730***) |
| | 5612vs378 | Inosine monophosphate biosynthesis (*M00048*)*, D-Methionine transport system (M00238)*, Lysine biosynthesis via succinyl-diaminopimelic acid (M00016)*, Lysine biosynthesis via diaminopimelic acid aminotransferase (M00527)*, Histidine biosynthesis (**M00026**), Leucine biosynthesis (M00432), Phosphonate (M00223) |
| | 6939vs378 | Inosine monophosphate biosynthesis (*M00048*)*, D-Methionine transport system (M00238), Peptides/nickel (M00239), Arabinogalactan oligomer/maltooligosaccharide (M00491), Lysine biosynthesis via succinyl-diaminopimelic acid (M00016), Lysine biosynthesis via diaminopimelic acid aminotransferase (M00527)*, VraS-VraR cell-wall peptidoglycan synthesis (***M00480***), Serine biosynthesis (**M00020**), Cationic antimicrobial peptide resistance VraFG transporter (***M00730***), Cationic antimicrobial peptide (***M00732***) |
| | 7210vs378 | Dissimilatory nitrate reduction (M00530)*, Osmoprotectant transport system (M00209)*, Phosphonate (M00223)* |
| Down | 3577vs378 | TCA cycle second carbon oxidation (*M00011*)*, Molybdate transport system (M00189)*, TCA cycle (*M00009*)*, Menaquinone biosynthesis (M00116), Succinate dehydrogenase prokaryotes (**M00149**)* |
| | 5612vs378 | TCA cycle (*M00009*)*, TCA cycle second carbon oxidation (*M00011*)*, Spermidine/ putrescine transport system (M00299)*, Succinate dehydrogenase prokaryotes (**M00149**)*, Menaquinone biosynthesis (M00116), TCA cycle first carbon oxidation (*M00010*), Molybdate transport system (M00189), Amino-acyl tRNA biosynthesis prokaryotes (***M00360***) |
| | 6939vs378 | Uridine monophosphate biosynthesis (*M00051*)*, Iron complex (M00240)*, Energy-coupling factor (M00582), TCA cycle first carbon oxidation (*M00010*), ABC-2 type transport system (M00254) |
| | 7210vs378 | TCA cycle (*M00009*)*, TCA cycle second carbon oxidation (*M00011*), Amino-acyl tRNA biosynthesis eukaryotes (***M00359***), Spermidine/ putrescine transport system (M00299), Adenine ribonucleotide biosynthesis (*M00049*), Succinate dehydrogenase prokaryotes (**M00149**), Amino-acyl tRNA biosynthesis prokaryotes (***M00360***), Nickel complex (M00440), Molybdate transport system (M00189), Menaquinone biosynthesis (M00116) |

Modules listed in order of normalized enrichment score from most to least change in pathway activity. * represents Gene Set Enrichment Analysis derived p-value<0.05. Bold font indicates a pathway with known association to *vraS*-driven antibiotic resistance. Italics font indicates a pathway with known association to vancomycin intermediate resistance lacking the *vanA* operon. Green font indicates a pathway with known association to linezolid resistance.

Table D-6. Leading-edge Pathways Associated with *vraS*-driven Resistance and Responses

| Panel | Signature | Module number |
|---|---|---|
| Up | HG001van (vancomycin treated vs untreated) | Leucine biosynthesis (M00432)*, Osmoprotectant transport system (M00209)*, Lysine biosynthesis via diaminopimelic acid aminotransferase (M00527)*, Biotin biosynthesis BioW pathway (M00577), Biotin biosynthesis (M00123), VraS-VraR cell-wall peptidoglycan synthesis (***M00480***), Betaine biosynthesis (M00555), Lysine biosynthesis via succinyl-diaminopimelic acid (M00016) |
| | HG001fluc (flucloxacillin treated vs untreated) | Inosine monophosphate biosynthesis (*M00048*)*, Lysine biosynthesis via succinyl-diaminopimelic acid (M00016)*, Dissimilatory nitrate reduction (M00530)*, D-Methionine transport system (M00238)*, Histidine biosynthesis (**M00026**)*, Lysine biosynthesis via diaminopimelic acid aminotransferase (M00527)*, Osmoprotectant transport system (M00209)*, Putative peptide (M00583)* |
| | HG001line (linezolid treated vs untreated) | Inosine monophosphate biosynthesis (*M00048*)*, Dissimilatory nitrate reduction (M00530)*, Lysine biosynthesis via diaminopimelic acid aminotransferase (M00527), Putative peptide (M00583)*, Lysine biosynthesis via succinyl-diaminopimelic acid (M00016), Leucine biosynthesis (M00432), Serine biosynthesis (**M00020**) |
| Down | HG001van (vancomycin treated vs untreated) | Menaquinone biosynthesis (M00116), Energy-coupling factor (M00582), Uridine monophosphate biosynthesis (*M00051*), ABC-2 type (M00254), Succinate dehydrogenase prokaryotes (**M00149**), Shikimate pathway (M00022), Molybdate transport system (M00189) |
| | HG001fluc (flucloxacillin treated vs untreated) | Iron complex (M00240)*, Spermidine/ putrescine transport system (M00299)*, Amino-acyl tRNA biosynthesis prokaryotes (***M00360***)*, Nickel complex (M00440)*, Amino-acyl tRNA biosynthesis eukaryotes (***M00359***), Menaquinone biosynthesis (M00116), Energy-coupling factor (M00582) |
| | HG001line (linezolid treated vs untreated) | Iron complex (M00240)*, Spermidine/ putrescine transport system (M00299)*, Menaquinone biosynthesis (M00116)*, Uridine monophosphate biosynthesis (*M00051*), Amino-acyl tRNA biosynthesis prokaryotes (***M00360***), Amino-acyl tRNA biosynthesis eukaryotes (***M00359***), TCA first carbon oxidation (*M00010*)*, Energy-coupling factor (M00582) |

Modules listed in order of normalized enrichment score from most to least change in pathway activity. * represents Gene Set Enrichment Analysis derived p-value<0.05. Bold

font indicates a pathway with known association to *vraS*-driven antibiotic resistance. Italics font indicates a pathway with known association to vancomycin intermediate resistance lacking the *vanA* operon. Underlined pathways indicate as oxacillin resistance association. Green font indicates a pathway with known association to linezolid resistance.

APPENDIX E. Significant Pathways Associated with Vancomycin Response in *S. aureus*

| Panel | Signature | Module number |
|---|---|---|
| Up | T8treatvsT8unt | Oligopeptide (M00439), Methionine transport system (M00238), Threonine biosynthesis (M00018), Energy-coupling factor (M00582), C5 isoprenoid biosynthesis mevalonate pathway(M00095), Twin-arginine translocation system (M00336), Lysine biosynthesis via succinyl-diaminopimelic acid (M00016), Formaldehyde assimilation ribulose monophosphate (M00345), Osmoprotectant transport system (M00209), VraS-VraR cell-wall peptidoglycan synthesis (*M00480*), Glyoxylate cycle (M00012), Betaine biosynthesis (M00555) |
| | C1treatvsC1unt | Threonine biosynthesis (M00018), VraDE transporter (*M00737*), Cationic antimicrobial peptide resistance lysyl-phosphatidylglycerol (L-PG) synthase MprF (*M00726*), Cationic antimicrobial peptide resistance VraFG transporter (*M00730*), Energy-coupling factor (M00582), Oligopeptide (M00439), D-Methionine transport system (M00238), Bacitracin transport system (M00314), Lysine biosynthesis via diaminopimelic acid aminotransferase (M00527), Lysine biosynthesis via succinyl-diaminopimelic acid (M00016), GraS-GraR two-component regulatory system (*M00733*), Riboflavin biosynthesis (M00125), Glyoxylate cycle (M00012), Inositol phosphate metabolism (M00131) |
| | PAfromT8treatvs<br>PAfromT8unt | Nickel complex (M00440), Iron complex (M00240), Spermidine/putrescine transport system (M00299), Multidrug resistance efflux pump MepA (M00705), F-type ATPase prokaryotes and chloroplasts (*M00157*), Glyoxylate cycle (M00012) |
| | PAfromC1treatvs<br>PAfromC1unt | Iron complex (M00240), Cationic antimicrobial peptide resistance VraFG transporter (*M00730*), Histidine biosynthesis (M00026), β-Lactam resistance Bla system (M00627), GraS-GraR two-component regulatory system (*M00733*), Lysine biosynthesis via diaminopimelic acid aminotransferase (M00527), Cationic antimicrobial peptide resistance, lysyl-phosphatidylglycerol synthase MprF (*M00726*), Peptides/nickel transport system (M00239), Betaine biosynthesis (M00555), Zinc transport system (M00242), Cytochrome c oxidase (M00154), Biotin biosynthesis (M00577) |

| Panel | Signature | Module number |
|---|---|---|
| Down | T8treatvsT8unt | Amino-acyl tRNA biosynthesis prokaryotes (*M00360*), TCA cycle second carbon oxidation (*M00011*), Dissimilatory nitrate reduction (M00530), Amino-acyl tRNA biosynthesis eukaryotes (*M00359*), Ribosome bacteria (*M00178*), Vancomycin resistance (M00651), TCA cycle (M00009), Nickel complex (M00440), Urea cycle (M00029), Siroheme biosynthesis (M00846), Pyruvate oxidation (M00307), Arginine biosynthesis (M00844), Glucose-specific II component (M00809), Cytochrome c oxidase (M00154), Succinate dehydrogenase (M00149), F-type ATPase prokaryotes and chloroplasts (*M00157*), Cystine transport system (M00234), Arginine biosynthesis (M00845), Trehalose-specific II component (M00270), Lysine degradation (M00032), NreB-NreC dissimilatory nitrate/nitrite reduction two-component regulatory system (M00483), Polyamine biosynthesis (M00134), Maltose and glucose-specific II component (M00266), N,N'-Diacetylchitobiose transport system (M00606), Glucose/mannose transport system (M00605) |
| | C1treatvsC1unt | Ribosome bacteria (*M00178*), Amino-acyl tRNA biosynthesis prokaryotes (*M00360*), Amino-acyl tRNA biosynthesis eukaryotes (*M00359*), Dissimilatory nitrate reduction (M00530), Nickel complex (M00440), Vancomycin resistance (M00651), Siroheme biosynthesis (M00846), Iron complex (M00240), RNA polymerase bacteria (M00183), Pyruvate oxidation (M00307), TCA cycle second carbon oxidation (*M00011*), Glucose-specific II component (M00809), F-type ATPase prokaryotes and chloroplasts (*M00157*), Molybdate transport system (M00189), NreB-NreC dissimilatory nitrate/nitrite reduction two-component regulatory system (M00483), Phosphate acetyltransferase-acetate kinase pathway (M00579), Cytochrome aa3-600 menaquinol oxidase (M00416), Fructose-specific II component (M00273), Spermidine/putrescine transport system (M00299), ResE-ResD two-component regulatory system (M00458) |
| | PAfromT8treatvs PAfromT8unt | Vancomycin resistance (M00651), Uridine monophosphate biosynthesis (*M00051*), Putative ABC transport system (M00211), Isoleucine biosynthesis (M00570), ABC-2 type transport system (M00254), Inosine monophosphate biosynthesis (*M00048*), Pyruvate oxidation (M00307), Pentose phosphate pathway archaea (*M00580*), Maltose and glucose-specific II component (M00266) |

| Panel | Signature | Module number |
|---|---|---|
| Down | PAfromC1treatvs PAfromC1unt | Vancomycin resistance (M00651), Uridine monophosphate biosynthesis (*M00051*), Ribosome bacteria (*M00178*), Siroheme biosynthesis (M00846), Molybdate transport system (M00189), Putative ABC transport system (M00211), Glucose-specific II component (M00809), ABC-2 type transport system (M00254), Glycolysis core module involving three-carbon compounds (M00002), Pentose phosphate pathway, non-oxidative phase (*M00007*), Cytochrome aa3-600 menaquinol oxidase (M00416), Phosphate acetyltransferase-acetate kinase pathway (M00579), LytS-LytR two-component regulatory system (M00492), Maltose and glucose-specific II component (M00266), ResE-ResD two-component regulatory system (M00458) |

Modules listed in order of normalized enrichment score from most to least change in pathway activity with all pathways achieving a Gene Set Enrichment Analysis derived p-value<0.05. Italics font indicates a pathway with known association to vancomycin intermediate resistance lacking the *vanA* operon. Red font are pathways associated with vancomycin resistance via the *vanA* operon.

APPENDIX F. KEGG Pathways Used in Pathway Signature Generation

| Category | Subcategory | No.[a] | Module Descriptions[a] |
|---|---|---|---|
| Carbohydrate and lipid metabolism pathway modules | Central carbohydrate metabolism | M00001 | Glycolysis (Embden-Meyerhof pathway) |
| | | M00002 | Glycolysis core module involving 3-carbon compounds |
| | | M00003 | Gluconeogenesis |
| | | M00004 | Pentose phosphate cycle |
| | | M00005 | Phosphoribosyl diphosphate biosynthesis |
| | | M00006 | Pentose phosphate pathway, oxidative phase |
| | | M00007 | Pentose phosphate pathway non-oxidative phase |
| | | M00008 | Entner-Doudoroff pathway |
| | | M00009 | Citrate cycle (TCA cycle, Kreb's cycle) |
| | | M00010 | Citrate cycle first carbon oxidation |
| | | M00011 | Citrate cycle second carbon oxidation |
| | | M00307 | Pyruvate oxidation |
| | | M00580 | Pentose phosphate pathway archaea |
| | Other carbohydrate metabolism | M00012 | Glyoxylate cycle |
| | | M00549 | Nucleotide sugar biosynthesis |
| | | M00632 | Galactose degradation (Leloir pathway) |
| | Fatty acid metabolism | M00082 | Fatty acid biosynthesis initiation |
| | | M00083 | Fatty acid biosynthesis elongation |
| | | M00086 | β-Oxidation acyl-CoA synthesis |
| | | M00087 | β-Oxidation |
| | Lipid metabolism | M00093 | Phosphatidylethanolamine biosynthesis |
| | | M00131 | Inositol phosphate metabolism |
| | Terpenoid backbone biosynthesis | M00095 | C5 isoprenoid biosynthesis (mevalonate pathway) |
| | | M00096 | C5 isoprenoid biosynthesis (non-mevalonate pathway) |
| | | M00364 | C10-C20 isoprenoid biosynthesis bacteria |
| | | M00365 | C10-C20 isoprenoid biosynthesis archaea |
| | | M00367 | C10-C20 isoprenoid biosynthesis non-plant eukaryotes |

| Category | Subcategory | No.[a] | Module Descriptions[a] |
|---|---|---|---|
| Nucleotide and amino acid metabolism pathway modules | Purine metabolism | M00048 | Inosine monophosphate biosynthesis |
| | | M00049 | Adenine ribonucleotide biosynthesis |
| | | M00050 | Guanine ribonucleotide biosynthesis |
| | Pyrimidine metabolism | M00051 | Uridine monophosphate biosynthesis |
| | | M00052 | Pyrimidine ribonucleotide biosynthesis |
| | | M00053 | Pyrimidine deoxyribonuleotide biosynthesis |
| | | M00089 | Triacylglycerol biosynthesis |
| | | M00098 | Acylglycerol degradation |
| | Serine and threonine metabolism | M00018 | Threonine biosynthesis |
| | | M00020 | Serine biosynthesis |
| | | M00555 | Betaine biosynthesis |
| | Cysteine and methionine metabolism | M00021 | Cysteine biosynthesis |
| | | M00034 | Methionine salvage pathway |
| | | M00035 | Methionine degradation |
| | Branched-chain amino acid metabolism | M00019 | Valine/isoleucine biosynthesis |
| | | M00036 | Leucine degradation |
| | | M00432 | Leucine biosynthesis |
| | | M00570 | Isoleucine biosynthesis |
| | Lysine metabolism | M00016 | Lysine biosynthesis (succinyl-diaminopimelic acid) |
| | | M00032 | Lysine degradation |
| | | M00527 | Lysine biosynthesis (diaminopimelic acid aminotransferase) |
| | Arginine and proline metabolism | M00015 | Proline biosynthesis |
| | | M00028 | Ornithine biosynthesis |
| | | M00029 | Urea cycle |
| | | M00844 | Arginine biosynthesis (ornithine => arginine) |
| | | M00845 | Arginine biosynthesis (glutamate => arginine) |
| | Polyamine biosynthesis | M00134 | Polyamine biosynthesis |
| | | M00135 | GABA biosynthesis eukaryotes |
| | Histidine metabolism | M00026 | Histidine biosynthesis |
| | | M00045 | Histidine degradation |

| Category | Subcategory | No.[a] | Module Descriptions[a] |
|---|---|---|---|
| Nucleotide and amino acid metabolism pathway modules | Aromatic amino acid metabolism | M00022 | Shikimate pathway |
| | | M00023 | Tryptophan biosynthesis |
| | | M00024 | Phenylalanine biosynthesis |
| | | M00025 | Tyrosine biosynthesis |
| | Other amino acid metabolism | M00027 | GABA (gamma-Aminobutyrate) shunt |
| | Cofactor and vitamin biosynthesis | M00115 | NAD biosynthesis |
| | | M00116 | Menaquinone biosynthesis |
| | | M00119 | Pantothenate biosynthesis |
| | | M00120 | Coenzyme A biosynthesis |
| | | M00123 | Biotin biosynthesis |
| | | M00125 | Riboflavin biosynthesis |
| | | M00126 | Tetrahydrofolate biosynthesis |
| | | M00140 | C1-unit interconversion prokaryotes |
| | | M00141 | C1-unit interconversion eukaryotes |
| | | M00577 | Biotin biosynthesis BioW pathway |
| | | M00842 | Tetrahydrobiopterin biosynthesis |
| | | M00846 | Siroheme biosynthesis |
| Energy metabolism pathway modules | Carbon fixation | M00166 | Reductive pentose phosphate cycle |
| | | M00375 | Hydroxypropionate-hydroxybutylate cycle |
| | | M00579 | Phosphate acetyltransferase-acetate kinase |
| | Nitrogen metabolism | M00530 | Dissimilatory nitrate reduction |
| | Sulfur metabolism | M00176 | Assimilatory sulfate reduction |
| Genetic information processing structural complexes | Methane metabolism | M00345 | Formaldehyde assimilation ribulose monophosphate |
| | DNA | M00260 | DNA polymerase III complex, bacteria |
| | RNA | M00183 | RNA polymerase bacteria |
| | | M00394 | RNA degradosome |
| | Ribosome | M00178 | Ribosome bacteria |

| Category | Subcategory | No.[a] | Module Descriptions[a] |
|---|---|---|---|
| Environmental information processing structural complexes | Mineral and organic ion transport system | M00188 | Glutathione biosynthesis |
| | | M00189 | Molybdate transport system |
| | | M00190 | Iron(III) transport system |
| | | M00209 | Osmoprotectant transport system |
| | | M00299 | Spermidine/ putrescine transport system |
| | Bacterial secretion system | M00335 | Secretion (sec) system |
| | | M00336 | Twin-arginine translocation (Tat) system |
| | | M00429 | Competence-related DNA transformation transporter |
| | Phosphotransferase system (PTS) II component | M00266 | Maltose and glucose-specific |
| | | M00267 | N-acetylglucosamine-specific |
| | | M00268 | Arbutin-like |
| | | M00270 | Trehalose-specific |
| | | M00273 | Fructose-specific |
| | | M00274 | Mannitol-specific |
| | | M00279 | Galactitol-specific |
| | | M00281 | Lactose-specific |
| | | M00283 | Ascorbate-specific |
| | | M00809 | Glucose- specific |
| Environmental information processing | ABC-2 type and other transport systems | M00251 | Teichoic acid |
| | | M00254 | ABC-2 type |
| | | M00257 | Hemin |
| | | M00258 | Putative ABC |
| | | M00314 | Bacitracin |
| | | M00583 | Putative peptide |
| | | M00731 | Bacitracin |
| | | M00732 | Cationic antimicrobial peptide |
| | | M00817 | Lantibiotic transport system |

| Category | Subcategory | No.[a] | Module Descriptions[a] |
|---|---|---|---|
| Environmental information processing | Metallic cation, iron-siderophore and vitamin B12 transport system | M00240 | Iron complex |
| | | M00242 | Zinc |
| | | M00581 | Biotin transport system |
| | | M00582 | Energy-coupling factor |
| | | M00792 | Manganese/zinc |
| | Peptide and nickel transport system | M00239 | Peptides/nickel |
| | | M00439 | Oligopeptide |
| | | M00440 | Nickel |
| | Phosphate and amino acid transport system | M00222 | Phosphate |
| | | M00223 | Phosphonate |
| | | M00234 | Cystine |
| | | M00238 | D-Methionine transport system |
| | Saccharide, polyol, and lipid transport system | M00196 | Multiple sugar transport system |
| | | M00211 | Putative ABC |
| | | M00491 | Arabinogalactan oligomer/maltooligosaccharide |
| | | M00605 | Glucose/mannose transport system |
| | | M00606 | N,N'-Diacetylchitobiose transport system |
| Energy metabolism structural complexes | ATP synthesis | M00149 | Succinate dehydrogenase prokaryotes |
| | | M00153 | Cytochrome D ubiquinol oxidase |
| | | M00154 | Cytochrome C oxidase |
| | | M00157 | F-type ATPase prokaryotes and chloroplasts |
| | | M00416 | Cytochrome aa3-600 menaquinol oxidase |
| Metabolism functional set modules | Amino-acyl tRNA | M00359 | Amino-acyl tRNA biosynthesis eukaryotes |
| | | M00360 | Amino-acyl tRNA biosynthesis prokaryotes |
| | Nucleotide sugar | M00361 | Nucleotide sugar biosynthesis eukaryotes |
| | | M00362 | Nucleotide sugar biosynthesis prokaryotes |

| Category | Subcategory | No.[a] | Module Descriptions[a] |
|---|---|---|---|
| Environmental information processing functional set modules | Drug efflux transporter/pump | M00737 | Bacitracin resistance VraDE transporter |
| | Two-component regulatory system | M00434 | PhoR-PhoB (phosphate starvation response) |
| | | M00454 | KdpD-KdpE (potassium transport) |
| | | M00458 | ResE-ResD (aerobic and anaerobic respiration) |
| | | M00459 | VicK-VicR (cell wall metabolism) |
| | | M00468 | SaeS-SaeR (staphylococcal virulence regulation) |
| | | M00479 | DesK-DesR (membrane lipid fluidity regulation) |
| | | M00480 | VraS-VraR (cell wall peptidoglycan synthesis) |
| | | M00483 | NreB-NreC (dissimilatory nitrate/nitrite reduction) |
| | | M00492 | LytS-LytR |
| | | M00495 | AgrC-AgrA (exoprotein synthesis) |
| | | M00716 | ArlS-ArlR (virulence regulation) |
| | | M00733 | GraS-GraR (cationic antimicrobial peptide transport) |
| | | M00734 | BraS-BraR (bacitracin transport) |
| Signature gene set module | Metabolic capability | M00616 | Nitrate assimilation |
| | Drug resistance | M00625 | Methicillin resistance |
| | | M00627 | β-Lactam resistance Bla system |
| | | M00651 | Vancomycin resistance |
| | | M00700 | Multi-drug resistance efflux pump AbcA |
| | | M00702 | Multi-drug resistance efflux pump NorB |
| | | M00704 | Tetracycline resistance efflux pump Tet38 |
| | | M00705 | Multi-drug resistance efflux pump MepA |
| | | M00725 | Cationic antimicrobial peptide resistance dltABCD operon |
| | | M00726 | Cationic antimicrobial peptide resistance lysyl-phosphatidylglycerol synthase MprF |
| | | M00729 | Fluoroquinolone resistance |
| | | M00730 | Cationic antimicrobial peptide resistance VraFG transporter |
| | | M00742 | Aminoglycoside resistance |

No. = KEGG Module number, [a] Listed respectively.